Hypoxia and cell death in grape berries (*Vitis vinifera* L.)

By

Zeyu Xiao

Bachelor of Viticulture and Oenology (Honours)

A thesis submitted for the partial fulfilment of the requirements for the degree of Doctor of Philosophy

The University of Adelaide

Faculty of Sciences

School of Agriculture, Food and Wine

Waite Campus

February 2018

Contents

Abstract

Cell death in the mesocarp of berries occurs late in the ripening process, and may influence berry sensory attributes and water retention. There are cultivar-dependent correlations between mesocarp cell death and berry shrivel. Cell death is likely to be associated with yield losses of up to 30% for Shiraz due to berry shrivel, which concentrates sugars and potentially leads to high alcohol content in wine. The main objective of this thesis was to investigate the association between berry internal oxygen concentrations and berry cell death.

Experiments were carried out at the Waite vineyards and at the SARDI research vineyard in Nuriootpa. Firstly, in Chapter 2, internal oxygen concentration ($[O_2]$) across the mesocarp was measured in berries from Chardonnay and Shiraz, both seeded, and Ruby Seedless, from the Waite vineyards, using an oxygen micro-sensor. Change of berry and seed respiration was investigated in Chardonnay. The lenticel density of Chardonnay and Shiraz berry pedicels (stem and receptacle) was assessed. We then tested the long-term effect of blocking pedicel lenticels on berry internal $[O_2]$ profiles and cell death. Air spaces within the Chardonnay berries at different developmental stages were visualized using x-ray micro-CT. Second, in Chapter 3, a factorial trial of two irrigation regimes was applied in season 2014/2015 and a factorial trial of two irrigation regimes and two temperatures was applied in season 2015/2016, in Nuriootpa. Midday stem water potential, stomatal conductance and photosynthetic rate were measured to examine the efficiency of drought and canopy heating treatments. The oxygen micro-sensor was used to measure oxygen concentration in grapes and their respiration rate. Lastly, in Chapter 4, we tested the effects of overhead shading (2014/2015), rootstocks and kaolin application (both in 2016/2017), on Shiraz berry cell death and berry shrivel.

In Chardonnay, Shiraz and Ruby Seedless grapes, steep $[O_2]$ gradients were observed across the skin and $[O_2]$ decreased toward the middle of the mesocarp. As ripening progressed, the

minimum [O_2] approached zero in the seeded cultivars and correlated to the profile of cell death across the mesocarp. Seed respiration declined during ripening, from a large proportion of total berry respiration early to negligible at latter stages. [O_2] increased towards the central axis corresponding to the presence of air spaces visualised using x-ray micro-CT. These air spaces connect to the pedicel where lenticels are located that are critical for berry O_2 uptake as a function of temperature, and when blocked caused hypoxia in Chardonnay berries, ethanol accumulation and cell death. This work has been published in the Journal of Experimental Botany in February 2018.

In Chapter 3, the results of a factorial field experiment comprising two thermal regimes (ambient and heated) and two irrigation regimes (irrigated and non-irrigated) are reported. Non-irrigation, in the first season, increased the rate of cell death relative to control irrigated Shiraz vines. In the second season, non-irrigation advanced the onset of cell death relative to the irrigated treatments independent of temperature. Non-irrigation treatments in the second season also decreased [O_2] within the berry mesocarp relative to the irrigated treatments. An association was established between mesocarp [O_2] and berry cell death. Berry respiration and total berry porosity were also found to decrease during berry ripening. This work has been submitted to the Australian Journal of Grape and Wine Research in February 2018.

In Chapter 4, three preliminary trials were undertaken to investigate possible mitigation strategies for berry cell death and dehydration. Trial 1 tested the effect of overhead shading on berry dehydration, cell death and internal oxygen concentrations [O_2]. Trial 2 tested the effect of rootstocks having different drought tolerance on berry dehydration and cell death. Trial 3 tested the effect of kaolin spray, which has been proposed to reduce leaf and cluster temperature and transpiration. Overhead shading reduced the rate of increase in cell death and berry dehydration in Shiraz. This treatment also affected the progression of hypoxia in the berry. Shiraz on the drought tolerant 140 Ruggeri had significantly less cell death and berry

dehydration than the less drought tolerant rootstocks (420 A and Schwarzmann). Kaolin spray application reduced berry shrinkage independently of either mesocarp cell death or cluster and leaf temperature.

In summary, grape internal [O_2] declined during fruit development and was correlated with the profile of mesocarp cell death. Lenticels on the pedicel provided a pathway for O_2 diffusion into the berry and when covered to restrict O_2 diffusion into the berry caused a large reduction in [O_2] in the centre of the berry, an increase in ethanol concentration and cell death. Differences in internal O_2 availability of berries between cultivars could be associated with seed development and differences in lenticel surface area. Higher rates of mesocarp cell death caused by water stress was also associated with hypoxia within grape berries. Rootstocks with different drought resistance properties can affect Shiraz berry dehydration and cell death. Kaolin can effectively reduce Shiraz dehydration after the peak berry mass was reached.

The data generated in this study provides the basis for further research into the role of berry gas exchange on berry quality and cultivar selection for adapting viticulture to a warming climate. Understanding the association between berry internal oxygen status and berry shrivel and cell death, as well as the effect of strategies to mitigate cell death and berry shrivel, will provide researchers and growers with new insights in berry ripening and is the basis for future research on berry flavour development and yield optimization.

Declaration

I certify that this work contains no material which has been accepted for the award of any other degree or diploma in my name, in any university or other tertiary institution and, to the best of my knowledge and belief, contains no material previously published or written by another person, except where due reference has been made in the text. In addition, I certify that no part of this work will, in the future, be used in a submission in my name, for any other degree or diploma in any university or other tertiary institution without the prior approval of the University of Adelaide and where applicable, any partner institution responsible for the joint-award of this degree.

I acknowledge that copyright of published works contained within this thesis resides with the copyright holder(s) of those works.

I also give permission for the digital version of my thesis to be made available on the web, via the University's digital research repository, the Library Search and also through web search engines, unless permission has been granted by the University to restrict access for a period of time.

I acknowledge the support I have received for my research through the provision of an Australian Government Research Training Program Scholarship.

Publications

Zeyu Xiao, Suzy Rogiers, Victor Sadras, Stephen Tyerman (2018)

Hypoxia in grape berries: the role of seed respiration and lenticels on the berry pedicel and the possible link to cell death.

Journal of Experimental Botany, ery039, https://doi.org/10.1093/jxb/ery039

Presented in Chapter 2

Zeyu Xiao, Siyang Liao, Suzy Rogiers, Victor Sadras, Stephen Tyerman

Effect of water stress and elevated temperature on hypoxia and cell death in the mesocarp of Shiraz berries.

Australian Journal of Grape and Wine Research (Submitted 2/2/2018)

Presented in Chapter 3

Zeyu Xiao, Lishi Cai, Xin Huang, Stephen Tyerman

Shade, rootstock and kaolin spray as possible mitigation strategies for berry cell death and berry shrivel in Shiraz.

Prepared manuscript

Presented in Chapter 4

Shifeng Cao, Zeyu Xiao, Vladimir Jiranek, Stephen Tyerman (2018)

The VvBAP1 gene is identified as a potential inhibitor of cell death in grape berries.

Plant Molecular Biology (Accepted)

Acknowledgements

First and foremost, I want to thank my supervisor Professor Stephen Tyerman. It has been an honour to be his Ph.D. student. He has taught me how good plant physiology and viticulture research is done. I appreciate his contributions of time, ideas and guidance to make my Ph.D. experience stimulating and rewarding. I am thankful for the excellent example he has set as a great teacher. I would also like to thank my co-supervisor Associate Professor Victor Sadras and external supervisor Dr. Suzy Rogiers for their help in developing my research and this thesis.

I would also like to take this opportunity to thank my friends and colleagues at The University of Adelaide. I am especially grateful for all the group members at the Plant Research Centre and The ARC Training Centre for Innovative Wine Production, past and present, that I have had the pleasure to work with or alongside of. I would like to thank Wendy Sullivan, for her expert technical advice and support throughout my Ph.D. and Siyang Liao, for her friendship and advice as we journey together along our Ph.D. path.

I would also like to acknowledge Martin Moran and Roger Maywald at The South Australian Research and Development Institute (SARDI) for the use of the vineyard in Nuriootpa. I thank Phil John Earl, Luciano Caravia and Benjamin Pike for their support at the Waite vineyards. I thank Gwenda Mayo and Ruth Williams at Adelaide Microscopy for their expert technical assistance in microscopy and micro-CT imaging. I also thank Yalumba Nursery for providing me with rootlings.

I gratefully acknowledge The ARC Training Centre for Innovative Wine Production and The University of Adelaide for funding my Ph.D.

I would like to thank my family, in particular Mum and Dad, for their love and support.

List of Abbreviations

A	Ambient (canopy temperature)
ACDT	Australian Central Daylight Time
ADH	Alcohol dehydrogenase
AL-DH	Aldehyde dehydrogenase
A_{sat}	Net CO_2 assimilation at light saturation (photon flux density = 919 µmol m^{-2} s^{-1})
CD	Cell death
CO_2	Carbon dioxide
DAA	Days after anthesis
FDA	Fluorescein diacetate
GDD	Growing degree days
g_s	Stomatal conductance
H	Heated (Canopy temperature)
H_2O_2	Hydrogen peroxide
I	Irrigated
IRGA	Infrared gas analyser
K^+	Potassium ion
Micro-CT	Micro-computed tomography
N_2	Nitrogen
NADH/NAD^+	Nicotinamide adenine dinucleotide
NI	Non-irrigated
O_2	Oxygen
PAR	Photosynthetically active radiation
PIP	Plasma membrane intrinsic protein
Q_{10}	Q_{10} temperature coefficient
RNA	Ribonucleic acid
ROS	Reactive oxygen species
TSS	Total soluble solids
v/v	Volume per volume
ψ_L	Leaf water potential
ψ_s	Stem water potential

Chapter 1 Literature review

Overview

Global warming is increasing the frequencies of heatwaves and drought events (Alexander and Arblaster, 2009; Perkins *et al.*, 2012). This challenges the wine grape industry particularly in warm climates (Webb *et al.*, 2007a), since temperature and water are important factors affecting the growth and physiology of grapevines, and in warm climates these factors may already be close to the upper limit for good quality grape production (Caravia *et al.*, 2016; Petrie and Sadras, 2008). Berries that ripen under stressful conditions can undergo substantial weight loss due to late-ripening berry shrivel, which ultimately affects the quality and potentially increases ethanol content in the final wine. This chapter reviews grape berry development, especially in later stages, with a focus on the changes in vascular delivery of water and sugar and the changes associated with the occurrence of cell death within the berry pericarp related to the structure of grape berries. How drought and heat stress affect the vine and how this may increase the severity of cell death in grape berries is also discussed. This is related to the role of molecular oxygen (O_2) in maintaining active cell metabolism and how reduced O_2 concentration ($[O_2]$) could affect plant tissues in general, and the grape berry. To test the hypothesis that reduced $[O_2]$ within the berry may be a cause of reduced cell vitality in the berry, measurements of $[O_2]$ across the berry pericarp were undertaken during normal berry development in different cultivars, after vines were drought and heat stressed in the field or otherwise treated in growth room conditions to investigate berry gas exchange. The aim was to enable a better understanding of the role of berry cell death in berry water relations and ripening.

Grape berry development

Grape berry development follows a double-sigmoid growth pattern, which can be divided into three main phases, berry formation, berry ripening and berry shrinkage, although the last phase is cultivar dependent (Coombe and McCarthy, 2000; Sadras and McCarthy, 2007). In the first phase (berry formation), berry size increases rapidly with cell division and enlargement. During this time, the accumulation and storage of organic acids, malate and tartrate, in the mesocarp occurs (Possner and Kliewer, 1985). The first phase is followed by the onset of ripening, veraison, marked by softening of the berries and colour change in pigmented varieties (Coombe, 1976; Coombe, 1992). Softening results from the reduction in apoplastic solute potential and turgor pressure (Thomas *et al.*, 2008; Wada *et al.*, 2009). Berry mass and size continues to increase and key compounds including sugars, pigments and important wine aroma precursors accumulate during the second phase (Castellarin *et al.*, 2016). The third phase is characterized by mass loss of the berries and is, depending on cultivar, correlated with loss of cell vitality within the berries (Fuentes *et al.*, 2010; McCarthy and Coombe, 1999; Tilbrook and Tyerman, 2008).

Sugar accumulation

The sugar concentration of berry juice is one of the major criteria for viticulture and winemaking decisions (Sadras *et al.*, 2008). The hexoses, glucose and fructose, are the major solutes that accumulate in berry flesh and skin (Coombe, 1992). Sucrose transported from the leaves is converted to glucose and fructose and accumulated in berry vacuoles. Hexoses generally start to accumulate 8 weeks after flowering and have been associated with a peak in invertase (Davies and Robinson, 1996). It is sometimes challenging to reach a desirable level of sugar with balanced water retention (Sadras *et al.*, 2008) and acidity, and the accumulation of phenolic and other aroma compounds (Dai *et al.*, 2010). Sugars are unloading into grape berries from the phloem primarily via the apoplastic pathway (Patrick, 1997). The phloem

unloading was shifted from symplastic to apoplastic at the beginning of berry ripening (Zhang *et al.*, 2006). Sugar accumulation can be affected by environmental factors, such as water status (Santesteban and Royo, 2006), but also by management practices such as cluster thinning (Keller *et al.*, 2005). Cultivar-dependent variations were found in the rate of change in concentration of soluble solids during berry ripening, which contributed to the differences in sugar maturity of each cultivar (Sadras *et al.*, 2008). The rate of sugar accumulation was also positively correlated with vine physiology such as stomatal conductance (Sadras *et al.*, 2008).

Berry cell vitality

Cell death can occur during late ripening in normally developing grape berries (Clarke *et al.*, 2010; Fuentes *et al.*, 2010; Krasnow *et al.*, 2008; Tilbrook and Tyerman, 2008). This process is hypothesised to contribute to flavour development due to enzymatic reactions leading to the breakdown of membranes and mixing of cell compartments, which are typical processes in plant cell death (Reape and McCabe, 2008; Tilbrook and Tyerman, 2008). Plant programmed cell death (PCD) can generally be categorized as developmental, abiotic stress triggered, or in response to pathogens (Van Doorn and Woltering, 2005). Late ripening cell death in the grape berry could be a developmental PCD and/or a response following abiotic stress, as no invading pathogenic microorganism has so far been reported to be associated with this phenomenon.

Several techniques have been used to measure the level of cell vitality in grape berries. The most common is the use of fluorescein diacetate (FDA) staining (Fuentes *et al.*, 2010; Krasnow *et al.*, 2008; Tilbrook and Tyerman, 2008). When using this method, berries were cut in halves, the clean-cut surface was submerged and incubated in staining solution containing FDA with sucrose used to adjust osmolality to match that of the cell sap. Permeable FDA enters living cells across the plasma membrane, then esterases in the

cytoplasm cleave the compound, producing fluorescein, which is membrane impermeable and fluorescent under UV light (Jones and Senft, 1985). Stained areas of the tissue indicate vital cells while non-stained areas indicate loss of enzymatic activity in cytoplasm or reduced membrane integrity, both indicating cell death (Krasnow *et al.*, 2008). Other staining agents have been reported to indicate grape berry cell vitality. Clarke *et al.* (2010) used nitroblue tetrazolium to indicate oxidative metabolism of living cells. Propidium iodide has also been used, since this only stains DNA of damaged cells and indicates the loss of membrane integrity (Krasnow *et al.*, 2008; Tilbrook and Tyerman, 2008). Impedance spectroscopy was also shown to detect loss of cell vitality in grape berries correlated against FDA staining, by reporting ion leakage into the apoplast and changed membrane integrity (Caravia *et al.*, 2015).

Berry shrivel

The occurrence of berry shrivel, most often observed for fully mature Shiraz berries on vines grown in warm climates (Coombe and McCarthy, 2000; McCarthy and Coombe, 1999), is likely due to a combination of several factors. First, based on the correlation between cell death and berry shrivel, membrane semi-permeability of the mesocarp cells may be lost causing loss of water from the cells (Clarke *et al.*, 2010; Tilbrook and Tyerman, 2008). Second, berry transpiration may continue but with decreased vascular inflow (Rogiers *et al.*, 2004b). This may be combined with backflow to the vine (Keller *et al.*, 2006; Keller *et al.*, 2015; Tilbrook and Tyerman, 2009; Tyerman *et al.*, 2004) through functional xylem, which is only partially blocked in the pedicel (Knipfer *et al.*, 2015). Berry shrivelling is cultivar dependent and may be linked to very different behaviours of berry hydraulic conductance in different cultivars late into ripening (Scharwies and Tyerman, 2017; Tilbrook and Tyerman, 2009).

Stress conditions and climate change

Berry shrivel and cell death is affected by abiotic stress. Elevated canopy temperature by 1.5 °C during the growing season can increase the rate of cell death in grapes (Bonada *et al.*, 2013a). Overhead shade can reduce berry cell death and loss of mass in Shiraz grapes due to the reduced impact of heat stress (Caravia *et al.*, 2016). There are increasing frequencies and intensities of heat waves and drought events in Australia (Alexander and Arblaster, 2009). The warming trend is predicted to have adverse effects on grapevine physiology (Webb *et al.*, 2007b). Grapevine phenology has shifted such that berry ripening occurs earlier and coinciding with higher seasonal temperatures (Petrie and Sadras, 2008). Consequently, berry quality can be affected (Bonada and Sadras, 2015; Caravia *et al.*, 2016; Fuentes *et al.*, 2010). The irrigation regime influences maximum and final berry size in various varieties and growing conditions (McCarthy, 1997; Reynolds and Naylor, 1994; Rogiers and Holzapfel, 2015). This is because water deficit shortly after fruit set reduces cell division rate in the pericarp (Coombe, 1976; Harris *et al.*, 1968). However, the rate of mass loss during late ripening in Shiraz berries was not linked to the degree of water deficit (McCarthy, 1997). Increased alternative oxidase (AOX) expression was found in water stressed grapevines (Cramer *et al.*, 2007). AOX synthesis is also induced by reactive oxygen species (ROS) and the protein suppresses further accumulation of ROS to harmful levels in plants (Pitzschke *et al.*, 2006)

Rootstock and vine water relations

Rootstocks are derivatives (generally hybrids) from American *Vitis* species used for their phylloxera (Granett *et al.*, 2001) and nematode (Anwar *et al.*, 2002) resistance properties. Rootstocks are also used for their ability to resist diseases (Wallis *et al.*, 2013), tolerate drought and salt stress (Serra *et al.*, 2014), and to control vigour of the scion according to soil fertility, water availability and climate conditions (Gambetta *et al.*, 2012; Walker *et al.*,

2002). Drought resistant rootstocks can maintain yield and dry matter production of the scion when under water stress (McCarthy *et al.*, 1997). Further, the use of rootstocks under water stress conditions can affect reproductive performance (Kidman *et al.*, 2014). Rootstock can affect sensory and composition of the fruit and wine, possibility due to the effect on vine vigour and cluster exposure (Olarte Mantilla *et al.*, 2017). Importantly, rootstocks were shown to delay the onset of Shiraz berry loss of mass during late ripening under deficit irrigation (Rogiers *et al.*, 2004a), while berry mass loss of own-rooted Shiraz was not affected by deficit irrigation (McCarthy, 1997; Rogiers *et al.*, 2004a). Common rootstocks considered to be drought tolerant are Ramsey, 110 Richter, 140 Ruggeri, 1103 Paulsen, SO4 and 99 Richter (Carbonneau, 1985; Williams, 2010), whereas 101-14 Mgt, 420 A and Schwarzmann are reported to be susceptible to drought (Carbonneau, 1985; Nicholas, 1997).

Structure of the grape berry

Pericarp

The grape pericarp (Figure 1), contains three anatomically distinct tissues: exocarp, mesocarp and endocarp, all developed from the ovary after flowering (Hardie *et al.*, 1996). These different tissue types are made of different cell types: The exocarp consists of cuticle covered epidermis, layers of thick-walled collenchyma-like cells, and cells that contain raphides. The mesocarp consists of thin-walled large parenchyma. The endocarp consists of druse-rich cells and an inner epidermis (Hardie *et al.*, 1996). The distribution of vascular bundles is thought to contribute to the spatial variations in solute concentrations within the berry, since higher sucrose and inorganic anion concentrations have been discovered in central and peripheral flesh, respectively, during late ripening stages (Coombe, 1987). Coombe (1987) also suggested these differences could be associated with phloem unloading as the berry senesces. Sugar unloading starts in the distal end of the berry (Castellarin *et al.*, 2011; Zhang and Keller, 2017).

The onset of berry ripening (veraison) is indicated by soluble solids accumulation and is concurrent with an increase in berry deformability (Nunan *et al.*, 1998). The softening of the berries after veraison is also associated with compositional changes of cell wall polysaccharide, protein and amino acids (Nunan *et al.*, 1998). Central mesocarp cells greatly increase in size during berry growth, compared to those cells closer towards the skin (Considine and Knox, 1979; Nunan *et al.*, 1998).

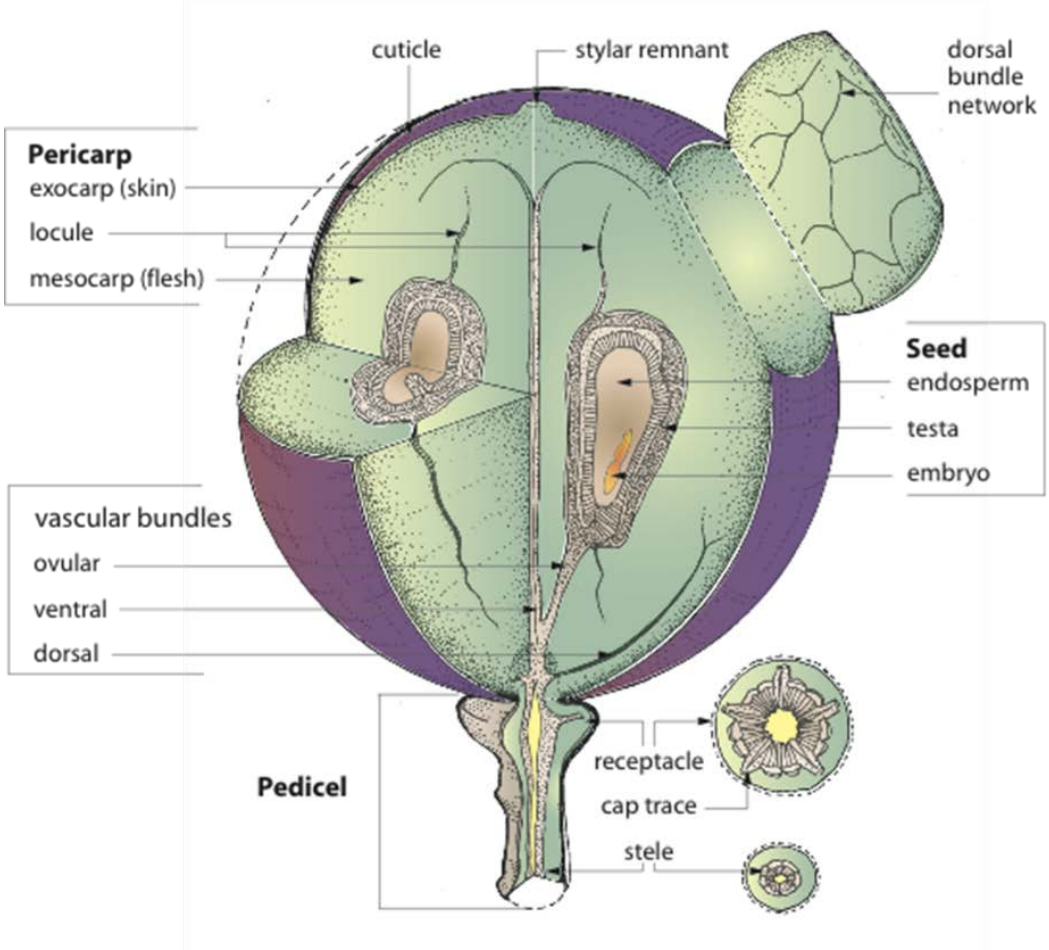

Figure 1. Basic grape berry structure (Iland *et al.* 2011).

Seeds

The growth of berry seeds, such as in Shiraz, can be allocated to three stages, each corresponding to certain stages in berry development (Ristic and Iland, 2005). During these stages, seeds undergo distinct morphological and chemical changes (Kennedy *et al.*, 2000;

Ristic and Iland, 2005). The growth of seeds is also highly correlated with increasing berry mass due to their positive effect on pericarp cell division (Coombe, 1960; Ojeda *et al.*, 1999). The biosynthesis of procyanidins coincide with the initial rapid period of berry growth (Coombe, 1973). These polyphenol compounds are highly concentrated in *Vitis vinifera* seeds and peak in accumulation at veraison, after which there is a steady decline (De Freitas *et al.*, 2000). After seeds reach their maximum fresh mass and size, development enters a transition where the seed coat changes colour and dehydration is initiated (Ristic and Iland, 2005). Although lignification of seeds is completed before berries begin to ripen (Cadot *et al.*, 2006), in Shiraz a sustained oxidation of tannins occurs (Ristic and Iland, 2005) and is concurrent with the oxidation of phenolic compounds such as flavan-3-ol monomers and procyanidins (Cadot *et al.*, 2006). Lignin polymerisation also requires the consumption of O_2 and generation of H_2O_2 for the final peroxidase reaction (Lee *et al.*, 2013), and this with oxidation of tannins could add additional stress to the mesocarp in seeded cultivars. Phenolics can also act as ROS-scavengers (Blokhina *et al.*, 2003).

Skin

Grape berries are covered by a cuticular membrane that plays an important role in controlling water movement between the epidermal cells and ambient atmosphere (Rogiers *et al.*, 2004b). Sun exposed berries have been recorded to reach 15°C above ambient temperature, whereas shaded berries are close to ambient temperature (Smart and Sinclair, 1976; Spayd *et al.*, 2002). The substantially higher temperature for sun-facing berries changed the morphology of the wax layer of the berries (Rogiers *et al.*, 2004b). Water stress increased anthocyanins and decreased flavonoids during berry ripening (Kennedy *et al.*, 2002). Cuticular conductance as well as surface area, air temperature and relative humidity determine the rate of berry ripening (Zhang and Keller, 2015). These factors also contribute to berry mass loss late in ripening (Rogiers *et al.*, 2004b).

Pedicel

Berry pedicels (Figure 2a) do not show accumulation of solutes during ripening (Coombe, 1992). Pedicel vessel functional efficiency changes over ripening and may have important implications for fruit development. It was earlier proposed that emboli occurred in the xylem of the pedicel and that this contributed to reduced hydraulic conductivity as ripening progressed (Coombe, 1992). In Chardonnay berries, there was a substantial reduction in hydraulic conductivity of the receptacle late in ripening associated with deposition of gels or solutes in xylem of the receptacle (Choat *et al.*, 2009). More recent measurements have shown that approximately 50% of vessel elements in the pedicel remain functional during late ripening (Knipfer *et al.*, 2015). This also appears to be cultivar dependent (Scharwies and Tyerman, 2017). The reduction in xylem conductance in the pedicel as well as within the fruit (brush region in grapes) could be a preventative mechanism for loss of solutes via xylem back-flow (Patrick, 1997) though a large proportion of phloem water appears to be recycled back to the vine by the xylem and is required for normal sugar accumulation (Zhang and Keller, 2017).

Lenticels

Lenticels occur on the mature grape berry skin as well as being particularly prominent on the pedicel (Figure 2). Lenticels develop from stomata during secondary growth of plant cuticles. They are multicellular structures with analogous functions to stomata as pathways for exchange of water vapour and gases (Lendzian, 2006). Lenticels are less regulated and have less gas exchange capacity than stomata, but provide “static pores” as a low-resistance pathway for oxygen and other gas exchange (Beikircher and Mayr, 2013; Groh *et al.*, 2002; Taiz and Zeiger, 2010). Less than ten stomata exist on the surface of an actively photosynthesizing young berry (Palliotti and Cartechini, 2001). Wax-occluded lenticels are formed below these stomata as the berry develops (Rogiers *et al.*, 2004b; Swift *et al.*, 1973).

Transpiration from grape berries is small due to the low frequency of stomata and lenticels on the berry surface, and transpiration is further hindered as the fruit matures (Mullins *et al.*, 1992). Lenticels on the surfaces of Riesling berries, receptacle and pedicels also appear to be involved in free water uptake (when berries are submerged) (Becker *et al.*, 2012). In their experiment, fluorescent dye movement indicated that lenticels on the pedicel were one of the primary entries points for liquid water. Lenticels on the berry skin and pedicels are pervious to excessive sulphur dioxide, which can result in localized skin bleaching of table grapes (Nelson, 1979; Nelson and Ahmedullah, 1973). Yet, there are still uncertainties about how efficient these structures are in facilitating gas exchange in grape berries. In tomato, less lenticels and smaller surface area of stem scar were correlated to lower loss of mass, fruit respiration and slower ripening under hypoxia (Paul and Srivastava, 2006). The diffusion of volatile compounds of pear into the air was found to be related to skin lenticel density (Ho *et al.*, 2016). Lenticels become obstructed by epicuticular wax on the grape berry skin as the fruit ages (Rogiers *et al.*, 2004b). Since lenticels on the pedicels are able to take up liquid water (Becker *et al.*, 2012), it is likely that they are not significantly obstructed by wax. Also gas permeability of lenticels could be affected by environmental conditions (Groh *et al.*, 2002; Lendzian, 2006; Mullins *et al.*, 1992). Previous research on potato showed lenticels on the skin are the main pathway for respiratory O_2 uptake (Wigginton, 1973).

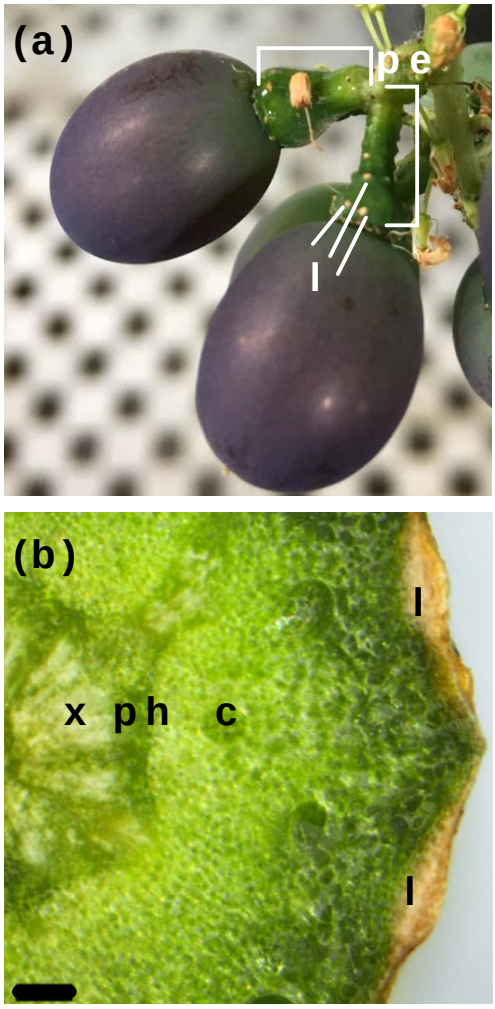

Figure 2. (a) Lenticels on Shiraz berry pedicel. (b) Cross-section of a grape pedicel. Scale bar is 0.1 mm. pe, pedicel; l, lenticel; x, xylem; ph, phloem; c, cortex.

Oxygen and reactive oxygen species in grape berries

Molecular O_2 is essential for efficient ATP production through oxidative phosphorylation as the terminal electron acceptor in mitochondria. In grape berries, O_2 is essential for berry respiration and metabolism and would need to be available within the pericarp to support the energy requirements of sugar accumulation and flavour development. Grape berries are non-climacteric fruit that do not exhibit a large rise in respiration rate or ethylene at the onset of ripening though ethylene may still play a role (Bottcher *et al.*, 2013). Rather, the onset of ripening is associated with the accumulation of hydrogen peroxide (H_2O_2) in the skin of Pinot

Noir berries, and there is increased catalase activity and peroxidation of galactolipids (Pilati *et al.*, 2014). Hypoxia also elevates hydrogen peroxide levels in plants (Vergara *et al.*, 2012). Reactive oxygen species (ROS) in plants occur as the by-products of aerobic metabolism and have been shown to regulate growth, development, stress defence (Considine *et al.*, 2017; Pilati *et al.*, 2007), and notably as modulators of PCD in plants (Gadjev *et al.*, 2008). Although H_2O_2 was considered to be a harmless signal in the case of Pinot Noir ripening, this cultivar also shows up to 50% cell death later in ripening (Fuentes *et al.*, 2010). The accumulation of H_2O_2, apart from a potential signal for ripening (Pilati *et al.*, 2014), is also characteristic for hypoxia and anoxia treated plant tissues (Blokhina *et al.*, 2001; Fukao and Bailey-Serres, 2004), suggesting that grape berries could also be under hypoxia stress during ripening. Plant tissues experience wide O_2 fluctuations under abiotic stress conditions (Bailey-Serres and Voesenek, 2008). Further, ROS induced decrease in cytosolic K^+ has been linked to the activation of PCD in plants due to sustained low K^+ levels within the cytosol (Shabala, 2017). Potassium accumulation in the apoplast was observed in Merlot berries (Keller and Shrestha, 2014), a cultivar that also shows substantial cell death during late ripening (Fuentes *et al.*, 2010). Linking these observations would suggest an association between ROS production induced by hypoxia/anoxia within berries, plasma membrane leakage (of K^+) and PCD. ROS production is kept tightly controlled in an anti-oxidative system by alternative oxidase (Pilati *et al.*, 2014; Pitzschke *et al.*, 2006), non-enzymatic low molecular weight compounds, such as ascorbic acid, glutathione (Ikbal *et al.*, 2014), carotenoid, tocopherols (DellaPenna and Pogson, 2006) and phenolic compounds (Blokhina *et al.*, 2003).

Metabolism and implications on water relations in an O_2 limited environment

The respiratory quotient increases in grape berries during ripening (Harris *et al.*, 1971), most probably due to increased ethanol fermentation (Famiani *et al.*, 2014; Terrier and Romieu,

2001) indicating a major change in berry metabolism. Other fruit also show evidence for restriction of aerobic respiration, for example in apple, tomato and chicory fruit, a clear effect of O_2 concentration on the level of respiration and on the occurrence of fermentation was found (Hertog *et al.*, 1998). Ethanol production is associated with normal fruit ripening, since alcohol dehydrogenase (ADH) activity increases and the ADH genes expression are up-regulate during normal fruit ripening in grapes and tomatoes (Longhurst *et al.*, 1990; Sweetman *et al.*, 2009). Fermentation is also one strategy that plant cells may invoke to allow some energy production and to maintain cell function under O_2-limiting conditions provided sugars are available, and interestingly both H_2O_2 and ethylene have been implicated in its regulation (Fukao and Bailey-Serres, 2004). Root tissue can lose reserves of sucrose quickly under anoxia due to fermentation but also due to reduced phloem unloading (Saglio, 1985). Gas permeability of fruit skin plays an important role in affecting ADH activity and the accumulation of ethanol (Shi *et al.*, 2007). Lactate fermentation can also occur under anaerobic stress (Davis, 1980), which can contribute to cytoplasm acidification (Roberts *et al.*, 1984). Alanine synthesis increases, when excessive pyruvate failed to be metabolized and accumulated under anoxia, to control supply of pyruvate for lactate and ethanol production (Good and Crosby, 1989; Good and Muench, 1992; Streeter and Thompson, 1972). Under anoxia stress, H^+ pumping ATPase was blocked which inhibits H^+ extrusion and this also initiates a cytosolic pH drop (Gout *et al.*, 2001). The induced more acidic cytosolic pH then results in reduction of membrane water transport capacity due to pH sensitivity of the water transport plasma membrane intrinsic proteins (Tournaire-Roux *et al.*, 2003; Zhang and Tyerman, 1999), which are highly expressed in grape berries during ripening (Choat *et al.*, 2009). We suspect the reduced membrane water permeation under hypoxia is accountable for the decrease in whole berry hydraulic conductance that is consistently observed for Chardonnay and Shiraz (Scharwies and Tyerman, 2017; Tilbrook and Tyerman, 2009) and

the decreased propensity of berries to split due to swelling in wet conditions (Clarke *et al.*, 2010).

Diffusion of O_2 in fruit

Fruit parenchyma can be regarded as a porous medium with air spaces distributed in between the elliptically tessellated cells (Gray *et al.*, 1999; Herremans *et al.*, 2015; Mebatsion *et al.*, 2006). The internal O_2 concentration of fruit depends on the respiratory demand, and the O_2 diffusion properties of the skin and internal tissues. These can show genotypic differences as is the case for apple fruit (Ho *et al.*, 2010). In pear fruit differences in porosity of tissue, the connectivity of intercellular spaces and cell distribution may account for variation between fruit (Ho *et al.*, 2009). For pear it was possible to reconcile the observed variation in gas diffusion with the irregular microstructure of the tissue using a microscale model of gas diffusion. This also appears to be the case for different cultivars of apple as assessed by X-ray micro computed tomography (Mendoza *et al.*, 2007). Apple skin also showed a very low O_2 diffusivity and likewise a steep concentration gradient across the skin (Ho *et al.*, 2010).

Porosity of fruit is considered to be an important factor in dry fruit and vegetable production (Mayor *et al.*, 2011). O_2 diffusion is significantly reduced in a porous matrix upon collapse of the system (White and Bell, 1999). Structural collapse reduces sugar degradation in a low-moisture matrix (White and Bell, 1999) and affects the rate of lipid oxidation (Shimada *et al.*, 1991). Shrinkage during the drying processes in food production and the porosity of the material together also determine rehydration capability in potatoes (McMinn and Magee, 1997). By investigating the morphological changes in air spaces and porosity in the grape berry, we might be able to further understand biological processes associated with berry shrivel and cell death.

Research questions

What is the profile of O_2 concentration across the berry from the surface to the interior regions?

Are there changes in berry internal O_2 profiles during berry development?

Are there differences in berry internal O_2 concentration between cultivars?

Is hypoxia in wine grape berries linked to cell death?

Does elevated temperature and water stress affect berry internal O_2 concentrations during ripening?

How do seeds affect O_2 demand in the berry mesocarp?

What is the potential pathway for O_2 uptake in grape berries?

How is berry respiration dependent on temperature at different ripening stages?

What mitigation strategies can be used to reduce berry shrivel?

Research objectives

1. Measure O_2 concentrations in difference grape cultivars

Hypotheses:

- Mesocarp becomes hypoxic during late ripening.
- Seed respiration is a significant demand on O_2 supply.
- There is a spatial difference in O_2 concentration within berries that is linked to the patterns of mesocarp cell death.
- Differences in the degree of cell death in different cultivars are linked to morphological differences that affect O_2 diffusion pathways.

2. Test whether stressful conditions (heat and water stress) is linked to berry internal oxygen concentration.

Hypotheses:

- Elevated temperature and water stress will affect berry internal oxygen profiles.

Grapes grown in stressful conditions in the field will show a greater degree of hypoxia that correlates to the advanced and exacerbated rate of cell death.

3. Test mitigation strategies that could reduce cell death and weight loss.

Hypotheses:

- Shade decreases canopy temperature and respiratory demand, and therefore affect berry internal oxygen concentration.
- Rootstock will influence vine/berry water relations of Shriaz scion and affect the level of berry shrivel.
- Kaolin spray will reduce berry water loss.
- Kaolin spray will delay and decrease berry cell death.

Significance/contribution to the discipline

Understanding the triggers of cell death in grape berries will help growers to better monitor the berry ripening process in order to produce fruit with balanced flavour development and water retention. Understanding the effect of rootstock on berry cell death will add valuable information to rootstock selection. Kaolin spray was tested to provide useful information on the effectiveness of this mitigation tool for reducing adverse effects caused by heatwaves and excessive sun exposure.

Chapter 2 Hypoxia in grape berries: the role of seed respiration and lenticels on the berry pedicel and the possible link to cell death

Published, Journal of Experimental Botany, ery039, https://doi.org/10.1093/jxb/ery039

Statement of authorship

Statement of Authorship

Title of Paper	Hypoxia in grape berries: the role of seed respiration and lenticels on the berry pedicel and the possible link to cell death
Publication Status	☐ Published ☑ Accepted for Publication ☐ Submitted for Publication ☐ Unpublished and Unsubmitted work written in manuscript style
Publication Details	Accepted in Journal of Experimental Botany 19/1/2018 MS ID JEXBOT/2017/214379

Principal Author

Name of Principal Author (Candidate)	Zeyu Xiao
Contribution to the Paper	ZX contributed to experimental design, performed the experiments, analysed the data and drafted the manuscript.
Overall percentage (%)	80%
Certification:	This paper reports on original research I conducted during the period of my Higher Degree by Research candidature and is not subject to any obligations or contractual agreements with a third party that would constrain its inclusion in this thesis. I am the primary author of this paper.
Signature	Date 1/2/2018

Co-Author Contributions

By signing the Statement of Authorship, each author certifies that:

i. the candidate's stated contribution to the publication is accurate (as detailed above);

ii. permission is granted for the candidate in include the publication in the thesis; and

iii. the sum of all co-author contributions is equal to 100% less the candidate's stated contribution.

Name of Co-Author	Suzy Y. Rogiers
Contribution to the Paper	Contributed to experimental design, co-supervised the research and assisted in editing the manuscript.
Signature	Date 1/2/2018

Name of Co-Author	Victor O. Sadras
Contribution to the Paper	Contributed to experimental design, co-supervised the research, assisted in analysing the data and editing the manuscript.
Signature	Date 1 - Feb - 2018

Name of Co-Author	Stephen D. Tyerman		
Contribution to the Paper	Contributed to experimental design, supervised the research and assisted in analysing the data and editing the manuscript.		
Signature		Date	31/1/2018

Abstract

Mesocarp cell death (CD) during ripening is common in berries of seeded *Vitis vinifera* L. wine cultivars. We examined if hypoxia within berries is linked to CD. Internal oxygen concentration ($[O_2]$) across the mesocarp was measured in berries from Chardonnay and Shiraz, both seeded, and Ruby Seedless, using an oxygen micro-sensor. Steep $[O_2]$ gradients were observed across the skin and $[O_2]$ decreased toward the middle of the mesocarp. As ripening progressed the minimum $[O_2]$ approached zero in the seeded cultivars and correlated to the profile of CD across the mesocarp. Seed respiration declined during ripening, from a large proportion of total berry respiration early to negligible at latter stages. $[O_2]$ increased towards the central axis corresponding to the presence of air spaces visualised using x-ray micro-CT. These air spaces connect to the pedicel where lenticels are located that are critical for berry O_2 uptake as a function of temperature, and when blocked caused hypoxia in Chardonnay berries, ethanol accumulation and CD. The implications of hypoxia in grape berries are discussed in terms of its role in CD, ripening and berry water relations.

Keywords: grape berry, lenticels, micro-CT, oxygen sensor, pedicel, programmed cell death, respiration, seed respiration, temperature, *Vitis vinifera*

Introduction

Onset and rate of cell death (CD) in berry mesocarp of *Vitis vinifera* L are genotype-dependent, and modulated by temperature and drought (Bonada *et al.*, 2013a; Bonada *et al.*, 2013b; Fuentes *et al.*, 2010; Krasnow *et al.*, 2008; Tilbrook and Tyerman, 2008). Evolutionarily, CD may have been selected as a trait favouring seed dispersal (Hardie *et al.*, 1996). It correlates with berry dehydration (Bonada *et al.*, 2013b; Fuentes *et al.*, 2010), a common phenomenon in warm wine growing regions, and is partially distinct from other forms of "berry shrivel" (Bondada and Keller, 2012; Keller *et al.*, 2016). Berry dehydration associated with CD is common in Shiraz (Syrah), resulting in increased sugar concentration (Caravia *et al.*, 2016; Rogiers *et al.*, 2004; Sadras and McCarthy, 2007). It is also associated with altered chemical composition (Šuklje *et al.*, 2016), and sensory characteristics (Bonada *et al.*, 2013a).

Grape berries are non-climacteric, though ethylene may still play a role (Bottcher *et al.*, 2013). However, the onset of ripening is associated with the accumulation of hydrogen peroxide (H_2O_2) in skin of Pinot Noir berries (Pilati *et al.*, 2014). Although H_2O_2 was considered a harmless signal, Pinot Noir berries also show up to 50% CD (Fuentes *et al.*, 2010). Accumulation of H_2O_2 is also characteristic of plant tissues exposed to hypoxia or anoxia (Blokhina *et al.*, 2001; Fukao and Bailey-Serres, 2004). Grape berry respiratory quotient increased during ripening (Harris *et al.*, 1971) associated with increased ethanolic fermentation (Famiani *et al.*, 2014; Terrier and Romieu, 2001). Other fruit also show restricted aerobic respiration and fermentation (Hertog *et al.*, 1998). Ethanolic fermentation contributes to maintain cell function under O_2-limiting conditions provided sugars are available. Interestingly, both H_2O_2 and ethylene have been implicated in its regulation (Fukao and Bailey-Serres, 2004).

Hypoxia-induced oxidative stress decreases lipid and membrane integrity (Blokhina *et al.*, 2001), the latter being clearly evident in most wine grape berries by vitality stains (Tilbrook and Tyerman, 2008). Increased CD in Shiraz grapes is reflected by decreased extracellular electrical resistance indicating electrolyte leakage (Caravia *et al.*, 2015). This leakage corresponds to the accumulation of potassium in the extracellular space of Merlot berries (Keller and Shrestha, 2014), a cultivar that also displayed CD (Fuentes *et al.*, 2010). O_2 deprivation diminishes intracellular energy status that reduces cell vitality in non-photosynthetic organs, as exemplified by roots under flooding or waterlogging (Voesenek *et al.*, 2006). Although grape berries show some photosynthesis in early stages of development (Ollat and Gaudillère, 1997), during ripening photosynthetic pigments and nitrogen content are reduced and atmospheric CO_2 is not fixed while re-fixation of respiratory CO_2 declines (Palliotti and Cartechini, 2001).

Shiraz berry CD can be accelerated by water stress and elevated temperature (Bonada *et al.*, 2013a). There are increasing frequencies and intensities of heat waves and drought events globally and in Australia (Alexander and Arblaster, 2009; Perkins *et al.*, 2012), and the warming trend is predicted to have adverse effects on grapevines (Webb *et al.*, 2007) and berry quality (Bonada and Sadras, 2015; Caravia *et al.*, 2016; Fuentes *et al.*, 2010). Higher temperature increases demand for O_2 to support increased oxidative respiration (Kriedemann, 1968). Meanwhile, O_2 diffusion into the berry may be limited by decreased gas exchange across the berry skin during ripening, as judged by declining transpiration (Rogiers *et al.*, 2004; Scharwies and Tyerman, 2017) and/or changes in berry internal porosity during ripening. Lenticels on the skin of potato tubers are the main channel for O_2 uptake for respiration (Wigginton, 1973) and phellem-lenticel complex of woody roots and trunks regulates O_2 exchange (Lendzian, 2006). In the grape berry, the small number of stomata on

skin develop into non-functional lenticels occluded with wax (Rogiers *et al.*, 2004), but lenticels are very prominent on the pedicel (Becker *et al.*, 2012).

Wine-grape cultivars are seeded, and have been selected for wine-related attributes, whereas table-grape cultivars have been selected for turgor maintenance, and markets increasingly demand seedless fruit; these differences in selective pressures between wine and table grape cultivars have led to differences in the dynamics of water during berry ripening (Sadras *et al.*, 2008). Table grape seedless cultivars show little or no CD well into ripening (Fuentes *et al.*, 2010; Tilbrook and Tyerman, 2008). Although lignification of seeds is complete before berries begin to ripen (Cadot *et al.*, 2006), oxidation of seed tannins is sustained (Ristic and Iland, 2005) and is concurrent with oxidation of phenolic compounds such as flavan-3-ol monomers and procyanidins (Cadot *et al.*, 2006). Lignin polymerisation requires consumption of O_2 and generation of H_2O_2 for the final peroxidase reaction (Lee *et al.*, 2013), and this, with oxidation of tannins, could add additional stress to the mesocarp in seeded cultivars. Phenolic compounds can also act as ROS-scavengers (Blokhina *et al.*, 2003). In grape, biosynthesis of procyanidins coincide with the initial rapid period of growth (Coombe, 1973) and flavan-3-ol accumulated during early ripening (Cadot *et al.*, 2006). Taken together, seed respiration and maturation deserves consideration in understanding mesocarp CD.

In this study we test the hypothesis that hypoxia (i.e. below normoxia as 20.95% air [O_2] (Sasidharan *et al.*, 2017)) occurs within the grape berry during ripening and that this may be correlated with CD in the pericarp. We compared the patterns of CD and [O_2] profiles across the berry flesh of two wine, seeded cultivars, Chardonnay and Shiraz, and a seedless table grape cultivar, Ruby Seedless. Respiratory demand of seeds and berry were measured for different ripening stages and different temperatures. The diffusion pathway of O_2 supply was assessed through examination of the role of lenticels on the berry pedicel and air space estimates using X-ray micro-computed tomography (micro-CT) of single berries.

Materials and methods

Details of sources of berries, vine age, sampling times and corresponding measurements are listed in Table 1. Berries from the Waite Campus (34°58'04.8"S 138°38'07.9"E) vineyards were sampled over the 2014-2015, 2015-2016 and 2016-2017 seasons. Mature Shiraz, Chardonnay and Ruby Seedless vines on own roots were grown under standard vineyard management with vertical shoot positioning, spur pruned (two buds), and drip irrigation, on dark brown clay soils with shale fragments, grading into red-brown mottled clay; overlying olive-brown mottled cracking clay (Du Toit, 2005). Rows (3m spacing) were north-south oriented. Three replicates each consisted of 2 vines per replicate for Shiraz and 3 vines per replicate for Chardonnay. Ten random clusters (combination of proximal and distal) were labelled within each replicate and 20 berries (2 from each cluster, randomly located within the cluster) per replicate were excised at the pedicel-rachis junction with sharp scissors at each sampling date. Ruby Seedless grapes were sampled from three vines with 5 clusters labelled for sampling on each vine and 20 berries were sampled from each vine. Timing of sampling during berry development was measured as days after anthesis (DAA, 50% of caps fallen from flowers). Berries were placed in sealed plastic bags into a cooled container, and taken to the laboratory, stored at 4 °C in the dark, and tested within 48 hours of sampling.

Berries from pot-grown vines

Shiraz and Chardonnay cuttings were taken from the Waite vineyards in April 2015 and propagated after storage at 4 °C in the dark for approximately two weeks. Propagation method and vine nutrition management were based on Baby *et al.* (2014). Briefly, after roots were initiated in a heated sand bed in a 4 °C cold room for 8 weeks, and after the root length reached approximately 6 cm, cuttings were transferred into vermiculite: perlite (1:1) mixture in 12 cm pots. Pots were placed in a growth chamber with a 16 h photo-period, 400 μmol photons/(m^2·s) at the plant level, 27 °C day/ 22 °C night, and 50% humidity. Pots were

irrigated with half strength Hoagland solution (Baby *et al.*, 2014). Fruitful vines at stage EL-12 (Coombe, 1995) were then transferred into a University of California (UC) soil mix: 61.5 L sand, 38.5 L peat moss, 50 g calcium hydroxide, 90 g calcium carbonate and 100 g Nitrophoska® (12:5:1, N : P : K plus trace elements; Incitec Pivot Fertilisers, Southbank, Vic., Australia), per 100 L at pH 6.8, in 20 cm diameter (4 L) pots irrigated with water thereafter. Five berries (each from 3 different vines) of each cultivar were used for light stereomicroscopy.

Chardonnay rootlings were obtained from Yalumba Nursery in April 2017 and planted with UC mix soil and in the same growth chamber with the same growth conditions as above. Seven vines, each with one cluster, were used for O_2 diffusion experiments.

$[O_2]$ profiles in berries

Berry $[O_2]$ was measured using a Clark-type O_2 microelectrode with a tip diameter of 25 µm (OX-25; Unisense A/S, Aarhus, Denmark). The microelectrodes were calibrated in a zero O_2 solution (0.1M NaOH, 0.1M $C_6H_7NaO_6$) and an aerated Milli-Q water (272 µmol/L at 22 °C), as 100% O_2 solution. Individual berries (equilibrated to room temperature) were secured on the motorized micromanipulator stage. To aid the penetration of the microelectrode into the berry skin, the skin was pierced gently with a stainless-steel syringe needle (19G), to a depth of 0.2 mm, at the equator of the berry. The microsensor was positioned in the berry through this opening and $[O_2]$ profiles were taken with depth towards the centre of the berry. For Shiraz, measurements were taken from 0.2 mm to 1.5 mm under the skin at 0.1 mm increments. The electrode was not moved beyond this point to avoid damaging the tip against a seed. For Ruby Seedless where seeds were not present and Chardonnay grapes, where the position of the seeds could be determined through the semi-transparent skin, measurements were taken at 0.5 mm intervals from 0.2 mm under the skin to the berry centre. Each measurement was applied for a 10s duration at each depth. Between each position, a 20s

waiting time was applied to ensure stable signals. To test whether puncturing of the skin by the needle and insertion of the microelectrode contaminated the berry internal O_2 by the surrounding air, a plastic ring was placed around the insertion site and a gentle stream (250 mL/min) of nitrogen gas was applied to the insertion point while obtaining the O_2 readings (Fig 1A). These readings were compared to those where no nitrogen gas was applied.

The O_2 readings were recorded using the Unisense Suite software (Unisense A/S, Aarhus, Denmark). Three berries were measured for each biological replicate. Means and SE of each step (n = 3) were calculated and [O_2] profiles were compiled using GraphPad Prism 7 (GraphPad Software Inc., La Jolla, CA, USA). Following the O_2 measurements, berry temperature was recorded using an IR thermometer (Fluke 568, Fluke Australia Pty Ltd, NSW, Australia) with a type-K thermocouple bead probe (Fluke 80PK-1). Berry diameters at the equator were measured with a digital calliper. [O_2] and respiration (see below) were measured under dim room lighting, less than 1 μmol photon/(m^2·s). Berry vitality was determined (see below) and total soluble solids (TSS) of the juice from individual berries was determined using a digital refractometer (Atago, Tokyo, Japan) as an indicator of berry maturity.

Testing the role of pedicel lenticels

[O_2] was measured as above but with the probe stationary at approximately 2 mm from the pedicel along the berry central axis. After a stable reading was obtained N_2 gas (250 mL/min) was then applied over the pedicel in order to test the contribution of pedicel lenticels to O_2 diffusion into the berry.

Berry and seed respiratory O_2 consumption

A Clark-type oxygen microsensor OX-MR and the MicroRespiration System (Unisense A/S, Aarhus, Denmark) were used for berry and seed respiration measurements. A replicate

consisted of 9 berries. The measuring chamber was filled with aerated MilliQ water, constantly stirred and was maintained at 25°C in a water bath. After the measurement of whole berry respiration, seeds of the 9 berries were extracted and the seed respiration rate measured using the same apparatus. Changes in the chamber's water [O_2] were monitored for at least 15 mins, with readings taken every 5 seconds in order to determine a steady respiration rate from the slope of the decline in [O_2].

Respiration was also measured for Shiraz and Chardonnay berries before and after the pedicels were covered with silicone grease (SGM494 silicone grease, ACC Silicones Limited, Bridgewater, England), which was known to restrict berry pedicel water uptake (Becker *et al.*, 2012), at 20 and 40 °C. Another batch of 9 Chardonnay berries was used to determine the respiratory contribution of excised pedicels.

The temperature dependence of berry respiration was determined with a water bath held at 10 °C, 20 °C, 30 °C and 40 °C.

Pedicel lenticel density

The lenticel density of Chardonnay and Shiraz berry pedicels (stem and receptacle) was assessed using a Nikon SMZ 25 stereo microscope with CCD camera (Nikon Instruments Inc., Melville, NY, USA). Lenticel area (%) was estimated using ImageJ (Schneider *et al.*, 2012) by first adjusting the colour threshold of the image to separate the pedicel from the background and then the lenticels from the pedicel. Subsequently the ROI managing tool was used to estimate the relative area of the pedicels and the lenticels.

Long term effect of blocking pedicel lenticels

The pedicel of approximately half of the berries on each cluster of growth chamber grown Chardonnay were covered with silicone grease at the onset of ripening (first signs of berry softening). Two or three pairs of berries, each pair containing one covered and one uncovered

(control) pedicel from one plant, were randomly sampled throughout the course of the experiment at 3, 5, 7, 10, 12, 14 and 18 days after application. Profiles of berry O_2 concentration were measured as above, and berries were subsequently assessed for cell vitality (see below). Three pairs of berries were sampled 12 and 20 days after silicone application and assessed for internal ethanol concentration (see below).

Berry ethanol concentration

Individual berries were ground to a fine powder under liquid nitrogen. Ethanol was quantified using an Ethanol Assay kit following the manufacturer's instructions (Megazyme International Ireland Ltd., Wicklow, Ireland). Briefly, alcohol dehydrogenase (ADH) catalysed the oxidation of ethanol to acetaldehyde. Acetaldehyde was then further oxidized to acetic acid and NADH in the presence of aldehyde dehydrogenase (AL-DH) and NAD^+. NADH formation was measured in a FLUOstar Omega plate reader (BMG LABTECH GmbH, Ortenbery, Germany) at 340 nm.

Pericarp cell vitality estimation

Cell vitality was estimated using a fluorescein diacetate (FDA) staining procedure on the cut medial longitudinal surface of berries as detailed in (Fuentes *et al.*, 2010; Tilbrook and Tyerman, 2008). Images were analyzed with a MATLAB (Mathworks Inc., Natick, MA, USA) code for determining berry cell vitality (Fuentes *et al.*, 2010). Using ImageJ, the FDA fluorescence signal, across the radius at the equator were analysed. The correlation between $[O_2]$ and fluorescence signal at corresponding distances within Chardonnay and Ruby Seedless berries were examined. The fluorescence signal of growth chamber grown Chardonnay berries with/without pedicel covered was also analysed in this way.

Air spaces within the berry

Chardonnay berries were sampled during season 2015-2016 for micro-CT, where three berries, each from a different replicate, were used for each sampling time. Grapes were imaged with a Skyscan 1076 (Bruker micro-CT, Kontich, Belgium) at the micro-CT facility at Adelaide Microscopy, where whole berries (pedicel attached) had 2D projections acquired with 59 kV, 149 uA, Al 0.5 mm filter, 2356 ms exposure, 0.4-degree rotation step and 8.5 µm pixel size (equivalent to 15 µm spatial resolution or 3×10^{-6} mm^3 voxel size). NRecon (bruker-microct.com) was used for greyscale image reconstruction. Using CT-Analyer (bruker-microct.com), Otsu thresholding was applied to the volume and despeckle was applied to accept only continuous volume over 500 voxels as connected air spaces. 3D images of the internal air spaces were generated using CTVox (bruker-microct.com), colour rendering modules were used to distinguish the internal air volume from the berry volume. 3D models were then longitudinally sectioned to reveal the internal air space distribution. Quantitative analysis of internal porosity between the berry proximal region and the top (hilum) of the seed(s) was performed by manually selecting the volume of interest and accepting 500 voxels as air spaces.

Statistical analysis

All data are presented as mean ± SEM. Two-way ANOVA was used for: effect of O_2 sensor depth and applying N_2 gas at the point of sensor entry on [O_2], effect of O_2 sensor depth and ripening stage on [O_2], effect of temperature and covering lenticels on respiration, effect of temperature and grape maturity on respiratory Q_{10}, effect of covering lenticels and the duration of coverage on [O_2], TSS, sugar per berry, ethanol and living tissue profiles. Deming regression was used to determine the association between fluorescent intensity of FDA stain and [O_2]; this type of regression takes account of error in both x and y (Strike, 1991). T-test was used for differences in: respiration of berry and seed of Chardonnay at two ripening

stages, lenticel area on pedicels between Chardonnay and Shiraz, activation energy of O_2 uptake of Chardonnay and Shiraz berries, porosity and connectivity index in Chardonnay at two ripening stages. Rates of CD in lenticel covered berries and control berries were determined using linear regression.

Results

Internal oxygen profiles of grape berries

In Chardonnay, [O_2] decreased from the skin towards the interior of the mesocarp to reach low concentration at depths of 2.2 mm to 4 mm (Fig. 1). The minimum [O_2] over this depth range was 5.5 ± 5.5 µmol/L. However, with further penetration towards the central axis of the berry, [O_2] increased and reached a maximum at 7 mm depth (Fig. 1). To test if the [O_2] profiles were affected by introduced O_2 via the penetration site, N_2 gas was gently applied on to the entry point of the sensor during the measurements. The [O_2] profiles were similar for control and nitrogen-treated berries (Fig. 1) indicating that leakage through the site of penetration did not affect the recorded profiles.

Changes in internal oxygen profiles and progression of cell death during ripening

To determine if there was a link between the progression of CD and hypoxia within the berry, we determined CD using FDA staining and recorded [O_2] profiles on berries sampled on the same days. Similar [O_2] profiles were observed for Chardonnay and Ruby Seedless (Fig. 2A, C), and for Shiraz over the first 1.5 mm (Fig. 2E), but the [O_2] dropped more steeply across the skins as ripening progressed in all cultivars resulting in overall lower [O_2] across the berry. This was manifest as much lower minimum [O_2] at the last ripening stage sampled: Chardonnay 0 µmol/L, Ruby Seedless 14.9 ± 8.86 µmol/L, Shiraz 0 µmol/L. Because seeds could not be visualised in Shiraz berries the micro oxygen sensor could not be moved further

into the berry than about 1.6 mm without risking the integrity of the sensor (Fig. 2E). Nevertheless, it was clear that [O_2] dropped precipitously towards 1 mm (Fig. 2E).

Vitality staining (Fig. 2B, F) indicated that, for both Chardonnay and Shiraz, CD increased over time as TSS accumulated and occurred predominately in the middle of the mesocarp corresponding to the minimum in [O_2]. Further, the change in fluorescent signal intensity across the radius at the equator of Chardonnay berries showed a similar trend as for berry internal [O_2] (Fig. 3A), indicating a correlation between cell vitality and internal [O_2] (Fig. 3B). On the other hand, Ruby Seedless berries maintained cell vitality close to 100% up to 132 DAA, when TSS was 20.7 °Brix (Fig. 2D). While a similar shape of [O_2] profile was observed within the mesocarp of Ruby Seedless berries when compared with that of Chardonnay berries (Fig. 2C), [O_2] did not reach zero.

Despite the decrease in [O_2] across the mesocarp during ripening, for Chardonnay and Ruby Seedless berries, [O_2] started to increase with depth from about 4.2 mm and reached a maximum at around 6.2 mm in Chardonnay and 8.2 mm in the larger Ruby Seedless berries (Fig. 2A, C). Standardising the position of the sensor relative to the diameter of each berry replicate (Fig. 4), showed that [O_2] peaked at the central vascular bundle region at all sampling times for both Chardonnay (Fig. 4A) and Ruby Seedless (Fig. 4B).

Consumption and supply pathways of oxygen within grape berries

Considering the link between CD and [O_2] (Fig. 3), and the lack of CD in well-developed berries of Ruby Seedless (Fig. 2D), we investigated the contribution of seeds to the respiratory demand of the berry in Chardonnay. Seed fresh weight peaks at the beginning of sugar accumulation and skin coloration; this stage is termed veraison (Ristic and Iland, 2005) and was reached around 63 DAA for Chardonnay here. Seed respiration at this stage was 5-fold higher than whole berry respiration on a per gram fresh weight basis. Berry respiration

reduced by about a third at 122 DAA compared to 63 DAA (Fig. 5A), however seed respiration decreased by 40-fold (Fig. 5B). Berry mass nearly doubled from 7.2 ± 0.5 g at 63 DAA to 13.9 ± 1.4 g at 122 DAA, thus on a per berry basis, respiration rate increased by about 18% from 63 DAA to 122 DAA (Fig. 5C). The contribution from the total number of seeds in the berry accounted for more than half of the respiratory demand in berries at veraison. This dropped to an insignificant proportion at 122 DAA (Fig. 5C).

Differences in resistance to diffusion into the berry may influence the [O_2] profiles. The pedicel lenticels may offer a pathway for O_2 entry that could account for the higher concentration towards the central axis of the berry. There were obvious differences in lenticel morphology between Chardonnay (Fig. 6A) and Shiraz berries (Fig. 6B). Individual lenticels on Chardonnay pedicels were larger, and also had 10-fold larger total surface area as a proportion of pedicel surface area compared to that of Shiraz berries (Fig. 6C).

To determine whether lenticels on the pedicel could be sites for berry gas exchange, respiration was measured on the same batches of berries with or without pedicels covered with silicone grease to impede gas exchange. This was examined at 20 and 40 °C as respiratory demand for O_2 increases with temperature (Hertog *et al.*, 1998). Fig. 7A shows that covering the berry pedicel (and lenticels) with silicone grease decreased berry respiration at 40 ºC for both Shiraz and Chardonnay berries, but had no effect on respiration at 20 ºC. The temperature dependence of respiration was examined in more detail for Chardonnay and Shiraz with both yielding similar activation energies and Q_{10} (Supplementary Fig. S1, S2) that did not differ between berries sampled on the two days for each cultivar. The decreased apparent respiration of berries with the covered pedicel was not due to the elimination of pedicel respiration, because pedicel respiration rate at 40°C was a small fraction of the total berry respiration (Fig. 7B) and did not account for the decrease observed when pedicels were

covered (Fig. 7A), where the decrease in respiration of pedicel-covered Shiraz and Chardonnay at 40 °C was 839.7 ± 101.8 and 1233.9 ± 229.4 nmol/h per berry.

A rapid decrease in [O_2] was observed at approximately 2 mm away from pedicel and close to the centre axis in the Ruby Seedless berries, when a N_2 stream was activated over the pedicel (Fig. 8).

An experiment was subsequently conducted using growth chamber grown Chardonnay vines to test whether covering the pedicel lenticels of berries attached to the vine would affect internal [O_2] profiles. Three days after covering the berry pedicel with silicone grease, a reduction in [O_2] at the central vascular region occurred and remained near 0 μmol/L over the subsequent 15 days (Fig. 9A). For control berries, a maximum of [O_2] was evident at the central axis across all days of measurement. Concentration of total soluble solids increased with time during the course of this experiment, and was higher for lenticel covered berries (Fig. 9B). Sugar/berry was not affected by covering the lenticels (Fig. 9C). Ethanol concentration of berries was measured at 12 and 20 days after covering the pedicel lenticels. These berries, showed higher ethanol content compared to control berries (Fig. 9D), consistent with more fermentation within the hypoxic berries. Cell death was significantly increased by limiting oxygen diffusion after 10 days of covering the lenticels (Fig. 9E) and this was also evident from examination of transects across the berry (Fig. 9F).

Air spaces within the grape berry shown by micro computed tomography (micro-CT)

Using micro-CT, the internal air spaces of Chardonnay berries at two time points during ripening, where air spaces within the berry greater in total volume than 500 voxels (1.5×10^{-3} mm^3), are shown in Figure 10. Colour rendering highlighted air space within the berries for both post-veraison (98 DAA, Fig. 10A) and post-harvest (154 DAA, Fig. 10B) berries. Air spaces were connected to the pedicel in the post-veraison berry, but not obviously in the post-

harvest berry. It was evident that there were larger air spaces within the locule. Porosity, pores and channels, between berry proximal region to seed(s) hilum, did not differ between berries sampled on the two days (Supplementary Fig. S3).

Discussion

The mesocarp of seeded wine grape berries typically shows a type of programmed cell death associated with dehydration and flavour development late in ripening (Fuentes *et al.*, 2010; Bonada *et al.*, 2013a; Tilbrook and Tyerman, 2008). Here we show a close similarity between the pattern of CD across the berry mesocarp and [O_2] profiles where the central regions of the mesocarp had both the highest CD and the lowest [O_2]. In both Shiraz and Chardonnay the oxygen deficit in the centre of the mesocarp increased as ripening and cell death progressed, essentially becoming anoxic after about 100 days from anthesis under our experimental conditions. This contrasted to the seedless, table-grape cultivar where O_2 concentrations remained above about 15 μmol L^{-1} (1.1 kPa) in the mid region of the mesocarp, still considered to be hypoxic (Saglio *et al.*, 1988), where CD was less apparent. In our experimental system, however, only three cultivars were tested and there is a confounded effect between cultivar types (wine vs table) with different water and sugar dynamics (Sadras *et al.*, 2008) and between seeded and seedless types. Separating these effects would require the comparison of seeded and seedless isogenic lines. Nonetheless, the strong correlation between CD and [O_2] profiles, the role of lenticels, seed respiration, ethanol fermentation and CT-images all converge to support our working hypothesis that hypoxia in the mesocarp contributes to CD in the grape berry.

The minimum [O_2] we measured in the pericarp for both Chardonnay and Shiraz berries (close to zero) may be at or below the K_m for cytochrome C oxidase (0.14 μM) (Millar *et al.*, 1994), and very likely resulted in restricted oxidative phosphorylation and a shift to fermentation as evidenced by the detection of ethanol in Chardonnay berries; testing other

cultivars for ethanol production would be of interest. All aerobic organisms require O_2 for efficient ATP production through oxidative phosphorylation. Lower ATP production occurs under hypoxia when cells shift from oxidative phosphorylation to fermentation (Drew, 1997; Geigenberger, 2003; Ricard *et al.*, 1994). The depletion of ATP has profound consequences on cell physiology, including a change in energy consumption and cellular metabolism (Bailey-Serres and Chang, 2005; Drew, 1997). Loss of membrane integrity responsible for browning disorder in pears is also linked to internal hypoxia and low ATP levels (Franck *et al.*, 2007; Saquet *et al.*, 2003).

Survival of grape berry mitochondria after imposed anaerobiosis (based on succinate oxidation rates) is cultivar dependent with survival ranging from 1 to 10 days (Romieu *et al.*, 1992). This work was based on the process of carbonic maceration, a wine making procedure where whole berries ferment in an anaerobic atmosphere prior to crushing. Ethanol alters the respiratory quotient of grape mitochondria and uncouples oxidative phosphorylation (Romieu *et al.*, 1992). These effects occurred above 1% (vol) ethanol and well above the concentrations we measured in Chardonnay berries (0.015%); however, it is possible that there are locally high concentrations of ethanol within the berry in our case. In a later paper, alcohol dehydrogenase (ADH) activity and ADH RNA were found to be already high in field grown Chardonnay berries before anaerobiosis treatment, suggesting a hypoxic situation already existed in the grapes as a result of some stressful conditions in the field (Tesnière *et al.*, 1993). Our results show that this may be the norm for certain regions within the berry mesocarp and likely exacerbated by high temperature (see below).

The internal [O_2] of fruit depends on the respiratory demand, and the O_2 diffusion properties of the skin and internal tissues. These can show genotypic differences as is the case for apple fruit (Ho *et al.*, 2010). In pear fruit, differences in porosity of the cortex, the connectivity of intercellular spaces and cell distribution may account for variation between cultivars (Ho *et*

al., 2009). For pear it was possible to reconcile the observed variation in gas diffusion with the irregular microstructure of the tissue using a microscale model of gas diffusion. This also appears to be the case for different cultivars of apple as assessed by micro-CT (Mendoza *et al.*, 2007). For grape berries the [O_2] profiles in our study would suggest a very low O_2 diffusivity for the skin since a steep gradient occurred across the skin. Apple skin also showed a very low O_2 diffusivity and likewise a steep concentration gradient across the skin (Ho *et al.*, 2010). Since sub-skin [O_2] of grape berries declined dramatically during ripening for all three grape cultivars it would suggest a decline in O_2 diffusivity during ripening that may result from the same epidermal and cuticle structural changes that cause a decline in berry transpiration (Rogiers *et al.*, 2004).

Changing properties of the skin, berry porosity and lenticels in the pedicel may all contribute to the reduced internal [O_2] in grape berries during ripening. Fruit parenchyma can be regarded as a porous medium with air spaces distributed in between the elliptically tessellated cells (Gray *et al.*, 1999; Herremans *et al.*, 2015; Mebatsion *et al.*, 2006). A maximum [O_2] at the central axis region of both seeded and seedless berries throughout berry development, indicates a channel connecting the source of O_2 intake and the central vascular bundles. Using different approaches, including blockage of pedicel lenticels with silicone grease or applying of N_2 over pedicels, our experiments demonstrated that the pedicel lenticels are a major pathway for O_2 diffusion into the grape berry. This corresponds to the predominant air canals observed in micro-CT from the receptacle into the central axis of the berry. Micro-CT to study air space distributions in fruit can reveal important properties that affect gas diffusion (Herremans *et al.*, 2015; Mendoza *et al.*, 2010) as well as internal disorders (Lammertyn *et al.*, 2003). In our work the visualisation of air space connecting the pedicel with the locular cavity around seeds provides the structural link to the measured peaks in [O_2] around the central vascular region in the berries. This also confirmed the potential O_2 uptake

pathway through the pedicel lenticels, and distribution through the vascular networks. The relatively higher [O_2] around both central and peripheral vascular bundles may be important for maintaining phloem unloading in the berry, and it is interesting to note that even with severe CD in berries the vascular bundles generally remain vital (Fuentes *et al.*, 2010). Despite this we observed higher sugar concentrations in hypoxic berries that had their lenticels covered while still on the vine. This anomaly may be accounted for by decreased water influx because of hypoxia, thereby causing an increase in sugar concentration. Hypoxia is associated with reduced plasma membrane water permeability (Zhang and Tyerman, 1991) caused by closing of water channels of the plasma membrane intrinsic protein (PIP) family (Tournaire-Roux *et al.*, 2003). This is due to sensitivity to lowered cytosolic pH under hypoxia. A PIP aquaporin (*VvPIP2;1*) that is highly expressed in the ripening berry (Choat *et al.*, 2009) would be predicted to have reduced water permeation under hypoxia (Tournaire-Roux *et al.*, 2003) perhaps accounting for the decrease in whole berry hydraulic conductance that is consistently observed for Chardonnay and Shiraz (Scharwies and Tyerman, 2017; Tilbrook and Tyerman, 2009).

Lenticels are multicellular structures produced from phellogen that replace stomata after secondary growth (Lendzian, 2006). The impact of lenticels on gas and water permeance compared to periderm of stems has been measured for some species. For *Betula pendula*, the presence of lenticels substantially increased the water permeability of the periderm by between 26 and 53-fold (Schönherr and Ziegler, 1980). Lenticels on the berry pedicel are a preferential site for water uptake for submerged detached berries (Becker *et al.*, 2012). Water vapour and O_2 permeance of tree phellem with and without lenticels showed that lenticels increased O_2 permeance much more than that for water, over 1000-fold for one species, yet the permeance for water vapour was higher than that for O_2 (Groh *et al.*, 2002). Interestingly, Schönherr and Ziegler (1980) showed that as the water vapour activity declined (increased

vapour pressure deficit), water permeability was strongly reduced. If declining water vapour activity also reduced O_2 permeability in grape berry lenticels this could restrict O_2 diffusion under the very conditions where respiratory demand is increased, i.e. under water stress and with high temperature and vapour pressure deficit.

The decrease in $[O_2]$ at the approximate central axis in the seeded Chardonnay berry during development suggests there could be either an increase in respiratory demand, a decrease in the intake of O_2 via the pedicel lenticels or decreased porosity through the central proximal axis. Ruby Seedless berries on the other hand did not show this reduction. This indicates there could be structural differences in lenticels between the seeded wine grape cultivar and the seedless table grape, or that the seeds themselves become a significant O_2 sink (unlikely based on the arguments presented below). The lower lenticel surface area in Shiraz could be indicative of a greater restriction to O_2 diffusion compared to Chardonnay. Shiraz is well known for its earlier and more rapid increase in CD under warm conditions (Bonada *et al.*, 2013b; Fuentes *et al.*, 2010). Unfortunately, it was not possible for us to probe for $[O_2]$ in the central region of the Shiraz berry to compare with Chardonnay due to not being able to visualise seed position relative to the sensor in Shiraz berries. The role of the pedicel lenticels in allowing grape berries to "breathe" and their variation between cultivars seems to have been overlooked and appears to be unique amongst fruit. Cluster compactness and pedicel length could also affect the gas diffusion via this passage, ultimately resulting in differences in berry internal oxygen availability throughout ripening.

Another possible explanation for the difference in oxygen profiles between the seeded and seedless cultivars is that seeds are a significant O_2 sink late in ripening. Oxygen supply to seeds is essential for seed growth, and deposition of protein and oil (Borisjuk and Rolletschek, 2009). On the other hand, low $[O_2]$ within seeds favours low levels of ROS thus preventing cellular damage (Simontacchi *et al.*, 1995). The seeded wine grape cultivars

Riesling and Bastardo, increased O_2 uptake from less than 0.45 µmol/h per berry to approximately 3 µmol/h per berry during early ripening, contrasting to seedless Sultana where the maximum O_2 uptake was 1.5 µmol/h per berry (Harris *et al.*, 1971). We observed that total seed respiration was more than half of whole berry respiration at around the beginning of ripening. This high O_2 demand from seeds, prior to the lignification of the outer layer (Cadot *et al.*, 2006), may create a significant O_2 demand within the berry that could lower O_2 concentrations in the locule, and potentially lowering the [O_2] in the mesocarp. However, seed respiration in Chardonnay dramatically declined later in ripening, accounting for the decrease in berry respiration on a per gram basis. During late ripening, [O_2] in the mesocarp of the seeded cultivar dropped to almost zero. Therefore, it is unlikely that the lower [O_2] in the mesocarp was caused by a respiratory demand from seeds directly.

Increased temperature advances the onset and increases the rate of CD in Chardonnay and Shiraz berries (Bonada *et al.*, 2013b). Using a modelling approach for pear fruit it was shown that increasing temperature should strongly increase respiration rate but not to affect the gas diffusion properties resulting in predicted very low core [O_2] (Ho *et al.*, 2009). Our direct measures of berry mesocarp [O_2] profiles concur with this prediction. We also observed typical Q_{10} and activation energy for respiration of 2.47 and 2.27 for whole berry respiration rates between 10 and 40 ^{o}C for Chardonnay and Shiraz berries respectively, and it was only at 40 ^{o}C that blocking the pedicel lenticels reduced respiration. The activation energies were similar to those reported by Hertog *et al.* (1998) for apple (52875 J/mol), chicory (67139 J/mol) and tomato (67338 J/mol). Unlike pear fruit, wine-grape berries ripen on the plant and can become considerably hotter than the surrounding air (Caravia *et al.*, 2016; Smart and Sinclair, 1976; Tarara *et al.*, 2008). Transient high temperatures would create a large respiratory demand and low [O_2] in the centre of the mesocarp as we observed. However, subsequent cooling during the night or during milder weather will reduce the respiratory

demand and increase internal [O_2] if the diffusivity for O_2 remains the same. This could then result in production of damaging ROS that may cause unrecoverable cell damage (Pfister-Sieber and Braendle, 1994; Rawyler *et al.*, 2002).

Conclusion

Grape internal [O_2] declines during fruit development and is correlated with the profile of mesocarp cell death. Lenticels on the pedicel provide a pathway for O_2 diffusion into the berry and when covered to restrict O_2 diffusion into the berry cause a large reduction in [O_2] in the centre of the berry, an increase in ethanol concentration and cell death. Differences in internal O_2 availability of berries between cultivars could be associated with seed development and differences in lenticel surface area. The data presented here provides the basis for further research into the role of berry gas exchange on berry quality and cultivar selection for adapting viticulture to a warming climate.

Figures

Table 1. Summary of berry source and traits measured

Source of berries	Cultivar	Plant date	Season	Traits	Sampling time	Replication
Waite vineyards	Chardonnay	1995	2015-2016;	O_2 profile	87, 104, 136 DAA	3 reps, 3 berries per rep
				Berry and seed respiration	63, 122 DAA	
				Micro-CT	98, 154 DAA	3 reps, 1 berry per rep
			2016-2017	O_2 profile when N_2 applied	90 DAA	
				Respiration (lenticel blockage)	86 DAA	
				Respiration (temperature change)	76, 120 DAA	
	Shiraz	1993	2014-2015;	O_2 profile	85, 114 DAA	3 reps, 3 berries per rep
			2016-2017	Respiration (lenticel blocked)	77 DAA	
				Respiration (temperature change)	71, 113 DAA	
	Ruby seedless	1992	2016-2017	O_2 profile	91, 132 DAA	3 reps, 3 berries per rep
				O_2 logging	132 DAA	
Growth chamber, cuttings from Waite vineyard	Chardonnay	2015	2015	Lenticel	At veraison	5 berries
	Shiraz	2015	2015	Lenticel	At veraison	5 berries
Growth chamber, rootlings from Yalumba	Chardonnay	2017	2017	Lenticel blockage on vines (O_2, cell vitality, ethanol)	3, 5, 7, 10, 12, 14 18 and 20 days after blockage	2 or 3 berries

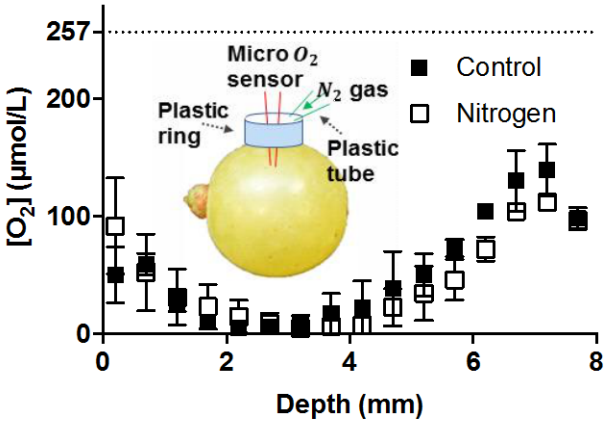

Fig. 1. [O_2] profiles of Chardonnay berries (90 DAA in season 2016-2017, Waite vineyards) measured with and without N_2 gas applied at the entry point during measurement. Inset: experimental set-up for measuring berry [O_2] profiles (not to scale). The O_2 sensor (tip diameter 25 µm) was inserted at the equator of the berry and moved inwards to the centre approximately across the radius. Around the entry of the sensor, a plastic ring was sealed and glued to the berry, to contain nitrogen gas gently flowing on to the entry point of the sensor. Data are means ± SEM, n=3. Two-way ANOVA (repeated measures) showed depth accounted for 68.73% of total variation (P<0.0001), treatments accounted for 0.55% of total variation (P=0.26) and interaction accounted for 3.72% of total variation (P=0.87).

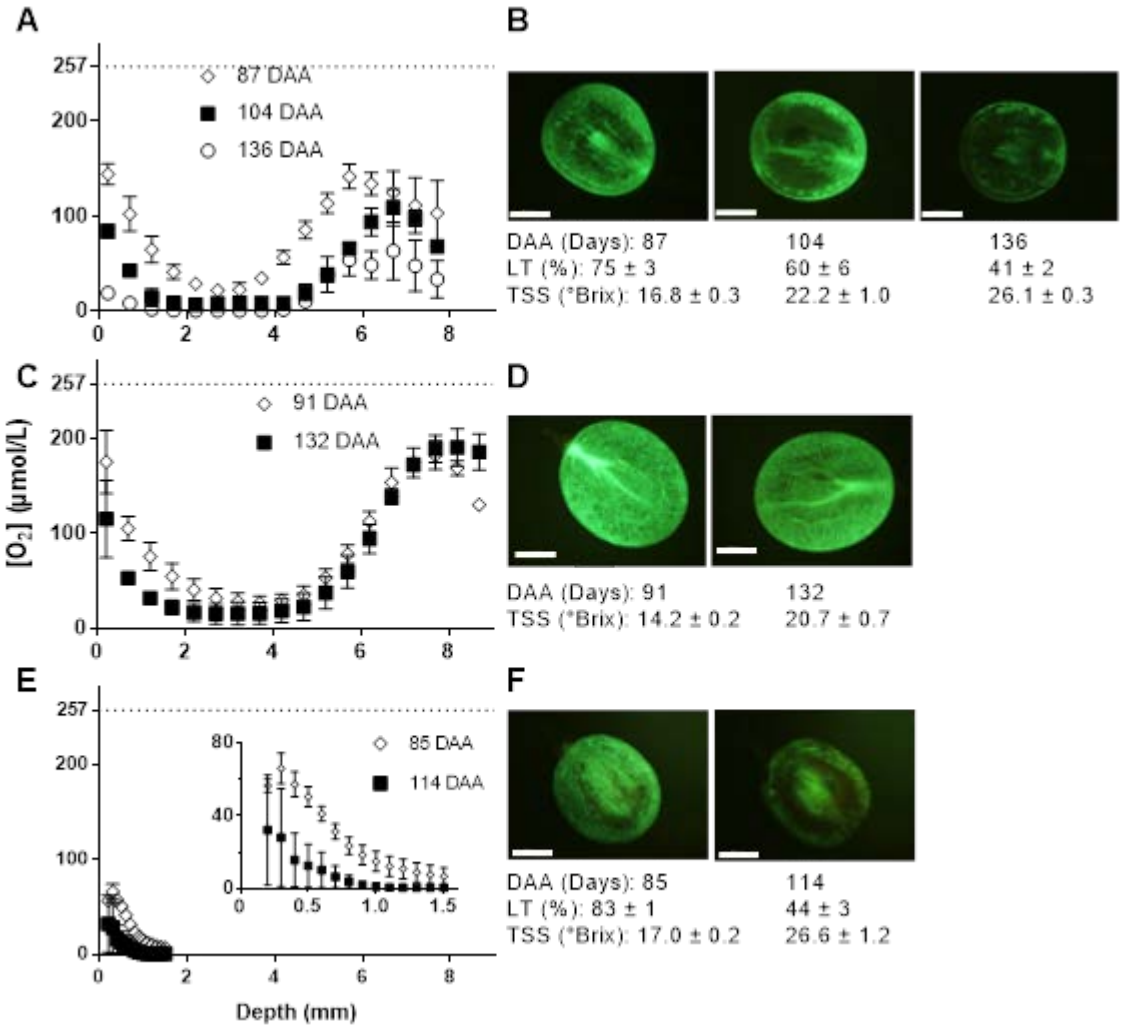

Fig. 2. [O_2] profiles of Chardonnay, Ruby Seedless and Shiraz berries (A,C,E) at various ripening stages and corresponding examples of living tissue (LT) in the pericarp for each variety (B,D,F). (A) Chardonnay berries were sampled at 87, 104 and 136 DAA in 2015-2016 season. Two-way ANOVA (repeated) showed depth accounted for 46.7% of total variation (P<0.0001), time accounted for 29.9% of total variation (P<0.0001) and interaction accounted for 8.0% of total variation (P=0.058). Horizontal dashed line indicates the approximate O_2 saturation value for Millipore water at room temperature, same as berries at the time of measurement. (B) Medial longitudinal sections (Chardonnay) stained with FDA hi-lighting LT differences at different stages of ripening (corresponding to A). (C) [O_2] profiles of Ruby Seedless berries sampled at 91 and 132 DAA in 2016-2017 season. Two-way ANOVA (repeated)

showed depth accounted for 85.2% of total variation (P<0.0001), time accounted for 1.2% of total variation (P=0.0025) and interaction accounted for 3.7% of total variation (P=0.048). (D) LT of Ruby Seedless was close to 100% for the two respective sampling days. (E) [O_2] profiles of Shiraz berries sampled on 85 and 114 DAA in 2014-2015 season. Inset shows detail of profile to 1.5 mm. Two-way ANOVA (repeated) showed depth accounted for 40.9% of total variation (P=0.0005), time accounted for 19.6% of total variation (P<0.0001) and interaction accounted for 6.4% of total variation (P=0.43). (F) LT of Shiraz. Data as means ± SEM, n=3 for A, C and E.

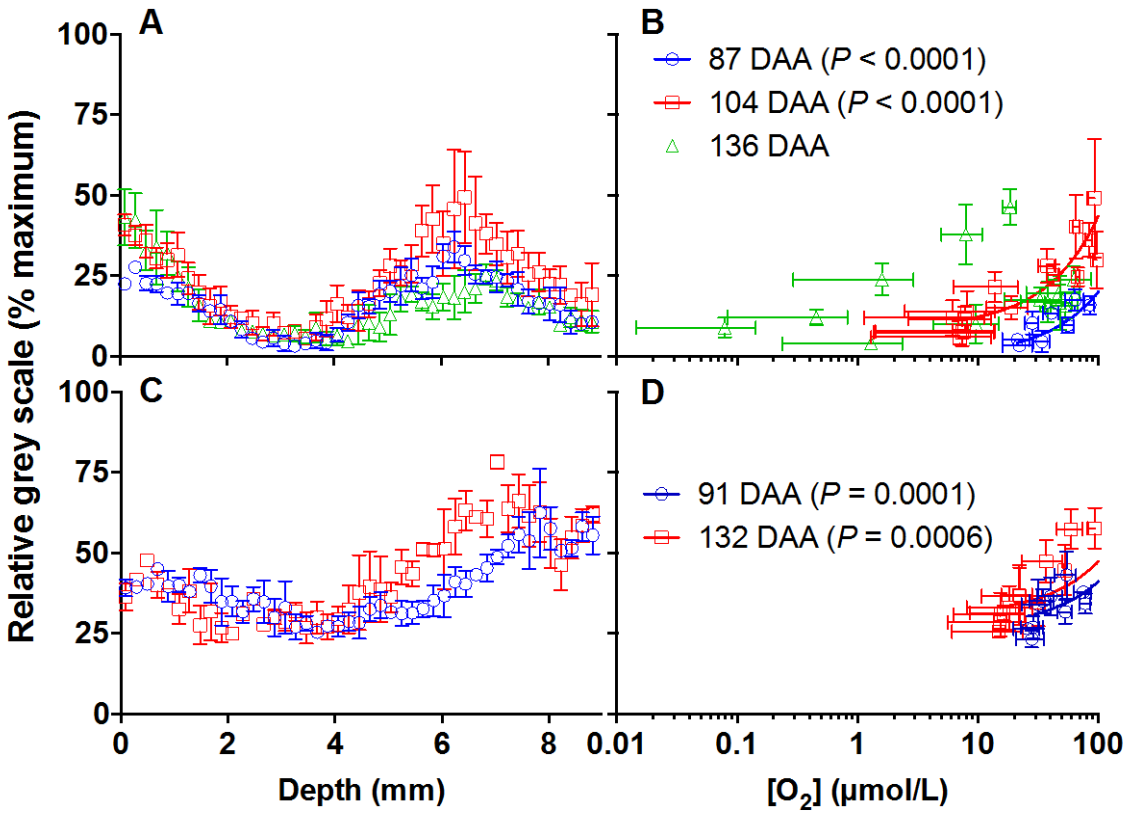

Fig. 3. Correlation between living tissue fluorescence signal and [O_2] profiles. Fluorescence signal (relative grey scale (% maximum)) from FDA stain (high value = higher living tissue) across radius at equator of Chardonnay (A) and Ruby Seedless (C). Correlation (Deming regression) between fluorescence signal intensity and [O_2] at corresponding depths (log scale) in Chardonnay on 87 and 104 DAA (B) and Ruby Seedless on 91 and 132 DAA (D) ([O_2] profiles shown in Fig. 1). Data are means ± SEM, n=3.

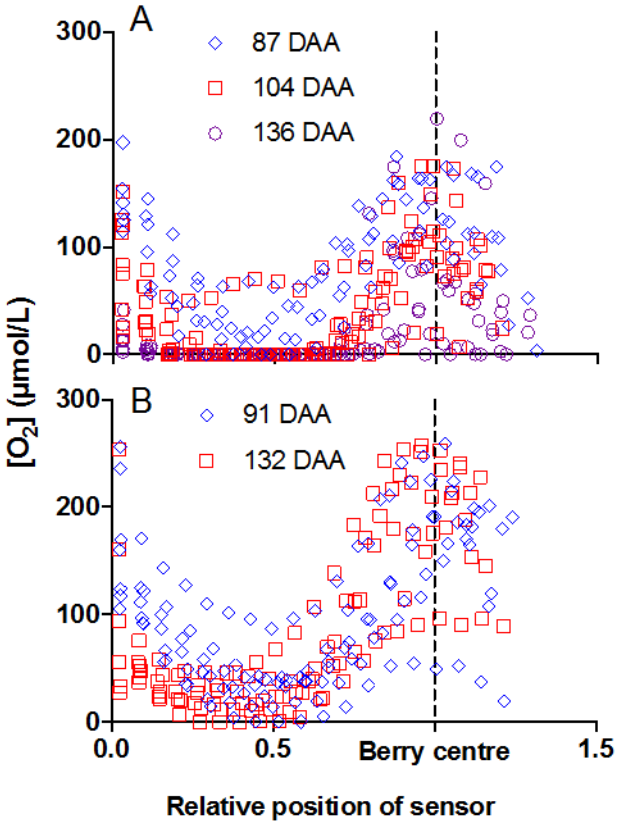

Fig. 4. Individual berry [O_2] profiles normalized to the berry radii. (A) [O_2] profiles of Chardonnay berries sampled at 87, 104 and 136 DAA in 2015-2016 season (Mean data shown in Fig. 2). (B) [O_2] profiles of individual Ruby Seedless berries sampled at 91 and 132 DAA in 2016-2017 season.

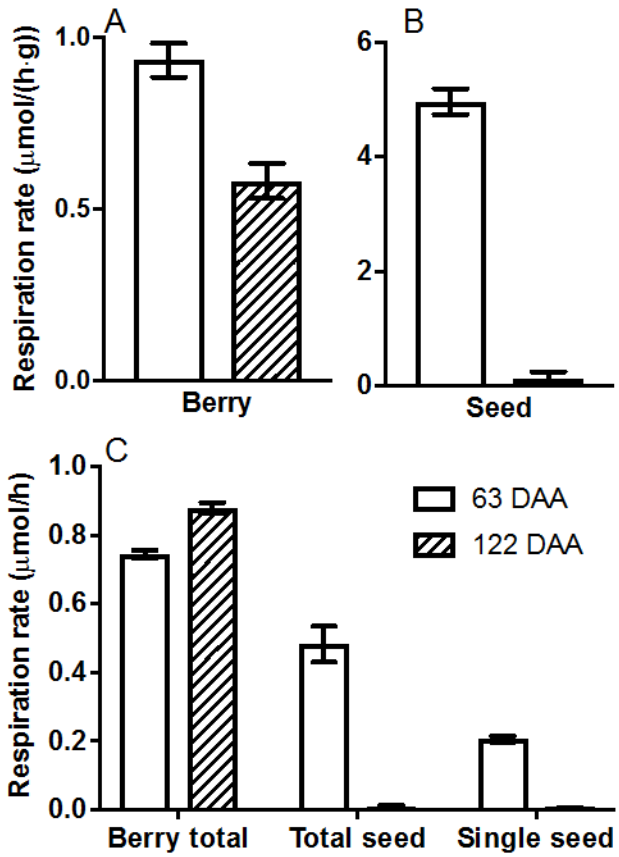

Fig. 5. Chardonnay berry and seed respiration (25 °C) at 63 and 122 DAA in 2015-2016 season. Respiration on a per gram fresh weight basis for berries (A) and seeds (B). (C) Comparison of respiration rates on a per berry basis (including seeds), total seeds basis, and single seed basis. Data are means ± SEM, n=3. All rates are different between 63 and 122 DAA (t-test, $P<0.05$).

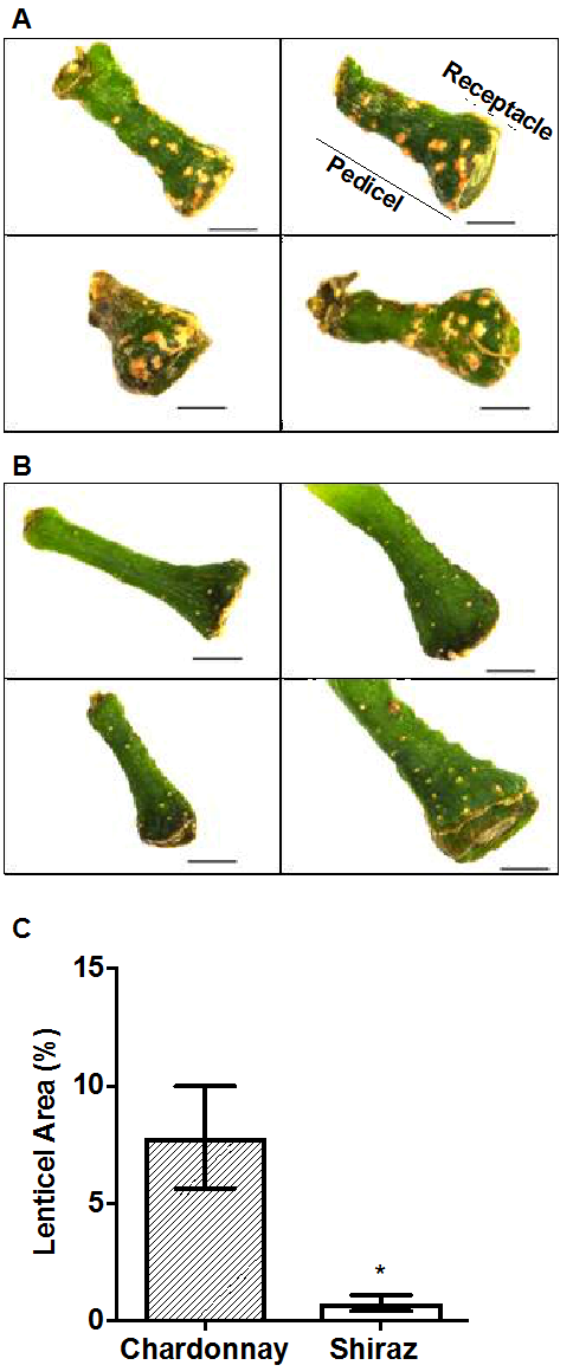

Fig. 6. Differences in lenticel morphology and relative lenticel area between Chardonnay (A) and Shiraz (B) berry pedicels. (C) Lenticel area relative to pedicel surface area of Chardonnay and Shiraz berries (chamber grown, 2015) estimated using ImageJ. Scale bars in A and B = 1mm. Data in C are means ± SEM, n=5, *=significantly different (t-test, $P< 0.05$).

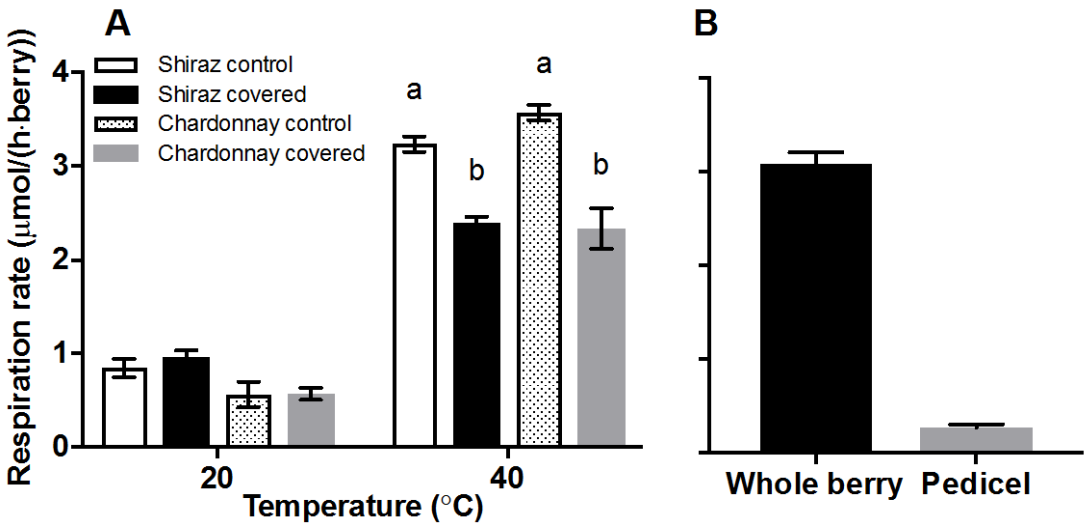

Fig. 7. Role of the pedicel in oxygen diffusion as a function of temperature. (A) Respiration of Chardonnay (86 DAA) and Shiraz (77 DAA) berries (per berry basis) at 20 and 40 °C with pedicels attached (2016-2017 season). Silicone grease covered the lenticels on the pedicel (covered berries). At 20°C no significant difference in apparent berry respiration was found between control and pedicel covered berries for both cultivars. Different lower-case letters indicate significant difference between treatments at 40°C within each cultivar (two-way ANOVA, $P<0.0001$). Shiraz and Chardonnay each showed a decrease of 839.7 ± 101.8 and 1377.3 ± 161.3 nmol/hour per berry in respiration at 40°C (26 and 39% decrease) respectively. (B) Respiration rate of whole berry including attached pedicel and respiration of separated pedicels for Chardonnay at 40°C. The pedicel accounted for 9% of the whole berry respiration rate. Data are means ± SEM, n=3.

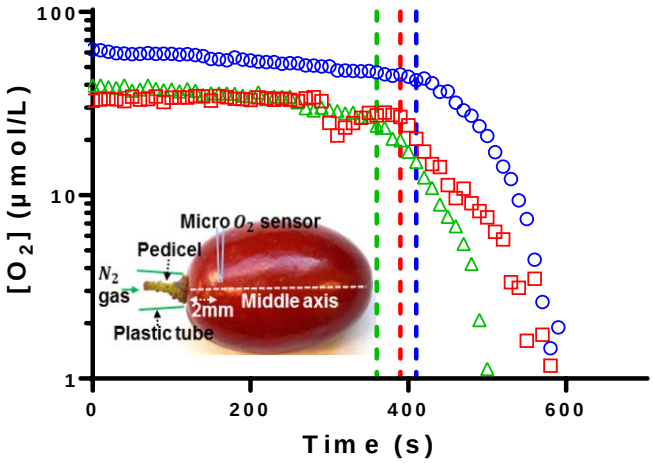

Fig. 8. The role of the pedicel in gas diffusion into Ruby Seedless grapes (132 DAA in 2016-2017 season). [O_2] of three individual berries as a function of time with the sensor inserted approximately at the central axis of Ruby Seedless around 2 mm from pedicel. Dashed lines indicate the start of external N_2 gas delivery over the pedicel. Different symbols indicate different berries. Inset: experimental set-up for applying N_2 gas over the berry pedicel while measuring [O_2].

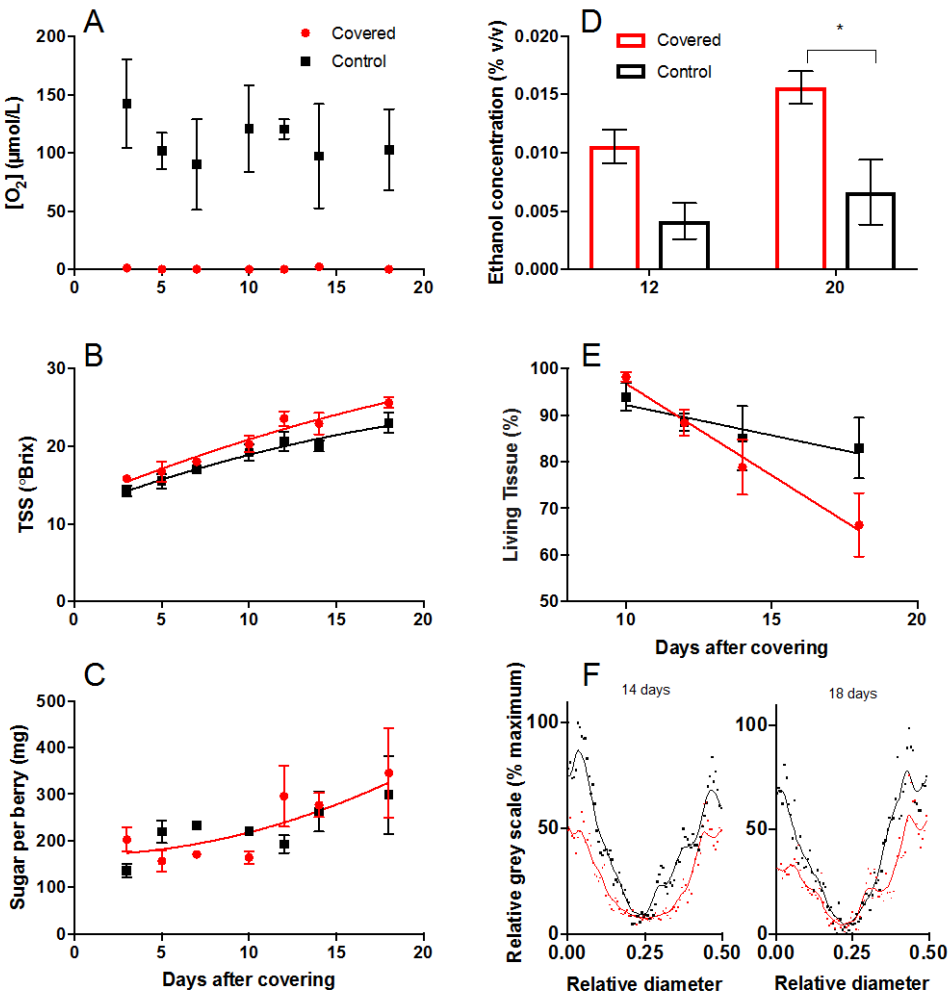

Fig. 9. The effect of covering berry pedicels with silicone grease on intact Chardonnay clusters during ripening (chamber grown 2017, black symbols=control, red symbols=covered). (A) $[O_2]$ at the approximate centre axis of berries as a function of time after covering pedicels. Two-way ANOVA showed covering pedicels reduced $[O_2]$ (P<0.0001). (B) Total soluble solids (TSS) concentration of berries as a function of time after covering pedicels. Pedicel covered berries showed significantly higher TSS during the course of the experiment compared to control berries (Two-way ANOVA P=0.003, fits are second order polynomials). (C) Sugar per berry as a function of time after covering pedicels. No significant difference was found between treatments in sugar/berry (combined fit is second order polynomial). (D) Ethanol concentration of berries after 12 and 20 days with (red) and without (black) silicone grease covering the pedicels. Two-way ANOVA (Tukey's multiple

comparisons test) showed significant difference at 20 days after covering (P=0.036). (E) Percentage living tissue as a function of time. Slope of fitted line for covered berries is non-zero (P=0.008) and different from slope of fitted line for uncovered berries (P=0.006). (F) Fluorescence signal (FDA stain, relative to maximum, high value = higher living tissue) across radius at equator normalised for variation in berry diameter at 14 and 18 days after covering. Locally weighted scatterplot smoothing fits (LOWESS) are shown for each. Covered versus control are significantly different at both times (Two-way ANOVA, P<0.001). Data are means ± SEM, n=3 except F where SEMs are not shown.

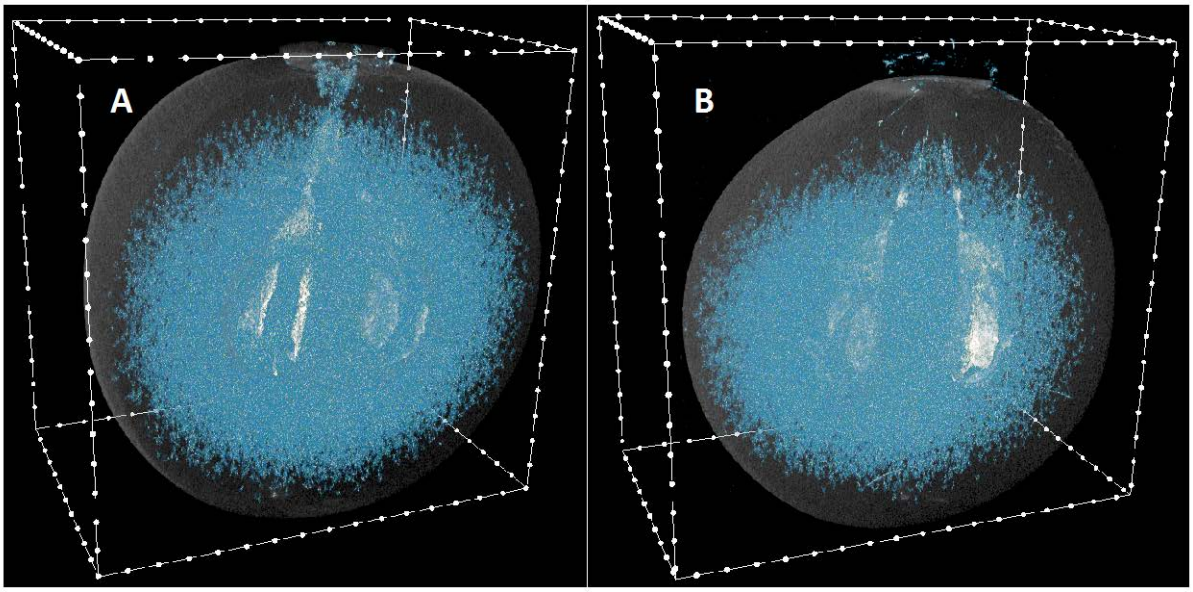

Fig. 10. Air spaces in Chardonnay berries as determined by X-ray micro-CT. (A) 98 DAA (19.3 °Brix), (B) 154 DAA (24.5 °Brix) in 2015-2016 season. Images have been manipulated to indicate berry outline. Minimum voxel cut-off was 500. White dots on box outline are at 1 mm intervals.

Supplementary materials

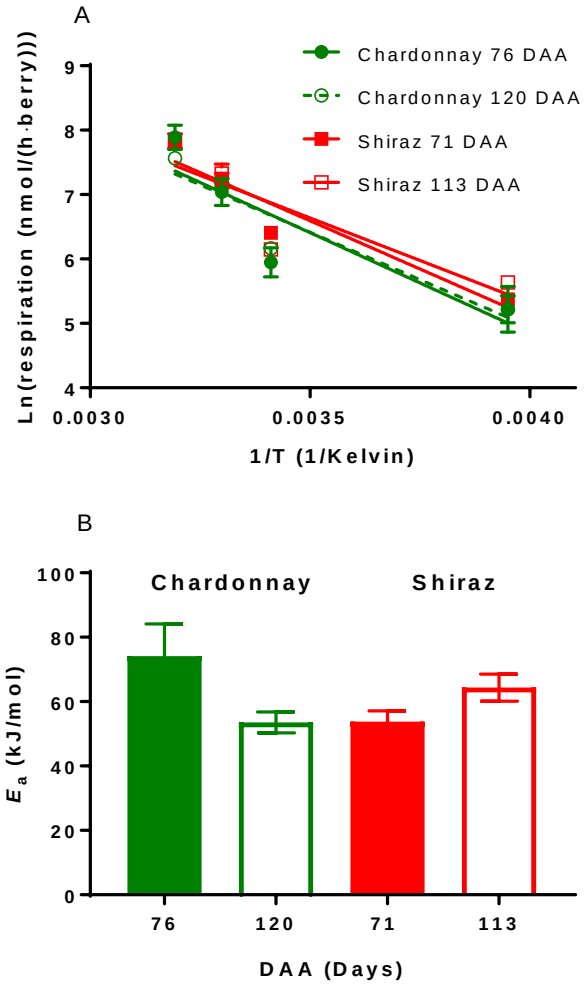

Supplementary Figure 1. Temperature dependence of berry respiration rate. Arrhenius plot of Chardonnay berries sampled on 76 and 120 DAA (11.2 ± 0.9 and 25.5 ± 0.1 °Brix), Shiraz berries sampled on 71 and 113 DAA (11.1 ± 0.4 and 26.2 ± 0.1 °Brix) in 2016-2017 season (A). Slopes (P=0.98) and intercepts (P=0.86) were similar between berries sampled, at the two times, within each cultivar. Activation energy of O_2 uptake by the berries (B). Error bars SEM (n=3).

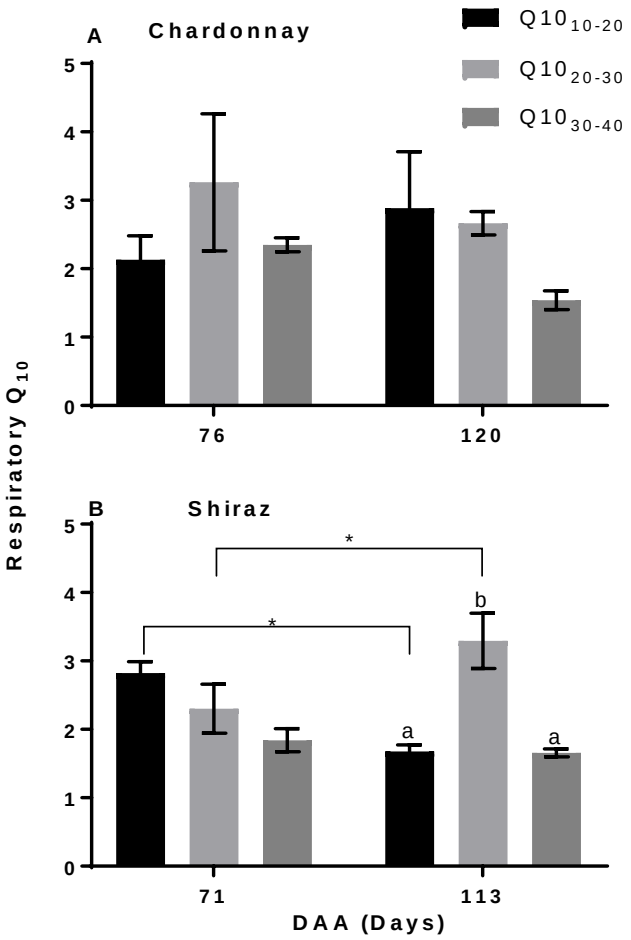

Supplementary Figure 2. Respiratory Q_{10} of Chardonnay (A) and Shiraz (B) in response to short-term measurement temperature and each at two maturity stages (2016-2017 season, Waite vineyards). No difference in the Q_{10} at different temperature classes for Chardonnay berries sampled within the two times were apparent. Q_{10} of Chardonnay berries, sampled at 76 and 120 DAA, at the same temperature classes did not differ from each other. For Shiraz berries sampled at 113 DAA, Q_{10} at 20-30 °C class was higher than the other two temperature classes, difference lower case letters indicate difference (Tukey's multiple comparisons test, $P<0.05$). At both temperature classes of 10-20 and 20-30 °C, Q_{10} were different between Shiraz berries sampled between 71 and 113 DAA, difference indicated by * (Sidak's multiple comparisons test, $P<0.05$). Error bars SEM (n=3).

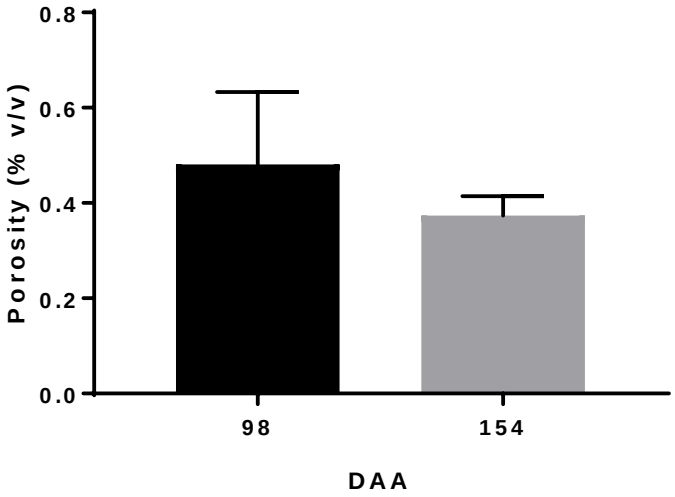

Supplementary Figure 3. Micro CT analysis of porosity, from berry proximal region to the top of seed(s) (hilum), of Chardonnay berries at two development stages (98 DAA, TSS = 18.7 ± 0.7 °Brix; 154 DAA, TSS = 26.8 ± 1.2 °Brix). Error bars SEM (n=3).

Literature cited

Alexander LV, Arblaster JM. 2009. Assessing trends in observed and modelled climate extremes over Australia in relation to future projections. *International Journal of Climatology* **29**, 417-435.

Baby T, Hocking B, Tyerman SD, Gilliham M, Collins C. 2014. Modified Method for Producing Grapevine Plants in Controlled Environments. *American Journal of Enology and Viticulture* **65**, 261-226.

Bailey-Serres J, Chang R. 2005. Sensing and Signalling in Response to Oxygen Deprivation in Plants and Other Organisms. *Annals of Botany* **96**, 507-518.

Becker T, Grimm E, Knoche M. 2012. Substantial water uptake into detached grape berries occurs through the stem surface. *Australian Journal of Grape and Wine Research* **18**, 109-114.

Blokhina O, Virolainen E, Fagerstedt KV. 2003. Antioxidants, oxidative damage and oxygen deprivation stress: a review. *Annals of Botany* **91**, 179-194.

Blokhina OB, Chirkova TV, Fagerstedt KV. 2001. Anoxic stress leads to hydrogen peroxide formation in plant cells. *Journal of Experimental Botany* **52**, 1179-1190.

Bonada M, Sadras V, Moran M, Fuentes S. 2013a. Elevated temperature and water stress accelerate mesocarp cell death and shrivelling, and decouple sensory traits in Shiraz berries. *Irrigation Science* **31**, 1317-1331.

Bonada M, Sadras VO. 2015. Review: critical appraisal of methods to investigate the effect of temperature on grapevine berry composition. *Australian Journal of Grape and Wine Research* **21**, 1-17.

Bonada M, Sadras VO, Fuentes S. 2013b. Effect of elevated temperature on the onset and rate of mesocarp cell death in berries of Shiraz and Chardonnay and its relationship with berry shrivel. *Australian Journal of Grape and Wine Research* **19**, 87-94.

Bondada B, Keller M. 2012. Not All Shrivels Are Created Equal—Morpho-Anatomical and Compositional Characteristics Differ among Different Shrivel Types That Develop during Ripening of Grape (Vitis vinifera L.) Berries *American Journal of Plant Sciences* **3**, 879-898.

Borisjuk L, Rolletschek H. 2009. The oxygen status of the developing seed. *New Phytologist* **182**, 17-30.

Bottcher C, Harvey KE, Boss PK, Davies C. 2013. Ripening of grape berries can be advanced or delayed by reagents that either reduce or increase ethylene levels. *Functional Plant Biology* **40**, 566-581.

Cadot Y, Minana-Castello MT, Chevalier M. 2006. Anatomical, histological, and histochemical changes in grape seeds from Vitis vinifera L. cv Cabernet franc during fruit development. *Journal of Agricultural and Food Chemistry* **54**, 9206-9215.

Caravia L, Collins C, Petrie PR, Tyerman SD. 2016. Application of shade treatments during Shiraz berry ripening to reduce the impact of high temperature. *Australian Journal of Grape and Wine Research* **22**, 422-437.

Caravia L, Collins C, Tyerman SD. 2015. Electrical impedance of Shiraz berries correlates with decreasing cell vitality during ripening. *Australian Journal of Grape and Wine Research* **21**, 430-438.

Choat B, Gambetta GA, Shackel KA, Matthews MA. 2009. Vascular Function in Grape Berries across Development and Its Relevance to Apparent Hydraulic Isolation. *Plant Physiology* **151**, 1677-1687.

Coombe BG. 1973. The regulation of set and development of the grape berry. International Society for Horticultural Science (ISHS), Leuven, Belgium, 261-274.

Coombe BG. 1995. Growth Stages of the Grapevine: Adoption of a system for identifying grapevine growth stages. *Australian Journal of Grape and Wine Research* **1**, 104-110.

Drew MC. 1997. Oxygen deficiency and root metabolism: Injury and acclimation under hypoxia and anoxia. *Annual Review of Plant Physiology and Plant Molecular Biology* **48**, 223-250.

Du Toit PG. 2005. The effect of partial rootzone drying on the partitioning of dry matter, carbon, nitrogen and inorganic ions of grapevines. PhD Thesis, The University of Adelaide, Australia.

Famiani F, Farinelli D, Palliotti A, Moscatello S, Battistelli A, Walker RP. 2014. Is stored malate the quantitatively most important substrate utilised by respiration and ethanolic fermentation in grape berry pericarp during ripening? *Plant Physiology and Biochemistry* **76**, 52-57.

Franck C, Lammertyn J, Ho QT, Verboven P, Verlinden B, Nicolaï BM. 2007. Browning disorders in pear fruit. *Postharvest Biology and Technology* **43**, 1-13.

Fuentes S, Sullivan W, Tilbrook J, Tyerman S. 2010. A novel analysis of grapevine berry tissue demonstrates a variety-dependent correlation between tissue vitality and berry shrivel. *Australian Journal of Grape and Wine Research* **16**, 327-336.

Fukao T, Bailey-Serres J. 2004. Plant responses to hypoxia - is survival a balancing act? *Trends in Plant Science* **9**, 449-456.

Geigenberger P. 2003. Response of plant metabolism to too little oxygen. *Current Opinion in Plant Biology* **6**, 247-256.

Gray JD, Kolesik P, Hoj PB, Coombe BG. 1999. Confocal measurement of the three-dimensional size and shape of plant parenchyma cells in a developing fruit tissue. *Plant Journal* **19**, 229-236.

Groh B, Hubner C, Lendzian KJ. 2002. Water and oxygen permeance of phellems isolated from trees: the role of waxes and lenticels. *Planta* **215**, 794-801.

Hardie WJ, O'Brien TP, Jaudzems VG. 1996. Morphology, anatomy and development of the pericarp after anthesis in grape, Vitis vinifera L. *Australian Journal of Grape and Wine Research* **2**, 97-142.

Harris J, Kriedemann P, Possingham J. 1971. Grape berry respiration: effects of metabolic inhibitors. *Vitis* **9**, 291-298.

Herremans E, Verboven P, Verlinden BE, Cantre D, Abera M, Wevers M, Nicolaï BM. 2015. Automatic analysis of the 3-D microstructure of fruit parenchyma tissue using X-ray micro-CT explains differences in aeration. *BMC Plant Biology* **15**, 264.

Hertog MLATM, Peppelenbos HW, Evelo RG, Tijskens LMM. 1998. A dynamic and generic model of gas exchange of respiring produce: the effects of oxygen, carbon dioxide and temperature. *Postharvest Biology and Technology* **14**, 335-349.

Ho QT, Verboven P, Mebatsion HK, Verlinden BE, Vandewalle S, Nicolai BM. 2009. Microscale mechanisms of gas exchange in fruit tissue. *New Phytologist* **182**, 163-174.

Ho QT, Verboven P, Verlinden BE, Schenk A, Delele MA, Rolletschek H, Vercammen J, Nicolai BM. 2010. Genotype effects on internal gas gradients in apple fruit. *Journal of Experimental Botany* **61**, 2745-2755.

Keller M, Shrestha PM. 2014. Solute accumulation differs in the vacuoles and apoplast of ripening grape berries. *Planta* **239**, 633-642.

Keller M, Shrestha PM, Hall GE, Bondada BR, Davenport JR. 2016. Arrested Sugar Accumulation and Altered Organic Acid Metabolism in Grape Berries Affected by Berry Shrivel Syndrome. *American Journal of Enology and Viticulture* **67**, 398-406.

Krasnow M, Matthews M, Shackel K. 2008. Evidence for substantial maintenance of membrane integrity and cell viability in normally developing grape (Vitis vinifera L.) berries throughout development. *Journal of Experimental Botany* **59**, 849-859.

Kriedemann P. 1968. Observations on gas exchange in the developing Sultana berry. *Australian Journal of Biological Sciences* **21**, 907-916.

Lammertyn J, Dresselaers T, Van Hecke P, Jancsok P, Wevers M, Nicolai BM. 2003. Analysis of the time course of core breakdown in 'Conference' pears by means of MRI and X-ray CT. *Postharvest Biology and Technology* **29**, 19-28.

Lee Y, Rubio MC, Alassimone J, Geldner N. 2013. A Mechanism for Localized Lignin Deposition in the Endodermis. *Cell* **153**, 402-412.

Lendzian KJ. 2006. Survival strategies of plants during secondary growth: barrier properties of phellems and lenticels towards water, oxygen, and carbon dioxide. *Journal of Experimental Botany* **57**, 2535-2546.

Mebatsion H, Verboven P, Ho Q, Verlinden B, Mendoza F, Nguyen T, Nicolaï B. 2006. Modeling fruit microstructure using an ellipse tessellation algorithm. *13th World Congress of Food Science & Technology 2006*, 246-246.

Mendoza F, Verboven P, Ho QT, Kerckhofs G, Wevers M, Nicolai B. 2010. Multifractal properties of pore-size distribution in apple tissue using X-ray imaging. *Journal of Food Engineering* **99**, 206-215.

Mendoza F, Verboven P, Mebatsion HK, Kerckhofs G, Wevers M, Nicolai B. 2007. Three-dimensional pore space quantification of apple tissue using X-ray computed microtomography. *Planta* **226**, 559-570.

Millar A, Bergersen F, Day D. 1994. Oxygen affinity of terminal oxidases in soybean mitochondria. *Plant Physiology and Biochemistry* **32**, 847-852.

Ollat N, Gaudillère J. 1997. Carbon balance in developing grapevine berries. *V International Symposium on Grapevine Physiology* Vol. 526, 345-350.

Palliotti A, Cartechini A. 2001. Developmental changes in gas exchange activity in flowers, berries, and tendrils of field-grown Cabernet Sauvignon. *American Journal of Enology and Viticulture* **52**, 317-323.

Perkins SE, Alexander LV, Nairn JR. 2012. Increasing frequency, intensity and duration of observed global heatwaves and warm spells. *Geophysical Research Letters* **39**, n/a-n/a.

Pfister-Sieber M, Braendle R. 1994. Aspects of plant behaviour under anoxia and post-anoxia. *Proceedings of the Royal Society of Edinburgh, Section B: Biological Sciences* **102**, 313-324.

Pilati S, Brazzale D, Guella G, Milli A, Ruberti C, Biasioli F, Zottini M, Moser C. 2014. The onset of grapevine berry ripening is characterized by ROS accumulation and lipoxygenase-mediated membrane peroxidation in the skin. *BMC Plant Biology* **14**, 87.

Rawyler A, Arpagaus S, Braendle R. 2002. Impact of oxygen stress and energy availability on membrane stability of plant cells. *Annals of Botany* **90**, 499-507.

Ricard B, Couée I, Raymond P, Saglio PH, Saint-Ges V, Pradet A. 1994. Plant metabolism under hypoxia and anoxia. *Plant Physiology and Biochemistry* **32**, 1-10.

Ristic R, Iland PG. 2005. Relationships between seed and berry development of Vitis Vinifera L. cv Shiraz: Developmental changes in seed morphology and phenolic composition. *Australian Journal of Grape and Wine Research* **11**, 43-58.

Rogiers SY, Hatfield JM, Jaudzems VG, White RG, Keller M. 2004. Grape Berry cv. Shiraz Epicuticular Wax and Transpiration during Ripening and Preharvest Weight Loss. *American Journal of Enology and Viticulture* **55**, 121-127.

Romieu C, Tesniere C, Than-Ham L, Flanzy C, Robin J-P. 1992. An examination of the importance of anaerobiosis and ethanol in causing injury to grape mitochondria. *American Journal of Enology and Viticulture* **43**, 129-133.

Sadras V, Collins M, Soar C. 2008. Modelling variety-dependent dynamics of soluble solids and water in berries of Vitis vinifera. *Australian Journal of Grape and Wine Research* **14**, 250-259.

Sadras VO, McCarthy MG. 2007. Quantifying the dynamics of sugar concentration in berries of Vitis vinifera cv. Shiraz: a novel approach based on allometric analysis. *Australian Journal of Grape and Wine Research* **13**, 66-71.

Saglio PH, Drew MC, Pradet A. 1988. Metabolic acclimation to anoxia induced by low (2-4 kPa partial pressure) oxygen pretreatment (hypoxia) in root tips of Zea mays. *Plant Physiology* **86**, 61-66.

Saquet AA, Streif J, Bangerth F. 2003. Energy metabolism and membrane lipid alterations in relation to brown heart development in 'Conference' pears during delayed controlled atmosphere storage. *Postharvest Biology and Technology* **30**, 123-132.

Sasidharan R, Bailey-Serres J, Ashikari M, Atwell BJ, Colmer TD, Fagerstedt K, Fukao T, Geigenberger P, Hebelstrup KH, Hill RD, Holdsworth MJ, Ismail AM, Licausi F, Mustroph A, Nakazono M, Pedersen O, Perata P, Sauter M, Shih MC, Sorrell BK, Striker GG, van Dongen JT, Whelan J, Xiao S, Visser EJW, Voesenek L. 2017. Community recommendations on terminology and procedures used in flooding and low oxygen stress research. *New Phytologist* **214**, 1403-1407.

Scharwies JD, Tyerman SD. 2017. Comparison of isohydric and anisohydric Vitis vinifera L. cultivars reveals a fine balance between hydraulic resistances, driving forces and transpiration in ripening berries. *Functional Plant Biology* **44**, 324-338.

Schneider CA, Rasband WS, Eliceiri KW. 2012. NIH Image to ImageJ: 25 years of image analysis. *Nature methods* **9**, 671-675.

Schönherr J, Ziegler H. 1980. Water permeability of Betula periderm. *Planta* **147**, 345-354.

Simontacchi M, Caro A, Puntarulo S. 1995. Oxygen-dependent increase of antioxidants in soybean embryonic axes. *The International Journal of Biochemistry & Cell Biology* **27**, 1221-1229.

Smart RE, Sinclair TR. 1976. Solar heating of grape berries and other spherical fruits. *Agricultural Meteorology* **17**, 241-259.

Strike PW. 1991. Chapter 8 - Measurement and control. *Statistical Methods in Laboratory Medicine*: Butterworth-Heinemann, 254-306.

Šuklje K, Zhang X, Antalick G, Clark AC, Deloire A, Schmidtke LM. 2016. Berry Shriveling Significantly Alters Shiraz (Vitis vinifera L.) Grape and Wine Chemical Composition. *Journal of Agricultural and Food Chemistry* **64**, 870-880.

Tarara JM, Lee J, Spayd SE, Scagel CF. 2008. Berry Temperature and Solar Radiation Alter Acylation, Proportion, and Concentration of Anthocyanin in Merlot Grapes. *American Journal of Enology and Viticulture* **59**, 235-247.

Terrier N, Romieu C. 2001. Grape berry acidity. . In: Roubelakis-Angelakis KA, ed. *Molecular Biology & Biotechnology of the Grapevine*: Springer Netherlands, 35-57.

Tesnière CM, Romieu C, Vayda ME. 1993. Changes in the Gene Expression of Grapes in Response to Hypoxia. *American Journal of Enology and Viticulture* **44**, 445-451.

Tilbrook J, Tyerman SD. 2008. Cell death in grape berries: varietal differences linked to xylem pressure and berry weight loss. *Functional Plant Biology* **35**, 173-184.

Tilbrook J, Tyerman SD. 2009. Hydraulic connection of grape berries to the vine: varietal differences in water conductance into and out of berries, and potential for backflow. *Functional Plant Biology* **36**, 541-550.

Tournaire-Roux C, Sutka M, Javot H, Gout E, Gerbeau P, Luu DT, Bligny R, Maurel C. 2003. Cytosolic pH regulates root water transport during anoxic stress through gating of aquaporins. *Nature* **425**, 393-397.

Voesenek L, Colmer TD, Pierik R, Millenaar FF, Peeters AJM. 2006. How plants cope with complete submergence. *New Phytologist* **170**, 213-226.

Webb LB, Whetton PH, Barlow EWR. 2007. Modelled impact of future climate change on the phenology of winegrapes in Australia. *Australian Journal of Grape and Wine Research* **13**, 165-175.

Wigginton MJ. 1973. Diffusion of oxygen through lenticels in potato tuber. *Potato Research* **16**, 85-87.

Zhang W, Tyerman S. 1991. Effect of low O2 concentration and azide on hydraulic conductivity and osmotic volume of the cortical cells of wheat roots. *Functional Plant Biology* **18**, 603-613.

Chapter 3 Effect of water stress and elevated temperature on hypoxia and cell death in the mesocarp of Shiraz berries

Manuscript submitted on 2 February 2018, to Australian Journal of Grape and Wine Research. AJGWR-18-015

Statement of authorship

Statement of Authorship

Title of Paper	Effect of water stress and elevated temperature on hypoxia and cell death in the mesocarp of Shiraz berries
Publication Status	☐ Published ☐ Accepted for Publication ☑ Submitted for Publication ☐ Unpublished and Unsubmitted work written in manuscript style
Publication Details	Submitted to Australian Journal of Grape and Wine Research 2/2/2018

Principal Author

Name of Principal Author (Candidate)	Zeyu Xiao
Contribution to the Paper	ZX contributed to experimental design and performed experiments, analysed the data and drafted the manuscript.
Overall percentage (%)	80%
Certification:	This paper reports on original research I conducted during the period of my Higher Degree by Research candidature and is not subject to any obligations or contractual agreements with a third party that would constrain its inclusion in this thesis. I am the primary author of this paper.
Signature	Date 1/2/2018

Co-Author Contributions

By signing the Statement of Authorship, each author certifies that:

i. the candidate's stated contribution to the publication is accurate (as detailed above);

ii. permission is granted for the candidate in include the publication in the thesis; and

iii. the sum of all co-author contributions is equal to 100% less the candidate's stated contribution.

Name of Co-Author	Suzy Y. Rogiers
Contribution to the Paper	Contributed to experimental design, co-supervised the research and editing the manuscript.
Signature	Date 1/2/2018

Name of Co-Author	Victor O. Sadras
Contribution to the Paper	Contributed to experimental design, co-supervised the research, assisted in analysing the data and editing the manuscript.
Signature	Date 1-Feb-18

Name of Co-Author	Siyang Liao		
Contribution to the Paper	Contributed to experimental design, field measurements and sample collection.		
Signature		Date	31/1/2018

Name of Co-Author	Stephen D. Tyerman		
Contribution to the Paper	Contributed to experimental design, supervised the research, assisted in analysing the data and editing the manuscript.		
Signature		Date	31/1/2018

Abstract

Background and aim: Berry shrivel during ripening is cultivar dependent and is correlated with berry cell death (CD). We hypothesized that under heat stress and water stress, regions of the pericarp in Shiraz berries would become hypoxic depending on berry porosity, and that this would induce CD.

Methods and Results: We measured CD and [O_2] across the pericarp in berries developed under the factorial combination of two thermal regimes (ambient and heated) and two irrigation regimes (irrigated and non-irrigated) in the Barossa Valley, South Australia. Heating increased ambient temperature by 0.6 °C for irrigated and 1 °C for non-irrigated vines but had no effect on water relations, while non-irrigation decreased stomatal conductance and stem water potential. Non-irrigation decreased berry [O_2] and increased both cell death and ethanol concentration relative to irrigation. An association was established between mesocarp [O_2] and CD. Berry respiration and total berry porosity decreased during berry ripening, but relative locule air-space measured by X-ray micro computed tomography increased late in ripening. Heating had little or no effect on CD or [O_2] but decreased berry porosity, which was not affected by irrigation.

Conclusion: Water stress increased berry CD, which was associated with increased hypoxia.

Significance of the Study: The association between berry [O_2] and CD provides insights in to berry ripening with implications for yield and berry flavour.

Keywords*: berry ripening, cell death, hypoxia, Vitis vinifera, water stress, heat*

Introduction

Vitis vinifera berry ripening in warm climates is sometimes associated with berry dehydration or shrivel. Increasing frequencies and intensities of heat waves and drought events with climate change (Alexander and Arblaster 2009, Perkins et al. 2012) are predicted to have adverse effects on grapevines (Bonada and Sadras 2015, Caravia et al. 2016, Webb et al. 2007) and frequency of shrivel is likely to increase (Bonada et al. 2013a, Fuentes et al. 2010a). Berry shrivel is particularly prevalent in Shiraz, where yield can be reduced by up to 30% (McCarthy 1997) and sensory and chemical composition of grapes and wine are altered (Bonada et al. 2013b, Šuklje et al. 2016). The phenomenon results from an imbalance between phloem influx to the berry (Rogiers et al. 2006), water back flow to the vine (Bondada *et al.* 2005, Keller *et al.* 2006, Tilbrook and Tyerman 2009,Tyerman *et al.* 2004) and berry transpiration (Greer and Rogiers 2009, Scharwies and Tyerman 2017). Dehydration and shrivelling can increase berry sugar concentration (Caravia et al. 2016, Rogiers et al. 2004b) leading to higher alcohol in the wine.

The onset of berry dehydration coincides with the occurrence of mesocarp cell death (CD) (Tilbrook and Tyerman 2008), which is modulated by water and temperature (Bonada et al. 2013b). The association between CD and berry shrinkage is evident in several wine grape cultivars (Fuentes et al. 2010b). The increase in CD indicates reduced lipid and membrane integrity and leakage of electrolytes from cells. This is evident as a decrease in extracellular electrical resistance of Shiraz berries during ripening (Caravia et al. 2015) that may be due to potassium leakage into the extracellular space as occurs in Merlot (Keller and Shrestha 2014). More importantly, CD involves breakdown of membranes and mixing of cellular components that are normally separated, thereby potentially influencing flavour development of wine grapes (Bonada et al. 2013b, Tilbrook and Tyerman 2008). Anecdotally, a small amount of late ripening dehydration sometimes favours flavour development in red wine berries. Berry

shrivel and CD are also correlated with ripe fruit sensory characteristics (Bonada et al. 2013b).

High temperature and water stress accelerate CD in Shiraz berries (Bonada et al. 2013b). Higher antioxidant activities are common in water stressed leaves indicative of oxidative stress (Flexas et al. 2006) and elevated temperature increases respiration in grapevine leaves (Zufferey 2016) and berries (Xiao et al. 2018). The increased demand for oxygen at high temperature or under water stress may induce hypoxic regions in the pericarp of berries depending on the diffusion resistance through the skin and air spaces (porosity) that connect to lenticels in the berry pedicel (Xiao et al. 2018). Xiao et al. (2018) showed that the pattern of mesocarp cell death correlated with hypoxic regions in Chardonnay and hypoxia was associated with CD late in ripening. Therefore, we hypothesized that under heat stress and water stress, regions of the pericarp in Shiraz grape berries would become hypoxic depending on berry porosity, and that this would induce CD. Hypoxic regions should lead to fermentation that will be reflected by elevated ethanol concentrations in the berry (Xiao et al. 2018). Here we examined the oxygen concentration profiles and CD across the pericarp of Shiraz berries during ripening under field conditions with treatments that induced water stress and elevated ambient temperature over two seasons. Berry porosity during ripening was measured using pycnometry and X-ray micro computed tomography (CT) to examine the potential for treatment induced changes in gas diffusion resistance within the berry. The goal of this study was to better characterize the physiological cause of CD late in ripening and its response to water and heat stress.

Materials and methods

Experimental site, vines and treatments

Shiraz vines (clone 1654) on own roots planted in 2004 were studied over two seasons (season 1, 2014-2015; season 2, 2015-2016) at the South Australian Research and

Development Institute, Nuriootpa Research Station in the Barossa Valley of South Australia (34°28'32.9"S 139°00'27.4"E). Vines were spur pruned to 40-50 buds per vine and trained to a single-wire trellis. Rows were oriented northwest to southeast. Row spacing was 3.0 m and vine spacing was 2.25 m.

This study was set up in an experiment established in 2010. It combined two water regimes (irrigated, I; non-irrigated, NI), and two thermal regimes (ambient, A; heated, H). An open-top chamber was used to passively heat vines, as described in Sadras et al. (2012). A split-plot design with three replicates was established where thermal regime was assigned to main plot, and water regime to subplots. Each replicate contained nine vines and seven centrally located vines were used for berry sampling. A guard row was also left on each side of the treated vines to minimise treatment interference.

Figure 1c,d summarises water inputs. In season 1, irrigated vines received 71 mm of water via dripper irrigation plus 10 mm effective rainfall (where effective rainfall is any event above 10 mm) between December 2014 and February 2015, and their non-irrigated counterparts received 10 mm in effective rainfall (Figure 1c). In season 2, irrigated vines received 74 mm through dripper irrigation and 31 mm effective rainfall between December 2015 and February 2016 (Figure 1d).

Ambient temperature and relative humidity were recorded at 15 min intervals using TinyTag Ultra2 loggers (Hastings Dataloggers, Port Macquarie, NSW, Australia) shielded in Stevenson-type screens and placed within canopy at bunch zone. Vapour pressure deficit was calculated based on canopy ambient temperature and relative humidity (Allan et al. 1998).

Sampling

In season 1, we sampled berries in control irrigated and control non-irrigated vines only, and in season 2 we sampled all four treatments from the factorial. Twenty bunches were

individually tagged in each season for each replicate. Bunches were chosen from the central part of the canopy when possible. Timing of berry development was recorded as days after anthesis (DAA) or growing degree days (GDD) from anthesis. Anthesis was taken as the date when an estimated 50% of the flower caps had dehisced. Growing degree days (GDD) was calculated for each replicate using actual temperature and 10°C base temperature (Amerine and Winkler 1944, Williams et al. 1985). During each growing season, 60 Shiraz berries per replicate were sampled weekly starting around veraison. Three berries, from top, middle, and proximal of each of the tagged bunches were carefully cut with the whole pedicel attached. Thirty berries were snap frozen in liquid nitrogen and stored in dry-ice during transport to the laboratory, and then stored in a -80 °C freezer. Zip-lock plastic bags with the remaining berries were placed into an ice-cooled container during transport and stored in 4 °C cold room in the laboratory for not more than 48 hours before cell vitality and oxygen measurements were made.

Berry cell vitality, total soluble solids (TSS) and fresh weight

A subsample of three berries of each replicate was used to determine cell vitality using a fluorescein diacetate (FDA) staining procedure on the cut medial longitudinal surface (Fuentes et al. 2010a, Tilbrook and Tyerman 2008). Each berry was weighed and cut in two halves. One half was used to measure TSS and osmolality, the other half was incubated in dark for 15 min, with 4.8 µM FDA solution on the cut surface with solution osmolality similar (to within 10%) of the grape juice (adjusted with sucrose). The stained berries were viewed under a Nikon SMZ 800 (Nikon Co., Toyko, Japan) dissecting microscope under ultraviolet light with a green fluorescent protein filter in place. Images were taken by a Nikon DS-5Mc digital camera (Tochigi Nikon Precision Co., Ltd, Otawara, Japan) and NIS-Elements F2.30 software with the same gain and exposure settings for all images. Images

were analysed with a MATLAB (Mathworks Inc., Natick, MA, USA) code for determining berry cell vitality (Fuentes *et al.* 2010a).

Stomatal conductance and leaf gas exchange

Stomatal conductance (g_s) and leaf gas exchange was measured on one occasion during both season 1 and season 2. In season 1, stomatal conductance was measured using a porometer (Model AP4 DeltaT Devices, Cambridge, UK) at 91 DAA. In season 2, we measured net CO_2 assimilation at light saturation A_{sat} (photon flux density = 919 µmol m^{-2} s^{-1} (Caravia et al. 2016)), leaf evaporation *E* and g_s, using an infrared gas analyser (LCpro-SD Portable Photosynthesis System, ADC BioScientific Ltd., UK) at 97 DAA. IRGA measurement was recorded after 2 min of enclosing the leaf. Measurements were performed between 12:00 to 14:00 (ACDT), at ambient temperature, CO_2 and humidity. Measurements were made on the southwestern side of the canopy on three mid-shoot, fully exposed and expanded leaves. Measurements on replicates of each treatment were taken in random order, to reduce the effect of changing environmental conditions associated with the order of measurement.

Stem water potential

Stem water potential (ψ_s) was measured at 49 and 119 DAA during season 2 using a pressure chamber (PMS Instrument Company, model 1005, Albany, OR, USA). For each replicate, two mid-shoot, fully exposed and expanded leaves were selected on the southwestern side of the canopy, and enclosed in foil covered plastic bags for 1 h before measurement. Measurements were carried out between 12:00 and 14:00 (ACDT). Each leaf with foil bag was placed in the chamber within 3s after excision of the petiole from the vines.

Berry internal O_2 concentration profiles

A subsample of three berries of each replicate was used to determine internal berry O_2 concentrations using a Clark-type oxygen microelectrode with a tip diameter of 25 µm (OX-

25; Unisense A/S, Aarhus, Denmark). The microelectrodes were calibrated in a zero O_2 solution (0.1M NaOH, 0.1M $C_6H_7NaO_6$) and an aerated Milli-Q water (272 µmol/L at 22 °C), as 100% O_2 solution. Individual berries (equilibrated to room temperature) were secured on the motorized manipulator stage. To aid the penetration of the microelectrode into the berry skin, a hole was initially punctured through the skin at the berry equator with a stainless-steel syringe needle (19G), to a depth of 200 µm. The microsensor was positioned through this narrow hole and profiles of oxygen were taken with depth towards the centre of the berry. Previous work had established that O_2 leakage around the site of skin penetration was insignificant (Xiao et al. 2018). O_2 measurements were conducted from 0.2 to 1.5 mm under the skin progressing at 0.1 mm steps. The electrode was not moved beyond this point to avoid damaging the tip against a seed. Each measurement at each position lasted 10s. Between each position, stable signals were recorded within 20s. Measurements were carried out and recorded using the Unisense Suite software. Means and SE of each step (n = 3) were calculated and O_2 profiles were compiled using GraphPad Prism 7. After the oxygen measurements, berry temperature was measured using an IR thermometer (Fluke 568) with a type-K thermocouple bead probe (Fluke 80PK-1). Berry diameters at the equator were determined using a digital calliper.

Berry O_2 uptake

A Clark-type oxygen microsensor OX-MR and the MicroRespiration System (Unisense A/S, Aarhus, Denmark) were used for berry O_2 uptake measurements. Each replicate consisted of nine berries. The measuring chamber containing 9 berries was filled with aerated MilliQ water, constantly stirred and was maintained at 25°C in a water bath. The measurement of O_2 concentration in the water inside the measuring chamber lasted at least 15 mins, with readings taken every 5 seconds to determine a steady respiration rate from the slope of the decline in O_2 concentration.

Berry ethanol concentration

A subsample of ten frozen berries from each replicate were ground to a fine powder in a liquid nitrogen-cooled A11 basic mill (IKA, Germany). Ethanol was quantified using an ethanol assay kit following the manufacturer's instructions (Megazyme International Ireland Ltd., Wicklow, Ireland). Briefly, alcohol dehydrogenase (ADH) catalysed the oxidation of ethanol to acetaldehyde. Acetaldehyde was then further oxidized to acetic acid and NADH in the presence of aldehyde dehydrogenase (AL-DH) and NAD+. NADH formation was measured in a FLUOstar Omega plate reader (BMG LABTECH GmbH, Ortenbery, Germany) at 340 nm.

Berry porosity using pycnometry

A subsample of three fresh berries from each replicate of all treatments in season 2 were used in this experiment. Berries, with pedicels carefully cut off, were submerged in de-gassed Milli-Q water and vacuum infiltrated at -740 mmHg using a vacuum pump (Sparmax TC-502V, Ding Hwa Co., Ltd, Taipei, Taiwan) and a desiccator (Art. 550, Kartell LABWARE, Noviglio, Italy). For every 270s of vacuum applied, the desiccator was depressurized for 30s. The total application time was 50 min. Individual berry weight was obtained before and after the vacuum application. Individual berry volume was estimated using a Hubbard-Carmick specific gravity bottle (25 mL, KIMAX, Kimble Chase, Vineland, NJ, USA). Berry volume (v_1) was calculated:

$$v_1 = \frac{m_0 + m_{f1} - m_{f2}}{\rho_{water}} \quad (1)$$

where m_0 is berry weight before vacuum, m_{f1} is weight of pycnometer filled only with water, m_{f2} is weight of pycnometer with one berry inside and filled with water. Density of water (ρ_{water}) = 1 g/cm^3. Volume of air space within berries was estimated assuming that after 50 min of vacuum infiltration, all air spaces were filled with water. No visible bubble

stream from berries could be observed under vacuum after 50 min. Volume of internal air space (v_2) was calculated as:

$$v_2 = \frac{m_{50} - m_0}{\rho_{water}} \quad (2)$$

where m_{50} is the weight of berries after 50 min of vacuuming application. Porosity of berries was then calculated as:

$$Porosity\ (\%) = \frac{v_2}{v_1} \times 100 \quad (3)$$

X-ray microCT to determine internal air space volumes of intact berries

To confirm berry porosity measurements using pycnometry and to image the structure of internal air space of the berries, x-ray micro computed tomography (microCT) was used to estimate the changes in the volume and distribution of air space within berries during berry ripening. One berry from each replicate of A+NI and A+I treatments in season 2 was imaged, using a Skyscan 1076 (Bruker microCT, Kontich, Belgium), at Adelaide Microscopy, the University of Adelaide. Imaging procedures and settings were the same as described by Xiao *et al.* (2018). Whole berry (pedicel attached) 2D projections were acquired with 59 kV, 149 uA, Al 0.5 mm filter, 2356 ms exposure, 0.4-degree rotation step. Transverse greyscale images of berries were obtained, using NRecon (bruker-microct.com), at 8.5 µm image pixel size (equivalent to 15 µm spatial resolution or 3×10^{-6} mm^3 voxel size). For 3D visualisation of air spaces in berries from the A+I treatment, Otsu thresholding was applied to the volume and the despeckle function was applied to accept only continuous volume over 500 or 1000 voxels as connected air spaces using CT-Analyser (bruker-microct.com). Inverted images only containing air space were reconstructed into 3D berry images using CTvox (bruker-microct.com). For locule volume calculation of berries from both I and NI vines, manual thresholding was applied by referring to the greyscale images and the despeckle setting was

applied to accept only continuous volume over 1000 voxels as locule volume using the CT-Analyser. Locule volumes were calculated using CT-Analyser.

Statistical analysis

All data are presented as mean ± SEM. In the first season only two treatments were compared (A+I vs A+NI), hence a t-test was used. In the second season, ANOVA was used to assess the effect of water regime, thermal regime and their interaction.

Segmental linear regressions were fitted to the change of percentage in berry living tissue over time as in Bonada et al. (2013a). Third order polynomials were fit to the [O_2] profile data for each treatment. For sugar accumulation and berry mass as a function of time either one of two equations were used to model the data as a function of time(t) depending on the presence of a stable plateau or a peak then decline in the variable with time:

$$Y = Y_0 + (Plateau - Y_0) \times (1 - e^{-K \times (t - t_0)}) \quad (4)$$

$$Y = B_0 + B_1 \times t + B_2 \times t^2 \quad (5)$$

Where Y_0 is the initial value, *Plateau* is the final value, K is the rate constant and t_0 is the first sampling time, and B_0, B_1, B_2 are the intercept and coefficients respectively of the quadratic equation. The better of these two models that fit to the data was determined by Akaike's Information Criteria. For the quadratic equation (5) the peak value was determined when the first derivative of the fitted line equalled zero. The Michaelis–Menten equation was fit to the relationship between percentages of berry living tissue and mean [O_2]. Linear regressions were fit to the changes in berry respiration or ethanol concentration of different treatments over time in season 2. Quadratic equations were fit to the data of berry and locule porosity as a function of TSS. Third order polynomial equations were fit to [O_2] as a function of depth in to the berry. The Extra Sum-of-Squares F-test was applied to test the differences of the fits

between treatments. All analyses were performed in Graphpad Prism 7 (Graphpad Software, La Jolla, CA, USA). A difference was taken as being significant when $P<0.05$.

Results

Growing conditions and phenology

Figure 1c,d summarises water inputs. In season 1, irrigated vines received 71 mm of water via dripper irrigation plus 10 mm effective rainfall between December 2014 and February 2015, and their non-irrigated counterparts received 10 mm in effective rainfall (Figure 1c). Frequent rain events were recorded around 70 DAA (Figure 1c). In season 2, irrigated vines received 74 mm through dripper irrigation and 31 mm effective rainfall between December 2015 and February 2016 (Figure 1d). There was a series of large rain events between 87 and 91 DAA (Figure 1d).

Between 40 and 125 DAA in season 2, daily maximum ambient temperature ranged from 21.2 to 44.5 °C in unheated irrigated treatments while daily minimum ranged from 6.3 to 22.8 °C. Over the same period, heating increased daily maximum temperature on average by 0.6 in I-H and 1.0 °C for NI-H (Figure 1a) and had no effect on minimum temperature. Larger canopies in irrigated vines diminished the effectiveness of passive heating. The VPD was elevated in proportion to the increase in maximum temperature (Figure 1b).

Full anthesis (stage EL 23) (Coombe 1995) occurred in season 1 on the 7th of November 2014 and in season 2 on the 3rd of November 2015 with no treatment differences evident. Veraison occurred on 63 and 70 DAA for season 1 and season 2 respectively again with no treatment differences.

Stem water potential, stomatal conductance and gas exchange

Lack of irrigation resulted in clear physiological indicators of water stress (Table 1). In the first season, we measured stomatal conductance on a bright sunny at day 91 DAA (average

PAR = 2852 ± 98 μmol/(m^2·s)) where g_s in non-irrigated vines was half of that in irrigated vines, and near a 50 mmol/(m^2·s) threshold proposed as an indicator of water stress by Flexas *et al.* (2002).

In the second season, midday stem water potential (ψ_s) reflected the water stress imposed on non-irrigated vines. Heated vines showed no indication of water stress and there was no interaction with irrigation in either gas exchange traits or ψ_s (Table 1). A similar depression of g_s for NI vines was observed on two occasions in season 2 and A_{sat} was significantly reduced relative to A+I vines (Table 1).

Berry ripening

The dynamics of berry total soluble solids (TSS), berry fresh mass and sugar per berry are compared between treatments for season 1 and season 2 in Figure 2. TSS as a function of time was best fit by EQN 4 and one curve adequately fit all the data sets rather than individual curves for each treatment (*P*=0.18). For berry mass EQN 5 best described the data returning peak biomass at 87 DAA and 89 DAA for ambient irrigated (A+I) and non-irrigated (A+NI) vines in season 1. In season 2 peaks in mass occurred at 99 DAA (A+I), 83 DAA (A+NI), 97 DAA (H+I) and 100 DAA (H+NI) (Figure 2c,d). Sugar per berry as a function of time was best fit by EQN 4 (Figure 2e,f). There was no significant difference between treatments in the rate constant for sugar accumulation (Extra Sum-of-Squares F-test, season 1, *P* = 0.287; season 2, *P* = 0.879) and one rate constant of 0.082/DAA (season 1) and 0.066/DAA (season 2) could fit all treatments, however fits were significantly different because of different final plateaus.

Berry living tissue

Figure 3 shows the effects of treatments on the dynamics of cell death during two seasons. Segmental linear regression identified a slow cell death stage (slope 1), and a fast cell death

stage (slope 2) after a developmental threshold (Bonada et al. 2013b). The onset of the fast cell death stage in both A+I and A+NI berries in season 1 was the same at 90-91 DAA, but separated in season 2 where A+NI vines had earlier onset but lower rate of cell death in the fast stage (Table 2). The earlier onset of the threshold for fast cell death corresponded to the peak in berry mass. There was no effect of heating on the onset of fast cell death or the rate of its development when examined over chronological time (Figure 3c,d) but there was a significant interaction with irrigation for both parameters (Table 2).

Plotting cell death against thermal time from anthesis in season 2 (Figure 3e) showed that A+NI vines had earlier onset of the rapid decline in living tissue (Figure 3f) and had reduced fast stage (slope 2) relative to A+I vines (Figure 3h). Heating increased the thermal time of onset of the fast stage of CD, and there was a significant interaction with irrigation (Figure 3f, Table 2). Water deficit slowed the rapid decline in living tissue for unheated vines (slope 2) with a significant interaction with temperature (Figure 3h, Table 2). There was no effect of treatment or interaction on the slope of the slow stage of CD before the onset of fast stage (Figure 3g, Table 2).

O_2 concentration profiles in berries

Oxygen concentration ($[O_2]$) as a function of depth into the berry is shown for season 1 and season 2 at different sampling dates (Figure 4). Irrespective of water regime and sampling time, $[O_2]$ decreased steeply with depth in to the berry (note log scale in Figure 4). In season 1 berries were sampled four times from veraison (63 DAA) to pre-harvest (106 DAA) (Figure 4a,b,c,d) and this revealed a reduction in $[O_2]$ with berry ripeness where $[O_2]$ at 0.2 mm depth at the last sampling date in season 1 was 22.90 ± 6.25 µmol/L for I berries and 6.71 ± 3.13 µmol/L for NI (Figure 4d). Differences between treatments were only found at 77 DAA $[O_2]$, when NI berries decreased to 3.10 ± 1.28 µmol/L at 1.5 mm depth, while for I berries $[O_2]$ was 25.93 ± 14.09 µmol/L at 1.5 mm (Figure 4b). At 106 DAA, both I and NI berries were

severely hypoxic at 1.5 mm (Figure 4d). Third order polynomial functions were fit to the profiles and comparison of fitted curves by Extra Sum-of-Squares F-test indicated berries from I showed a different evolution of [O_2] profiles where [O_2] was on average higher in I than NI for berries at 77 and 91 DAA.

In season 2 similar patterns of [O_2] profiles were observed with depth in the berry and with berry ripeness (Figure 4e,f,g,h). In contrast to season 1, ambient irrigated (A+I) berries did not become severely hypoxic at 1.5 mm at the last sample date (112 DAA), but all other treatments had extremely low [O_2] between 1.0 and 1.5 mm (Figure 4h). Comparison of third order polynomials showed berries from A+I and H+I at 105 DAA (Figure 4g) had significantly higher [O_2] than the NI treatments ($P < 0.0001$). Berries from I and H+I had similar parameters for their fitted functions, while the models for NI and H+NI were different ($P < 0.0001$). At 112 DAA, H+NI berries showed lower [O_2] compared to the other treatments (Figure 4h).

Associations between cell death and oxygen concentration

The relationships between berry living tissue and mean [O_2] (0.2 to 1.5 mm) are shown in Figure 5. In season 1 a strong global association fit by the Michaelis–Menten equation was found regardless of water regime ($R^2 = 0.91, P = 0.023$) (Figure 5a). At the same concentration of oxygen, berries in season 2 maintained higher proportion of living tissue than in season 1 (solid vs dashed lines in Fig. 5b). A similar association between proportion of living tissue and oxygen concentration was found for A+I, A+NI and H+I berries ($R^2 = 0.74, P = 0.0035$), but H+NI required a different fit to the data (Figure 5b).

Berry respiration

Berry respiration measured as O_2 uptake at 25 °C declined during ripening both on a per berry basis and on a fresh mass basis (Figure 6). On a per berry basis respiration rates in both

season 1 and season 2 differed between treatments (Figure 6 a,c). For season 2 berries from irrigated vines had higher respiration rates on a per berry basis compared to non-irrigated irrespective of thermal treatment. On a berry fresh mass basis, there was a difference in respiration rate only between I and NI in season 1 at 84 DAA, but no difference amongst all treatments in season 2 (Figure 6d).

Berry ethanol concentrations

Berry ethanol concentration was measured three times during ripening in season 1 and four times in season 2 (Figure 7). There was a significant trend in both seasons for ethanol to increase with time. In season 1 the increase was larger for berries from non-irrigated vines compared to their irrigated counterparts. This was not evident in season 2 where there was no difference between the linear regression lines for the treatments by Extra Sum-of-Squares F-test. The overall ethanol concentrations in berries were similar in both seasons.

Berry porosity and relative locular volume from X-ray microCT

3D models of total air space within the berries (Figure 8a-d) showed berries with lower TSS had a small proportion of locule volume (Figure 8a) and a large proportion of small-sized air spaces in the pericarp (Figure 8c). The small-sized air spaces diminished later in ripening compared to earlier while the locule air space became more dominant (Figure 8b,d). There are continuous air space connections from the locule area to the pedicel. Total berry porosity measured from pycnometry declined as ripening progressed (Figure 8e). In contrast to other measured traits there was no effect of water regime on porosity (Figure 8e). Heating decreased porosity for the same TSS particularly early in ripening irrespective of water regime (dashed line in Figure 8e).

X-ray microCT was used to measure the locule relative volume for A+I and A+NI grapes. Contrary to the total porosity the locule volume increased with increasing TSS. Locule

volumes as a function of TSS were similar across water regimes (solid red line, Figure 8e). The curves of locule volume and porosity intersected at a TSS of about 25-27 °Brix.

Discussion

This study connects two parallel streams of previous research. First, it was shown that restricted O_2 diffusion into Chardonnay berries may cause severe hypoxia, ethanol accumulation, presumed to result from fermentation, and earlier cell death (Xiao et al. 2018). Profiles of low [O_2] across the pericarp correlated with regions of cell death in both Chardonnay and Shiraz (Xiao et al. 2018). Second, it was shown that elevated temperature and water stress increased the rate of fast cell death in Shiraz berries (Bonada et al. 2013a,b). Here we thus explored the connection between stress-modulated cell death and berry internal [O_2]. Decreased berry porosity (air spaces), perhaps induced by stress could potentially restrict the diffusion of O_2 and lead to hypoxia and CD, thus we also examined how porosity and internal air space structure, defined by X-ray micro CT, changed during development under the imposed treatments.

Our results for Shiraz berry cell death during development confirm those of Bonada et al. (2013b), with stress modulating both onset and rate of cell death in the second stage. Our measurements showed correspondingly higher degree of hypoxia, and higher ethanol production in berries from non-irrigated vines in season 1 and CD correlated with mean [O_2] in berries during development. In contrast to Bonada et al. (2013b), however, heating did not shift the onset of fast cell death in chronological time under our experimental conditions. Consistently, heating did not alter the degree of hypoxia in berries, despite the decrease in berry porosity (proportion of volume as air space) earlier in ripening that would be expected to increase the diffusion resistance to O_2 (see below). Heating increased berry mass after veraison compared to control vines with or without irrigation and this was reflected in increased sugar per berry since TSS was not affected. Water deficit (Table 1) reduced berry

mass, reflecting the sensitivity of both cell division and expansion (Hardie and Considine 1976, Ojeda et al. 2001, Rogiers et al. 2004a).

Water deficit and elevated temperature modulate mesocarp CD and berry shrivel in Shiraz (Bonada et al. 2013a,b, Caravia et al. 2015,2016). Under our experimental conditions the effect of water stress was dominant, where the rate of cell death was accelerated in season 1 and the onset of cell death was advanced in season 2 in water stressed vines. In contrast to Bonada et al. (2013b) we found no thermal effects on the dynamics of cell death. There are three non-mutually exclusive reasons for this disagreement. First, the intensity of heat stress was larger in the experiment of Bonada et al. (2013b). Second, there were differences in the background conditions of rainfall, radiation and other relevant environmental factors (Sadras et al. 2017). Third, we measured berry responses in vines that where continuously exposed to the warmer temperature during 4-5 years, hence the potential for acclimation (Kozlowski and Pallardy 2002, Wang and Li 2006). Notwithstanding these reasons, it is interesting to note the very large difference in the onset of cell death in thermal time between the two studies, but the similarity in time after anthesis, which is consistent across many previous studies on Shiraz berry cell death.

Internal [O_2] decreased dramatically across skin and mesocarp region up to 1.5 mm from the skin surface (note log scale in Figure 4), for all treatments in both seasons. It was not possible to probe the Shiraz berries greater than 1.5 mm from the surface due to the possibility of impacting the seeds with the expensive O_2 probe (Xiao et al. 2018). The mean berry internal [O_2] to 1.5 mm of all treatments also decreased during ripening in both seasons. This decrease in mean [O_2] correlated well with the progression of cell death during berry ripening (Figure 5). The association between cell vitality and mean [O_2] was generally independent of seasonal and stress conditions (Figure 5). The Michaelis–Menten equation that fitted the data for CD as a function of mean [O_2] may be related to the relationship between respiration rate

and [O_2] observed in other plant tissues (Armstrong et al. 2009, Thomson and Greenway 1991). At very low [O_2] cytochrome oxidase would be inhibited and potentially the reduced energy production and increase in fermentation (increase in ethanol production, discussed below) may lead to increased leakiness of berry cell membranes and ultimately CD (Pfister-Sieber and Braendle 1994); this has been observed in other plant tissues under severely and prolonged hypoxic situations (Rawyler et al. 1999). The spatio-temporal change of internal berry [O_2] reported here is consistent with previous research on Shiraz, Chardonnay and Ruby Seedless grapes (Xiao et al. 2018). In other fruits such as pear, limited O_2 availability in the core of the fruit can lead to the physiological disorder of core breakdown, which is related to severe hypoxia in the tissue (Franck et al. 2007).

Berries from non-irrigated vines showed lower internal [O_2] during ripening in both seasons. In grapevine, transcript abundance of genes involved in ROS scavenging increased under water stress (Cramer et al. 2007). ROS accumulation at veraison was regarded as a harmless and normal berry ripening phenomenon (Pilati et al. 2014). ROS production is enhanced under stress and may function as a signal that triggers defence responses. On the other hand, prolonged drought stress can break the balance of ROS generation and scavenging and result in oxidative stress and cell death (Cruz de Carvalho 2008).

Hypoxia in large tissues can result from gas diffusion limitation and high O_2 demand from respiration (Sasidharan et al. 2017). Respiration is highly correlated with internal [O_2] of plant tissues (Zabalza et al. 2009) and in the grape berry is affected by the developmental stage (Harris et al. 1971). On a per berry basis, lower respiration rate was found in water stressed berries in both seasons very likely due to the smaller berry size, since on a per gram basis there was little or no difference in respiration rates between treatments. On a per gram basis berries under water stress showed a significantly higher respiration prior to the onset of CD in the first season. This is possibly associated with the lower mean [O_2] around the same

time during ripening (Figure 4b) that could result in more cell death under water stress. An overall decrease in respiration rate was observed in all treatments from veraison to late ripening (Figure 6). This is probably an indication of decreased O_2 availability combined with decreased proportion of living tissue within the berry.

Ethanol is the major end product of fermentation (Noctor and Foyer 1998) favoured by hypoxia or anoxia (e.g. in Arabidopsis (Zabalza et al. 2009)). Plants can adapt to severe hypoxia by utilising fermentation instead of oxidative respiration thereby maintaining some cell function (Geigenberger 2003). The increase in ethanol in berries indicates this metabolic change and confirms that the high respiration, possibly drought induced, first results in faster depletion of internal [O_2] ultimately leading to severe hypoxia.

Oxygen uptake and the diffusion properties within grape berries change during berry ripening (Xiao et al. 2018). Differences in volume of air spaces and density of pores in fruit parenchyma contribute to the differences in internal O_2 availability between apple and pear (Verboven et al. 2008). Interestingly, the berries grown under elevated temperature showed lower proportion of airspace particularly earlier in ripening. Since berries were larger under heating treatments this may indicate that the actual air space volume was approximately the same. However, the proportional increase in mass for the heated treatments early in ripening (i.e. at 10 ^{o}Brix) was small while the relative difference in porosity between heated and control treatments was greatest at this stage (compare Figure 2d and Figure 8). Porosity of the berries decreased throughout development for all treatments in season 2 (Figure 8e) with the heated and control treatments converging as locular air space volume increased as measured by microCT. Previous research showed that intracellular air spaces existed in the brush region throughout berry development (Findlay et al. 1987). Using microCT 3D visualization, we found that Shiraz berry internal air space occurs as fine pores in the pericarp. Later in ripening, these fine pores became less dense corresponding to the decrease

in porosity measured using pycnometry. These air channels connect to the pedicel where lenticels occur at high density. This is essentially similar to the situation in Chardonnay berries (Xiao et al. 2018). An interesting observation made by microCT was that the locule air space relative volume became larger later in ripening. Comparing this with the pycnometry measurements it would suggest that the total berry air space was mostly accounted for by the locule air space when berries become ripe at 25-27 ^{o}Brix. The relative locule volume increased thereafter, probably indicative of berry shrivel. The reduction of fine air-filled pores in the pericarp could be due to sap leaking from non-vital cells and this would reduce oxygen diffusion to any cells that were still vital and respiring in the pericarp.

Conclusions

Berry internal [O_2] decreased with both depth in Shiraz berry tissues and berry ripeness irrespective of growing conditions. The progression of CD during berry ripening correlated with mean berry internal [O_2] across growing conditions. Water stress decreased Shiraz berry internal [O_2] and increased ethanol accumulation and CD. Elevated temperature did not affect berry [O_2] and CD under our experimental conditions. Porosity of the berries decreased throughout development for all treatments. Relative volume of locule air space became larger later in ripening which could be an indicator of berry shrivel. The increase in berry mass of heated berries, resulting in lower porosity compared to smaller sized controls, was likely due to similar air volume within the berries irrespective of treatment. The reduced berry internal [O_2] was related to the reduction in porosity and percentage of living tissue. Cell death, and by implication berry shrivel, are strongly linked to oxygen supply and demand. Potentially any biotic or abiotic stress that may influence oxidative processes, berry respiration or berry anatomy will likely impact on cell death, with implications for oenologically relevant berry traits.

Figures

Table 1 Physiological indicators of water stress under the treatments imposed over the two seasons of this study and the results of 2-way ANOVA.

Season	DAA	Variable	Treatment				*P* value		
			Ambient irrigated (A+I)	Ambient non-irrigated (A+NI)	Heated irrigated (H+I)	Heated non-irrigated (H+NI)	Temperature	Water	Interaction
1	91	g_s	162 ± 7	72 ± 21				0.015	
2	49	Ψ_S	-1.21 ± 0.04	-1.63 ± 0.01	-1.27 ± 0.04	-1.67 ± 0.02	0.164	0.000	0.798
	97	A_{sat}	7.6 ± 0.4	4.9 ± 0.4	8.7 ± 0.9	5.4 ± 0.2	0.190	0.001	0.593
		g_s	88 ± 3	37 ± 9	116 ± 18	44 ± 5	0.138	0.000	0.382
	119	Ψ_S	-1.63 ± 0.02	-1.81 ± 0.06	-1.62 ± 0.04	-1.90 ± 0.05	0.406	0.001	0.331

Units for variables: g_s (mmol/(m^2·s)), A_{sat} (µmol/(m^2·s)), Ψ_S (MPa).

Table 2. Rates of cell death before (slope 1) and after (slope 2) the onset of rapid cell death in chronological (DAA) and thermal (°Cd) scales for Shiraz for season 2, and the results of 2-way ANOVA.

Scale	Variable	Treatment				*P* value		
		Ambient irrigated (A+I)	Ambient non-irrigated (A+NI)	Heated irrigated (H+I)	Heated non-irrigated (H+NI)	Temperature	Water	Interaction
DAA	Slope 1	-0.25±0.095	-0.15±0.132	-0.26±0.063	-0.55±0.232	0.205	0.533	0.211
	Onset	111±2	96±3	108±2	108±3	0.117	0.013	0.011
	Slope 2	-5.17±0.868	-2.35±0.190	-3.56±0.445	-3.89±0.489	0.925	0.050	0.022
°Cd	Slope 1	-0.01±0.005	-0.01±0.009	-0.02±0.004	-0.04±0.016	0.190	0.540	0.320
	Onset	1411±7	1213±33	1428±23	1390±22	0.003	0.001	0.009
	Slope 2	-0.30±0.020	-0.17±0.012	-0.24±0.025	-0.24±0.014	0.933	0.007	0.007

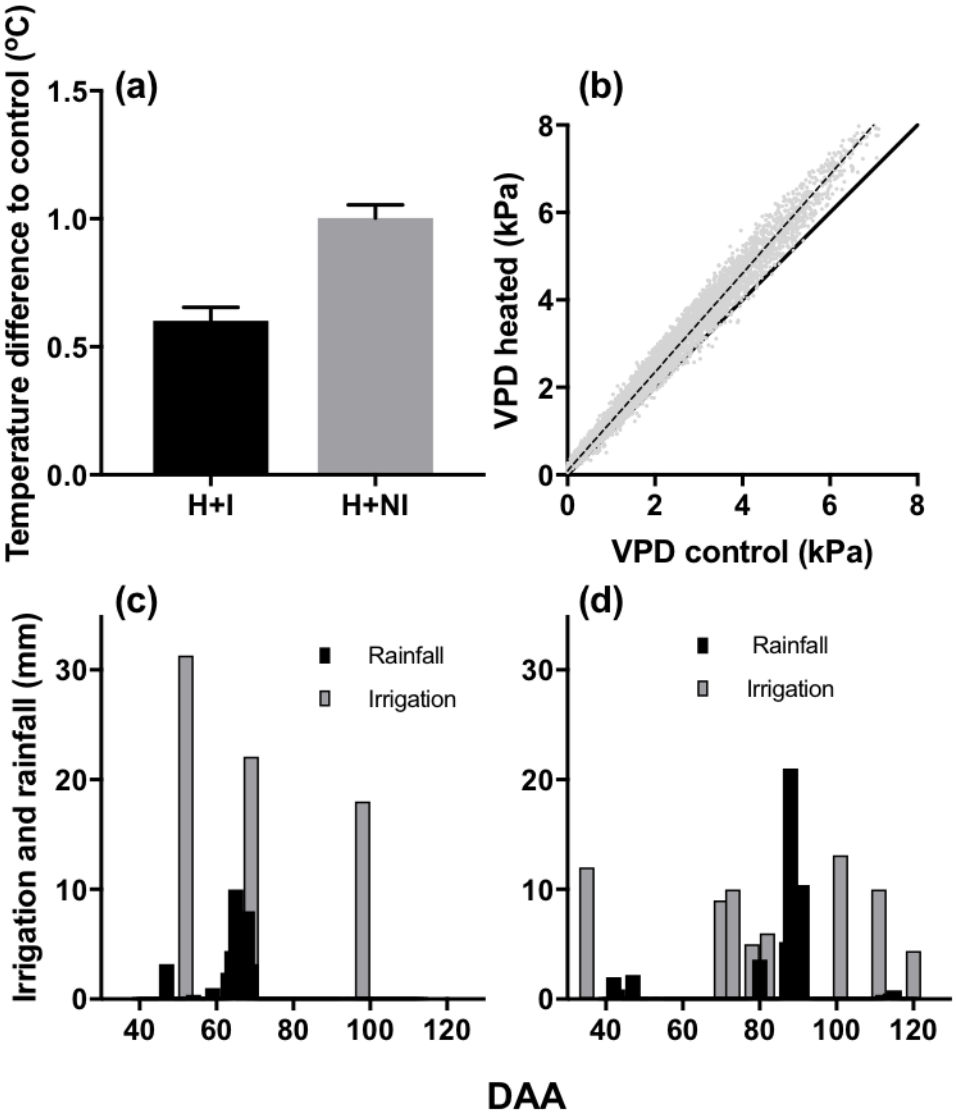

Figure 1. (a) Canopy ambient temperature difference of heated irrigated (H+I) and heated non-irrigated (H+NI) vines to ambient irrigated (A+I) vines 40 DAA to harvest in S2. Data are means ± SE, n=3. Temperature differences are greater than zero in both cases (P<0.0001). (b) Comparison of H+I canopy vapour pressure deficit to that of the A+I vines, solid line is y = x. Fitted line (Deming regression) (dashed): $VPD_{heated} = 1.13 \times VPD_{irrigated} + 0.09$. Daily rainfall from 40 DAA to harvest in S1 (c) and S2 (d).

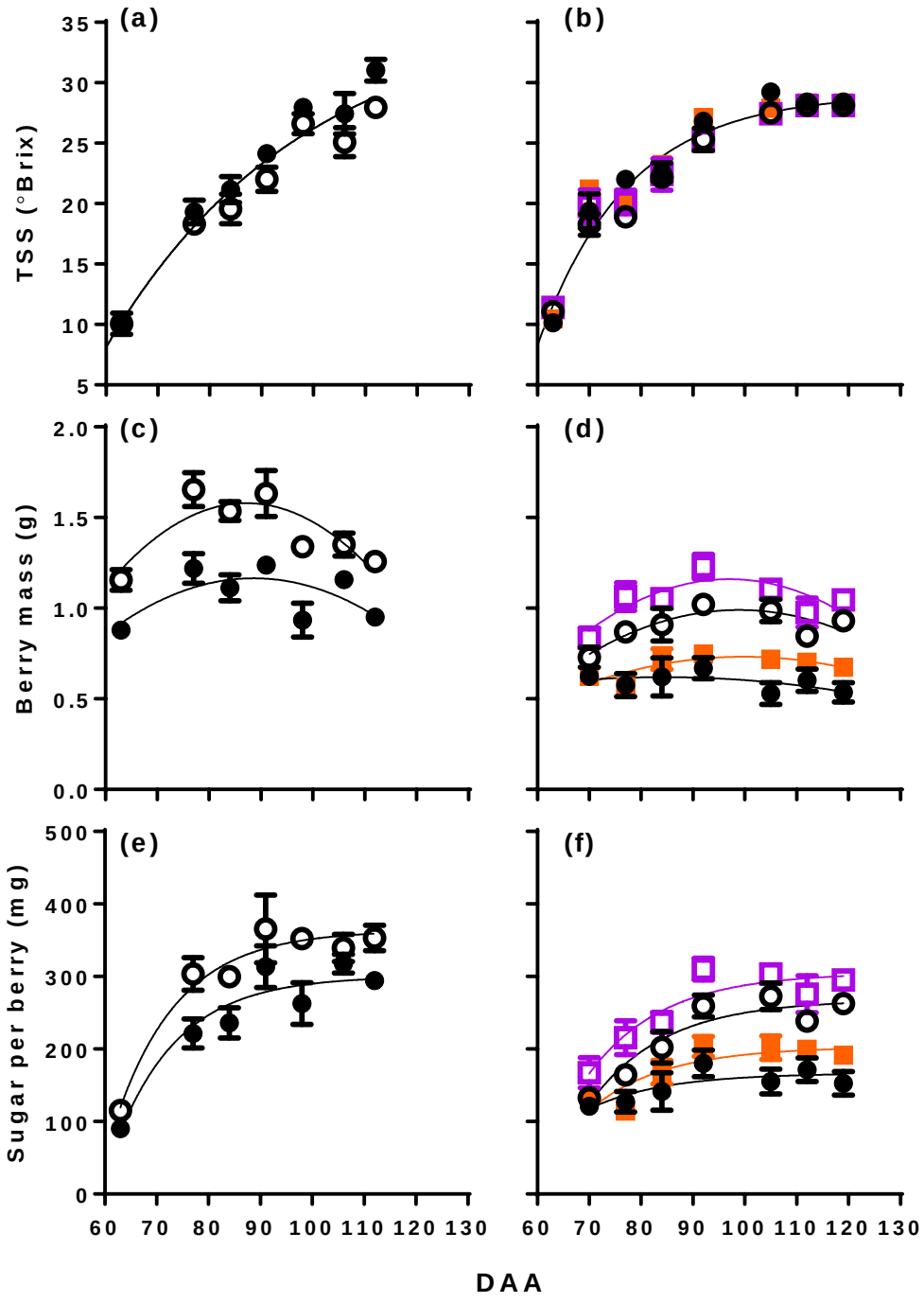

Figure 2. Berry ripening during season 1 (2014-2015. a,c,e) and season 2 (2015-2016, b,d,f) showing TSS (a,b), berry fresh mass (c,d) and sugar per berry (e,f). Treatments are: ambient irrigated (A+I, open circle), ambient non-irrigated (A+NI, black closed circle), heated & irrigated (H+I, open cyan square), heated & non-irrigated (H+NI, orange closed square). Data

are means ± SE, n=3. Where separate lines are shown this indicates that there were significant differences between the fitted lines (Extra Sum-of-Squares F-test, $P<0.05$).

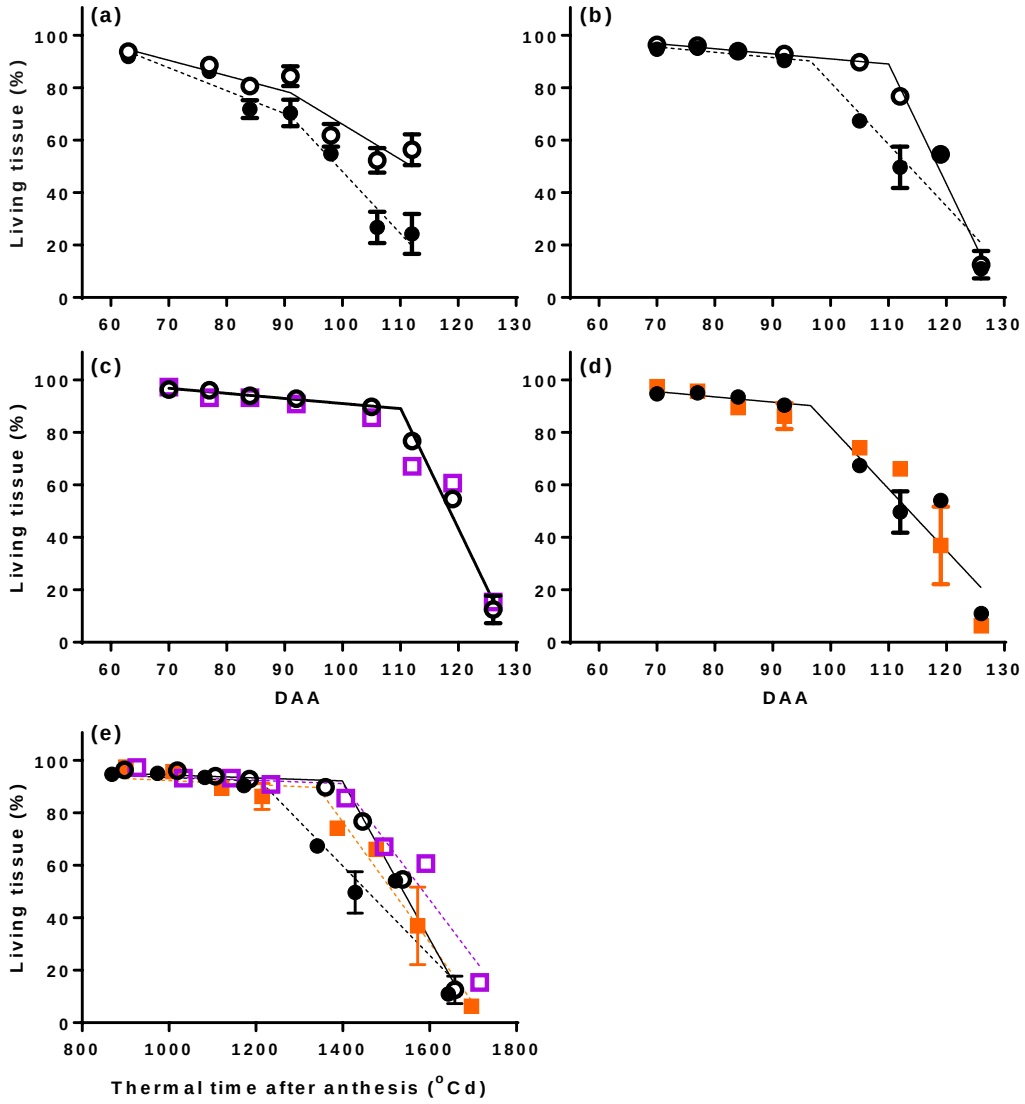

Figure 3. Proportion of berry living tissue over time from anthesis (DAA) for season 1 (a) and season 2 (b,c,d,e) over time and thermal time (°Cd) from anthesis comparing the treatments indicated as: ambient irrigated (A+I, open circle), ambient non-irrigated (A+NI, black closed circle), heated irrigated (H+I, open cyan square), heated non-irrigated (H+NI, orange closed square). In each case a segmented linear regression has been fit to the data for each treatment and for clarity, ambient irrigated have been duplicated in (c) to compare with heated irrigated, and ambient non-irrigated has be duplicated in (d) to compare with heated non-irrigated. All data for season 2 is shown in (e) against thermal time. Data are means ± SEM, n=3.

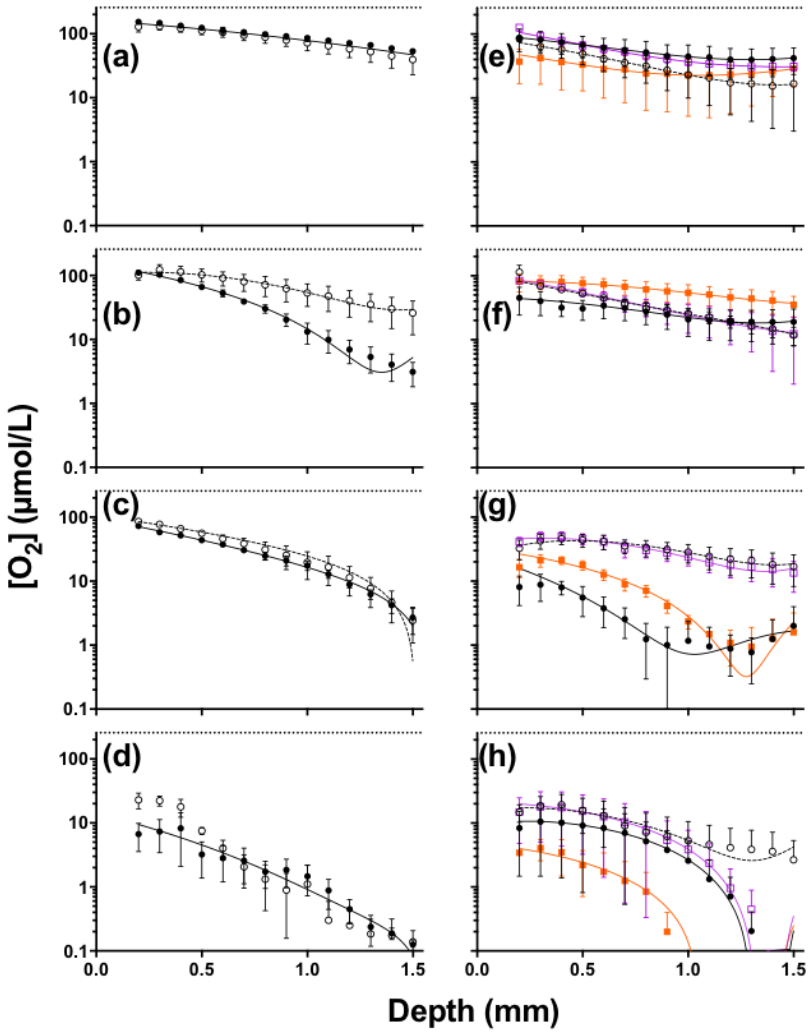

Figure 4. Oxygen concentration profiles (log scale) from 0.2 mm beneath the skin to 1.5 mm towards the centre of the berry at different stages of development for the two seasons (S1: a,b,c,d; S2: e,f,g,h) under the treatments: ambient irrigated (A+I, open circle) and non-irrigated (A+NI, black closed circle), heated irrigated (H+I, open cyan square), heated non-irrigated (H+NI, orange closed square). The sampling times were different for S1 and S2. S1: (a) 63 DAA, (b) 77 DAA, (c) 91 DAA, (d) 106 DAA. S2: (e) 70 DAA, (f) 84 DAA, (g) 105 DAA, (h) 112 DAA. Dashed lines indicate the approximate O_2 saturation value for water at 25 °C. Data are means ± SE, n=3. Third order polynomial functions were fit to the data for each treatment. Where separate curves are shown on each panel the fitted lines were significantly different by F-test (P<0.05).

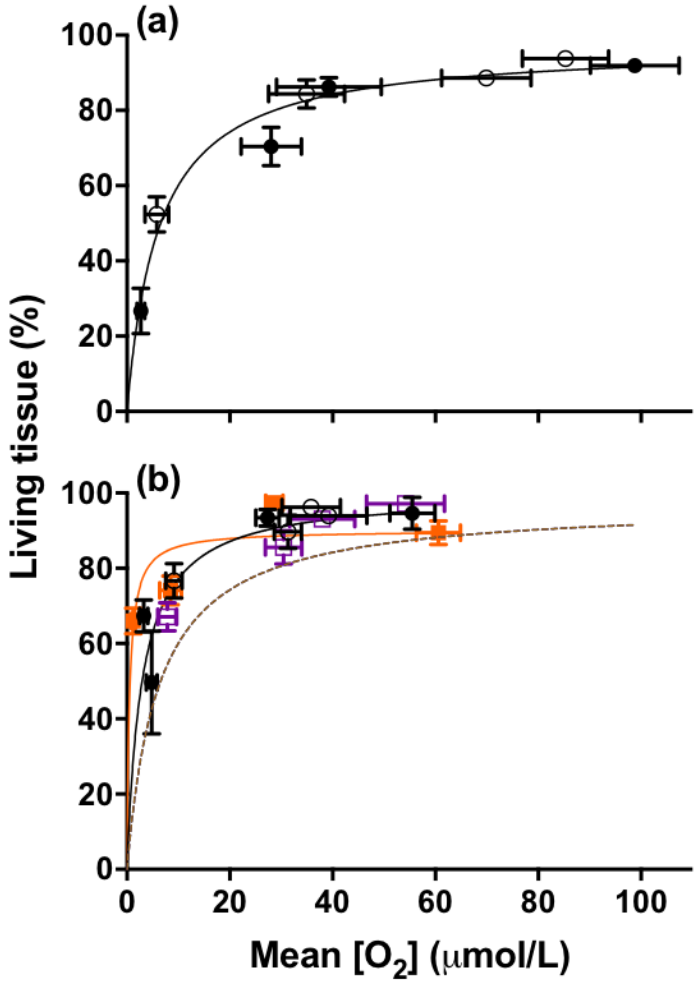

Figure 5. Dependence of berry living tissue on mean [O_2] from 0.2 mm to 1.5 mm depth from the surface of the berry. Data are means ± SE, n=3. Fitted curves are the Michaelis–Menten equation: Living Tissue (LT) = $LT_{max} \times [O_2]/(K_d + [O_2])$. (a) There was no significant difference in the fits for A+I (open circles) and A+NI (filled circles) in S1 (combined R^2=0.91). LT_{max} = 97.2 ± 2.7 (SE) %, K_d = 6.2 ± 0.03 (SE) µmol/L. (b) For S2, A+I (open circles), A+NI (filled black circles) and H+I (cyan open squares) were not significantly different (fit=solid black line, R^2=0.66), LT_{max} = 99.9 ± 2.9 (SE) %, K_d = 2.9 ± 0.53 (SE) µmol/L. The fit for H+NI (orange filled squares) was significantly different from the other treatments (fit = solid orange line, R^2 = 0.59) LT_{max} = 90.1 ± 3.5 (SE) %, K_d = 0.50 ± 0.17 (SE) µmol/L. The fit for season 1 in (a) is shown for comparison with data for season 2 in (b) (dashed line).

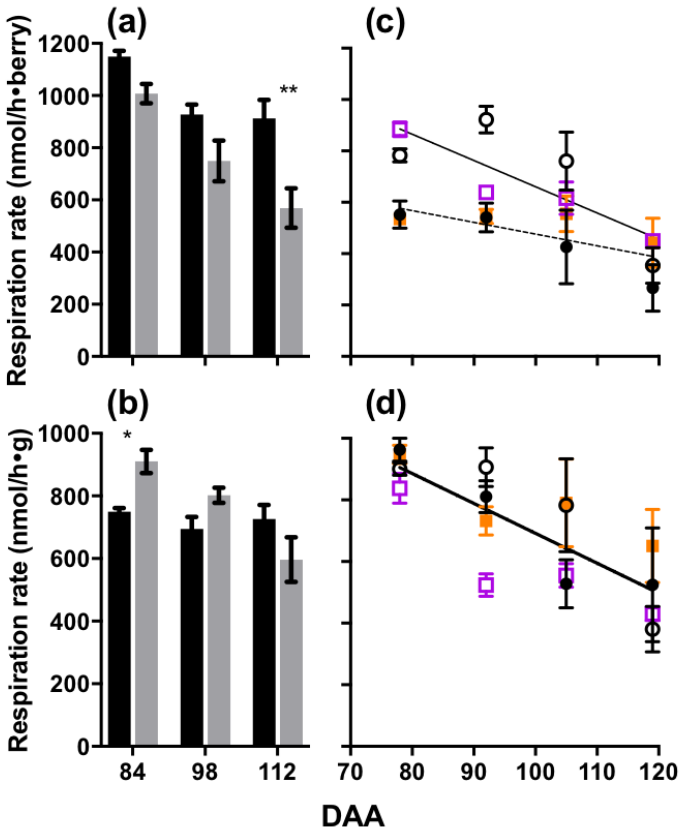

Figure 6 Respiration rate of Shiraz berries at 25°C as a function of days after anthesis (DAA), per berry (a, c) or per gram of berry fresh mass (b, d) for season 1 (a,b) and season 2 (c,d). For season 1 there were two treatments, A+I (black) and A+NI (grey). Data are means ± SE, n=3. From two-way repeated ANOVA: (a) treatment, time and interaction were significant $P<0.05$; (b) treatment and time were significant, *, ** = significantly different from control ($P<0.05$, $P<0.01$, Fisher's LSD). For Season 2 (c,d) there was a significant reduction in respiration with time. For (c) Irrigated treatments (A+I, open black circles, H+I, open cyan squares) had significantly higher respiration rates per berry than for non-irrigated treatments (A+NI, closed black circle, H+NI, closed orange square) and separate regressions are shown (solid line = I treatments, respiration rate = -10.22 × DAA + 1683; dashed line = NI treatments, respiration rate = -4.56 × DAA + 933). For (d) there was no significant difference between the linear regression lines for the treatments (Extra Sum-of-Squares F-test) and one regression line is shown for all the data [respiration rate = -9.71 × DAA + 1662 nmol/(h g), R^2=0.45].

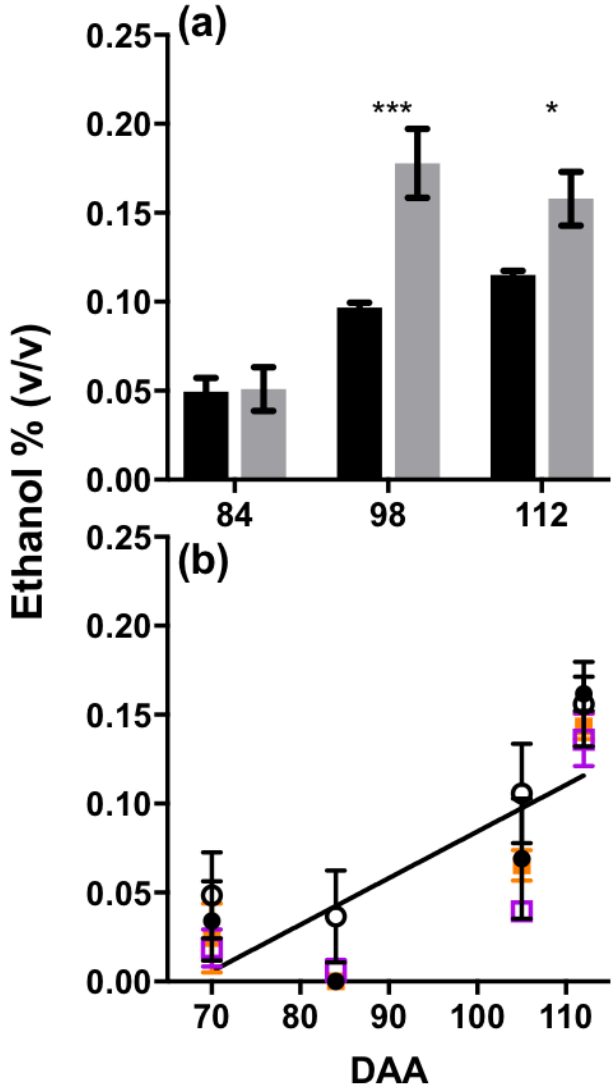

Figure 7 Ethanol concentration in berries as a function of days after anthesis (DAA) for: (a) S1 comparing I (black) and NI (grey) treatments. Data are means ± SE, n=3. Two-way repeated ANOVA showed treatment and time were significant (P<0.002), ***, * indicate significant difference (P < 0.001, P < 0.05, Fisher's LSD). (b) Increase in ethanol with time was also found in season 2. There was no difference between the linear regression lines for the treatments (A+I, open black circles, A+NI, closed black circle, H+I, open cyan squares and H+NI, closed orange square) by Extra Sum-of-Squares F-test and one regression line is shown for all the data ([Ethanol] = 0.0026 × DAA - 0.18, R^2 =0.52).

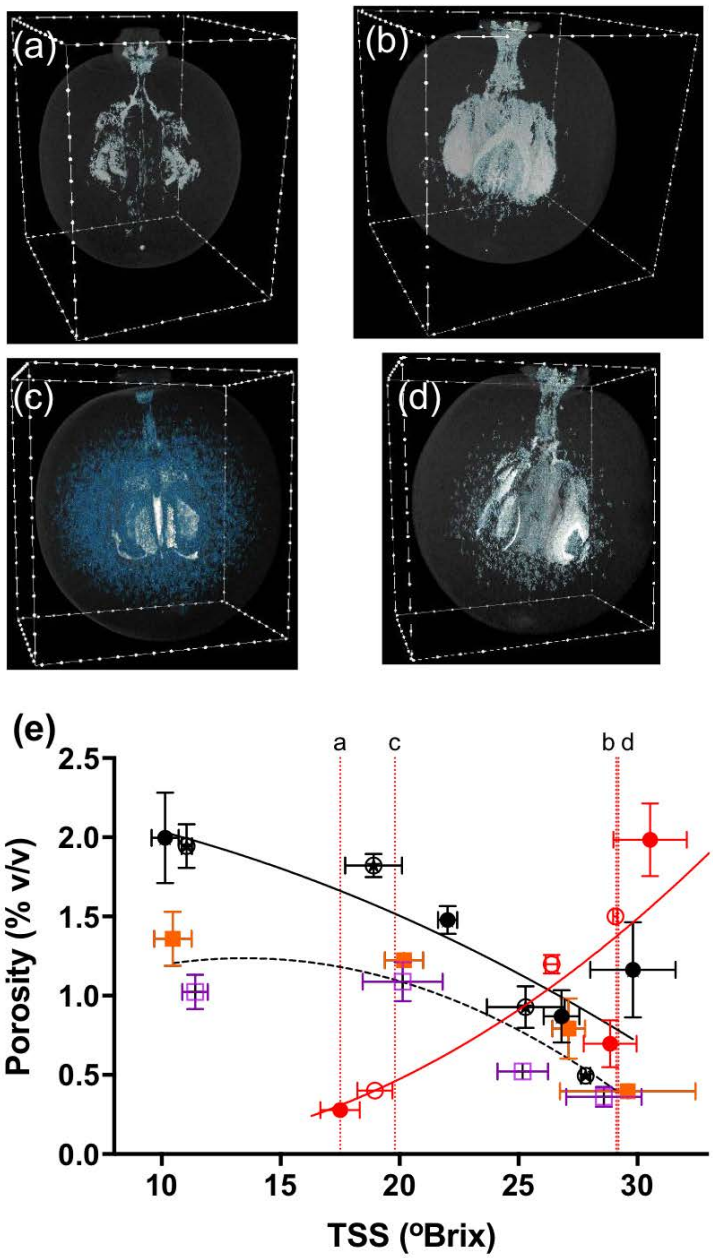

Figure 8. Air spaces in Shiraz berries determined by X-ray micro-CT and pycnometry. 3D images represent four Shiraz berries (control irrigated) of (a) 17.5 °Brix, (b) 29.2 °Brix, (c)19.8 °Brix and (d) 29.1 °Brix (also shown as vertical red dotted lines in (e)). In (a) and (b), minimum voxel cut-off was 1000. In (c) and (d), minimum voxel cut-off was 500, longitudinally sectioned 3D berries were shown for easy visualisation of locule. White dots on box outline are at 1 mm intervals. Blue to white colour indicates increasing volume of connected space. (e) Total berry porosity measured in S2 using pycnometry and relative volume of the locule using microCT, as a function of TSS. There was no significant

difference in total porosity (pycnometry) between ambient irrigated (A+I) and non-irrigated (A+NI) berries so one fitted line is shown (quadratic equation, solid black line). There was also no significant difference between the two heated treatments and one fitted line is shown (quadratic equation, dashed black line). There was a significant difference between heated and ambient treatments F-test, $P < 0.05$). Locule relative volume is shown measured by microCT for ambient irrigated (A+I) (open red circles) and non-irrigated (A+NI) (solid red circles) berries. There was no significant difference between locule relative volume for the two treatments so one fitted line shown (quadratic, red solid line). Treatments indicated as: ambient irrigated (A+I) (open circle), ambient non-irrigated (A+NI) (black or red closed circle), heated irrigated (H+I) (open cyan square), heated non-irrigated (H+NI) (orange closed square).

Literature cited

Alexander, L.V. and Arblaster, J.M. (2009) Assessing trends in observed and modelled climate extremes over Australia in relation to future projections. International Journal of Climatology **29**, 417-435.

Allan, R.G., Pereira, L.S., Raes, D., and Smith, M. (1998) Crop evapotranspiration-Guidelines for computing crop water requirements. in *FAO Irrigation and drainage paper 56* (Food and Agricultural Organization, Rome, Italy, 1998), Vol. 56.

Amerine, M. and Winkler, A. (1944) Composition and quality of musts and wines of California grapes. Hilgardia **15**, 493-675.

Armstrong, W., Webb, T., Darwent, M. and Beckett, P.M. (2009) Measuring and interpreting respiratory critical oxygen pressures in roots. Annals of Botany **103**, 281-293.

Bonada, M. and Sadras, V.O. (2015) Critical appraisal of methods to investigate the effect of temperature on grapevine berry composition. Australian Journal of Grape and Wine Research **21**, 1-17.

Bonada, M., Sadras, V.O. and Fuentes, S. (2013a) Effect of elevated temperature on the onset and rate of mesocarp cell death in berries of Shiraz and Chardonnay and its relationship with berry shrivel. Australian Journal of Grape and Wine Research **19**, 87-94.

Bonada, M., Sadras, V.O., Moran, M. and Fuentes, S. (2013b) Elevated temperature and water stress accelerate mesocarp cell death and shrivelling, and decouple sensory traits in Shiraz berries. Irrigation science **31**, 1317-1331.

Bondada, B.R., Matthews, M.A. and Shackel, K.A. (2005) Functional xylem in the post-veraison grape berry. Journal of Experimental Botany **56**, 2949-2957.

Caravia, L., Collins, C., Petrie, P.R. and Tyerman, S.D. (2016) Application of shade treatments during Shiraz berry ripening to reduce the impact of high temperature. Australian Journal of Grape and Wine Research **22**, 422-437.

Caravia, L., Collins, C. and Tyerman, S.D. (2015) Electrical impedance of Shiraz berries correlates with decreasing cell vitality during ripening. Australian Journal of Grape and Wine Research **21**, 430-438.

Coombe, B.G. (1995) Growth Stages of the Grapevine: Adoption of a system for identifying grapevine growth stages. Australian Journal of Grape and Wine Research **1**, 104-110.

Cramer, G.R., Ergül, A., Grimplet, J., Tillett, R.L., Tattersall, E.A., Bohlman, M.C., Vincent, D., Sonderegger, J., Evans, J. and Osborne, C. (2007) Water and salinity stress in grapevines: early and late changes in transcript and metabolite profiles. Functional & Integrative Genomics **7**, 111-134.

Cruz de Carvalho, M.H. (2008) Drought stress and reactive oxygen species: production, scavenging and signaling. Plant Signaling & Behavior **3**, 156-165.

Findlay, N., Oliver, K.J., Nil, N. and Coombe, B.G. (1987) Solute accumulation by grape pericarp cells IV. Perfusion of pericarp apoplast via the pedicel and evidence for xylem malfunction in ripening berries. Journal of Experimental Botany **38**, 668-679.

Flexas, J., Bota, J., Escalona, J.M., Sampol B. and Medrano, H. (2002) Effects of drought on photosynthesis in grapevines under field conditions: an evaluation of stomatal and mesophyll limitations. Functional Plant Biology **29**, 461-471.

Flexas, J., Bota, J., Galmés, J., Medrano, H., and Ribas-Carbó, M. (2006) Keeping a positive carbon balance under adverse conditions: responses of photosynthesis and respiration to water stress. Physiologia Plantarum **127**, 343-352.

Franck, C., Lammertyn, J., Ho, Q.T., Verboven, P., Verlinden, B. and Nicolaï, B.M. (2007) Browning disorders in pear fruit. Postharvest Biology and Technology **43**, 1-13.

Fuentes, S., Sullivan, W., Tilbrook, J. and Tyerman, S. (2010a) A novel analysis of grapevine berry tissue demonstrates a variety-dependent correlation between tissue vitality and berry shrivel. Australian Journal of Grape and Wine Research **16**, 327-336.
Fuentes, S., Sullivan, W., Tilbrook, J. and Tyerman, S. (2010b) A novel analysis of grapevine berry tissue demonstrates a variety-dependent correlation between tissue vitality and berry shrivel. Australian Journal of Grape and Wine Research **16**, 327-336.
Geigenberger, P. (2003) Response of plant metabolism to too little oxygen. Current Opinion in Plant Biology **6**, 247-256.
Greer, D.H. and Rogiers, S.Y. (2009) Water flux of Vitis vinifera L. cv. Shiraz bunches throughout development and in relation to late-season weight loss. American Journal of Enology and Viticulture 60, 155-163.
Hardie, W. and Considine, J. (1976) Response of grapes to water-deficit stress in particular stages of development. American Journal of Enology and Viticulture **27**, 55-61.
Harris, J., Kriedemann, P. and Possingham, J. (1971) Grape berry respiration: effects of metabolic inhibitors. Vitis **9**, 291-298.
Keller, M. and Shrestha, P.M. (2014) Solute accumulation differs in the vacuoles and apoplast of ripening grape berries. Planta **239**, 633-642.
Keller, M., Smith, J.P. and Bondada, B.R. (2006) Ripening grape berries remain hydraulically connected to the shoot. Journal of Experimental Botany **57**, 2577-2587.
Kozlowski, T. and Pallardy, S. (2002) Acclimation and adaptive responses of woody plants to environmental stresses. The Botanical Review **68**, 270-334.
McCarthy, M.G. (1997) The effect of transient water deficit on berry development of cv. Shiraz (Vitis vinifera L.). Australian Journal of Grape and Wine Research **3**, 2-8.
Noctor, G. and Foyer, C.H. (1998) Ascorbate and glutathione: keeping active oxygen under control. Annual Review of Plant Biology **49**, 249-279.
Ojeda, H., Deloire, A. and Carbonneau, A. (2001) Influence of water deficits on grape berry growth. Vitis **40**, 141-146.
Perkins, S., Alexander, L. and Nairn, J. (2012) Increasing frequency, intensity and duration of observed global heatwaves and warm spells. Geophysical Research Letters **39**, 20.
Pfister-Sieber, M. and Braendle, R. (1994) Aspects of plant behaviour under anoxia and post-anoxia. Proceedings of the Royal Society of Edinburgh, Section B: Biological Sciences **102**, 313-324.
Pilati, S., Brazzale, D., Guella, G. ,Milli, A., Ruberti, C., Biasioli, F., Zottini, M. and Moser ,C. (2014) The onset of grapevine berry ripening is characterized by ROS accumulation and lipoxygenase-mediated membrane peroxidation in the skin. BMC Plant Biology **14**, 87.
Rawyler, A., Pavelic, D., Gianinazzi, C., Oberson, J. and Braendle ,R. (1999) Membrane lipid integrity relies on a threshold of ATP production rate in potato cell cultures submitted to anoxia. Plant Physiology **120**, 293-300.
Rogiers, S., Hatfield, J.M. and Keller, M. (2004a) Irrigation, nitrogen, and rootstock effects on volume loss of berries from potted Shiraz vines. Vitis **43**, 1-6.
Rogiers, S.Y., Greer, D.H., Hatfield, J.M., Orchard, B.A. and Keller M. (2006) Solute transport into Shiraz berries during development and late-ripening shrinkage. American Journal of Enology and Viticulture **57**, 73-80.
Rogiers, S.Y., Hatfield, J.M., Jaudzems, V.G., White, R.G. and Keller, M. (2004b) Grape berry cv. Shiraz epicuticular wax and transpiration during ripening and preharvest weight loss. American Journal of Enology and Viticulture **55**, 121-127.
Sadras, V.O., Bubner, R. and Moran, M.A. (2012) A large-scale, open-top system to increase temperature in realistic vineyard conditions. Agricultural and Forest Meteorology **154-155**, 187-194.

Sadras, V.O., Moran, M.A. and Petrie, P.R. (2017) Resilience of grapevine yield in response to warming. OENO ONE: Journal international des sciences de la vigne et du vin= International Journal of Vine and Wine Sciences **51**, 381-386.

Sasidharan, R., Bailey-Serres, J., Ashikari, M., Atwell, B.J., Colmer, T.D., Fagerstedt, K., Fukao, T., Geigenberger, P., Hebelstrup, K.H. and Hill, R.D. (2017) Community recommendations on terminology and procedures used in flooding and low oxygen stress research. New Phytologist **214**, 1403-1407.

Scharwies, J.D. and Tyerman, S.D. (2017) Comparison of isohydric and anisohydric Vitis vinifera L. cultivars reveals a fine balance between hydraulic resistances, driving forces and transpiration in ripening berries. Functional Plant Biology **44**, 324-338.

Šuklje, K., Zhang, X., Antalick, G., Clark, A.C., Deloire, A. and Schmidtke, L.M. (2016) Berry shriveling significantly alters Shiraz (Vitis vinifera L.) grape and wine chemical composition. Journal of Agricultural and Food Chemistry **64**, 870-880.

Thomson, C.J. and Greenway, H. (1991) Metabolic evidence for stelar anoxia in maize roots exposed to low O_2 concentrations. Plant Physiology **96**, 1294-1301.

Tilbrook, J. and Tyerman, S.D. (2008) Cell death in grape berries: varietal differences linked to xylem pressure and berry weight loss. Functional Plant Biology **35**, 173-184.

Tilbrook, J. and Tyerman, S.D. (2009) Hydraulic connection of grape berries to the vine: varietal differences in water conductance into and out of berries, and potential for backflow. Functional Plant Biology **36**, 541-550.

Tyerman, S.D., Tilbrook, J., Pardo, C., Kotula, L., Sullivan, W. and Steudle, E. (2004) Direct measurement of hydraulic properties in developing berries of Vitis vinifera L. cv Shiraz and Chardonnay. Australian Journal of Grape and Wine Research **10**, 170-181.

Verboven, P., Kerckhofs, G., Mebatsion, H.K., Ho, Q.T., Temst, K., Wevers, M., Cloetens, P. and Nicolaï, B.M. (2008) Three-Dimensional Gas Exchange Pathways in Pome Fruit Characterized by Synchrotron X-Ray Computed Tomography. Plant Physiology **147**, 518-527.

Wang, L.-J. and Li, S.-H. (2006) Thermotolerance and related antioxidant enzyme activities induced by heat acclimation and salicylic acid in grape (Vitis vinifera L.) leaves. Plant Growth Regulation **48**, 137-144.

Webb, L., Whetton, P. and Barlow E. (2007) Modelled impact of future climate change on the phenology of winegrapes in Australia. Australian Journal of Grape and Wine Research **13**, 165-175.

Williams, D., Andris, H., Beede, R., Luvisi, D., Norton, M. and Williams L. (1985) Validation of a model for the growth and development of the Thompson Seedless grapevine. II. Phenology. American Journal of Enology and Viticulture **36**, 283-289.

Xiao, Z., Rogiers, S., Sadras, V. and Tyerman S.D. (2018) Hypoxia in the grape berry linked to mesocarp cell death: the role of seed respiration and lenticels on the berry pedicel. Journal of Experimental Botany (in press)

Zabalza, A., van Dongen, J.T., Froehlich, A., Oliver, S.N., Faix, B., Gupta, K.J., Schmälzlin, E., Igal, M., Orcaray, L., Royuela, M. and Geigenberger P. (2009) Regulation of respiration and fermentation to control the plant Internal oxygen concentration. Plant Physiology **149**, 1087-1098.

Zufferey, V. (2016) Leaf respiration in grapevine (Vitis vinifera'Chasselas') in relation to environmental and plant factors. Vitis **55**, 65-72.

Chapter 4 Shade, rootstock and kaolin spray as possible mitigation strategies for berry cell death and berry shrivel in Shiraz

Zeyu Xiao[1 2], Lishi Cai[1 2], Xin Huang[1 2] and Stephen D. Tyerman[1 2]

[1]School of Agriculture, Food and Wine, Waite Research Institute, The University of Adelaide, PMB1, Glen Osmond, SA 5064, Australia.

[2]The Australian Research Council Training Centre for Innovative Wine Production, University of Adelaide, Glen Osmond, SA, Australia

Authorship declaration: All authors have contributed significantly, and all authors agree with the manuscript.

Corresponding author: Professor Stephen D. Tyerman, School of Agriculture, Food and Wine, Waite Research Institute, The University of Adelaide, PMB1, Glen Osmond, SA 5064, Australia. Email steve.tyerman@adelaide.edu.au; Phone: 0411776050

Acknowledgements

We thank Wendy Sullivan for expert technical assistance. This research was conducted by the Australian Research Council Training Centre for Innovative Wine Production (www.adelaide.edu.au/tc-iwp/), which is funded as a part of the ARC's Industrial Transformation Research Program (Project No IC130100005) with support from Wine Australia and industry partners.

Disclosure statement: Authors declare that there is no conflict of interest.

Running Title: Berry cell death and shrivel mitigation strategies

Statement of authorship

Statement of Authorship

Title of Paper	Shade, rootstock and kaolin spray as possible mitigation strategies for berry cell death and berry shrivel in Shiraz
Publication Status	☐ Published ☐ Accepted for Publication ☐ Submitted for Publication ☑ Unpublished and Unsubmitted work written in manuscript style
Publication Details	Intended to submit to Australian Journal of Grape and Wine Research.

Principal Author

Name of Principal Author (Candidate)	Zeyu Xiao
Contribution to the Paper	Contributed to experimental design, field measurements on the rootstock and kaolin trials, performed experiments on the shading trial, co-supervised the rootstock and kaolin trials, analysed the data and drafted the manuscript.
Overall percentage (%)	40%
Certification:	This paper reports on original research I conducted during the period of my Higher Degree by Research candidature and is not subject to any obligations or contractual agreements with a third party that would constrain its inclusion in this thesis. I am the primary author of this paper.
Signature	Date 28/6/2017

Co-Author Contributions

By signing the Statement of Authorship, each author certifies that:

i. the candidate's stated contribution to the publication is accurate (as detailed above);

ii. permission is granted for the candidate in include the publication in the thesis; and

iii. the sum of all co-author contributions is equal to 100% less the candidate's stated contribution.

Name of Co-Author	Lishi Cai
Contribution to the Paper	Contributed to experimental design, performed the experiments on the rootstock trial and analysed the data.
Signature	Date 27/6/2017

Name of Co-Author	Xin Huang
Contribution to the Paper	Contributed to experiment design, performed the experiment on the kaolin trial and analysed the data.
Signature	Date 27/06/2017

Name of Co-Author	Steve Tyerman
Contribution to the Paper	Contributed to experimental design, supervised the research, assisted in analysing the data and editing the manuscript.
Signature	Date 28/06/2017

Abstract

Background and Aim: Berry cell death and dehydration (shrivel) in Shiraz during late ripening can be accelerated by drought and high temperature. In order to provide possible mitigation strategies to the industry for berry cell death and dehydration three preliminary trials were undertaken: Trial 1 (T1) tested the effect of overhead shading on berry dehydration, cell death and internal oxygen concentrations [O_2], since previously it had been shown that shading could reduce cell death, and in a separate study, that cell death could be correlated to hypoxia in the berry. Trial 2 (T2) tested the effect of rootstocks having different drought tolerance on berry dehydration and cell death. Trial 3 (T3) tested the effect of kaolin spray, which has been proposed to reduce leaf and cluster temperature and transpiration.

Methods and Results: For T1 berries were sampled from an overhead shade treatment (62% absorption, from veraison) since this had the most consistent high temperature mitigation according to a previous study. For T2 berries were sampled from Shiraz scions on three rootstocks differing in drought tolerance (Schwartzman, Ruggeri 140 and 420 A). For T3, Shiraz vines were treated with a kaolin spray (and mock control). For T2 and T3, vine water status, leaf gas exchange, and berry ripening evolution were measured from veraison to harvest. For T1 previous research had reported vine water relations. For all experiments the progression of mesocarp cell vitality was determined and correlated with loss of berry mass. Additionally [O_2] profiles were examined for T1.

Both kaolin treatments resulted in a significant increase in berry mass compared with control vines, while only T2 showed a significant decrease in photosynthesis (light saturation) at a given stomatal conductance corresponding to a trend of lower TSS accumulation over time. Cell vitality measured with a vital stain decreased linearly with time after peak berry mass was reached for all treatments. No significant difference in leaf and berry temperature, leaf gas exchange, water status, TSS and berry vitality were detected between treatments."

Conclusion: Overhead shading can reduce the rate of increase in cell death and berry dehydration in Shiraz. This treatment also affects the progression of hypoxia in the berry. Shiraz on the drought tolerant 140 Ruggeri had significantly less cell death and berry dehydration than the less tolerant rootstocks. Kaolin spray application can reduce berry shrinkage independently of mesocarp cell death, and independently of berry and leaf temperature.

Significance of Study: There are potential mitigation strategies for reducing mesocarp cell death and berry dehydration in Shiraz. Use of drought tolerant rootstocks and kaolin application from veraison to harvest show promise but further research is required across multiple seasons on both rootstocks and kaolin treatments and their effects on berry oxygen concentration.

Keywords: *Vitis vinifera, berry, cell death, rootstock, shading, kaolin*

Introduction

Because of global warming, the ripening process of grapes grown in warmer regions has been advancing (earlier onset) and shortened into warmer months that have also increased frequencies of heatwaves (Jones 2007,Petrie and Sadras 2008,Rahmstorf and Coumou 2011,Sadras and Petrie 2012,Webb, et al. 2011). This can increase the rate of cell death in Shiraz berries and exacerbate berry dehydration (shrivel), since berry shrivel and cell death are correlated and are highly sensitive to increased temperature and drought stress (Bonada, et al. 2013). Shrivel can result in up to 30% yield loss during the late ripening stage of Shiraz (McCarthy 1999). Berry shrivel and cell death in Shiraz are also correlated with other berry quality parameters and ultimately can affect wine quality (Bonada, et al. 2013,Šuklje, et al. 2016).

Cell death has been suggested to be one cause for berry dehydration late in ripening, and this has been linked to hypoxia in the berry in response to water stress (Xiao, et al. 2018) (paper 2). Despite these advances in our knowledge of the phenomena, the wine industry has yet to receive clear mitigation strategies or even prediction methods for the occurrence of cell death and berry dehydration. Here we investigate three strategies that could impact on the occurrence of cell death and dehydration: shading to reduce temperature and water stress, root stocks to improve drought tolerance, and kaolin spray to reduce leaf and cluster temperature.

Shading of grapevines has been studied as a mitigation strategy for heat and solar radiation stress. Artificial shading using shade cloth can reduce canopy temperatures (Caravia, et al. 2016,Greer, et al. 2011,Greer, et al. 2010,Rojas-Lara and Morrison 1989) and also positively influence vine water status, however, the timing /duration and orientation of shading are important (Caravia *et al*., 2016). Carbon fixation of the vines can be reduced if shading is applied to whole canopy prior to the establishment of the canopy (Greer, et al. 2010). Cluster

shading can reduce skin tannins and flavonoid synthesis (Downey, et al. 2004,Oliveira, et al. 2014,Ristic, et al. 2007). Lower temperature caused by shading pre-flowering might also affect cell division during berry formation (Ebadi, et al. 1996). Nevertheless, overhead shade applied to Shiraz vines from veraison to harvest was found to delay berry cell death and dehydration so that resultant wines had lower alcohol but limited effects on other wine characteristics compared to unshaded controls (Caravia, et al. 2016). Given that cell death has been recently linked to hypoxia in the berry and that water stress can exacerbate this, we investigated berry internal [O_2] status and the link to berry cell death of overhead shaded berries compared to unshaded controls.

Grapevine rootstocks play important roles in increasing tolerance to both biotic and abiotic stress (Ferris, et al. 2012,Rosa, et al. 2011,Walker, et al. 2004,Wallis, et al. 2013). Rootstocks have been used in grapevine cultivation to increase drought tolerance (Serra, et al. 2014). Due to differences in root growth and physiological characteristics and root hydraulic conductance, rootstocks can affect the water retention of the scion (Gambetta, et al. 2012). Rootstock interaction with irrigation can affect yield (McCarthy, et al. 1997) and berry shrivel in Shiraz (Rogiers, et al. 2004). Here we investigated whether different rootstocks (Schwarzmann, Ruggeri 140 and 420 A) that have been reported to impart different drought tolerance to the scion (Soar, et al. 2006) can affect Shiraz berry dehydration and cell death.

Kaolin particle film has been applied to crops to mitigate biotic and abiotic stress including: protection from insect pests, limiting radiation and sunburn, reducing canopy temperature, and to increase photosynthesis (Glenn 2012,Glenn and Puterka 2005,Rosati, et al. 2007,Steiman, et al. 2007). In grapevines, kaolin was found to reduce canopy temperature by increasing reflection of solar radiation, and also to increase water use efficiency, but with variations between cultivars (Glenn, et al. 2010). Kaolin application was also found to improve berry anthocyanin accumulation in vines grown under water stressed and warm

conditions (Shellie and King 2013,Song, et al. 2012). Here we investigated the effectiveness of kaolin application on reducing Shiraz berry cell death and dehydration.

Materials and methods

Experimental site and vines

Shading trial

Shiraz (*Vitis vinifera* L.) vines (clone BVRC12) on own roots, planted in 1992, were studied in season 2014-2015, for the overhead shading experiment, at Coombe vineyard, Waite Campus, The University of Adelaide (34°58'03.12" S and 138°38'00.21"E). Vines were trained to a vertical shoot positioned trellis with north-south row orientation and vine and row spacing of 2.7 by 3 m respectively. The application of overhead shading treatment was as described in Caravia, et al. (2016) and the experiments reported herein were obtained from the season 3 Coombe vineyard trial as reported in Caravia et al. (2016). Briefly, overhead shading using shade cloth (Premium Hortshade, medium grade, Pacific, Braeside, Victoria, Australia), was imposed from veraison, 71 days after anthesis (DAA), to harvest. Standard irrigation and viticulture practices typical for the region were applied. Three replicates each containing one panel (two vines), located in different rows, with adjacent panels as controls without overhead shading, were used in this study.

Rootstocks and kaolin trial

Two studies were conducted in season 2016-2017 at Coombe vineyard, in the same vineyard block as above, examining the effects of different rootstocks and application of kaolin spray. Standard irrigation was applied to all vines. A total of 0.426 kilolitre/vine or 63.4 mm of water through dripper irrigation was applied during the growing season from December 2016 to March 2017. During this time the vineyard also received 119.4 mm of effective rainfall (sum of any event > 10 mm).

For the rootstock trial: Shiraz (clone BVCR12), planted in 1993, on Schwarzmann, 140 Ruggeri and 420 A rootstocks were used. For each rootstock, four replicates each comprising of two panels (4 vines in total), located in difference rows were used.

For the kaolin trial, Shiraz scion on Schwarzmann rootstock was used. Four replicates, located in different rows, each consisting of two vines were used for each treatment. Within each replicate, two kaolin treatments were imposed in two adjacent vines from the same panel and control (mock sprayed on canopy or cluster zone) were located in adjacent panels from the other four different rows. Treatments were: control (canopy), mock sprayed whole canopy with tap water only, control (cluster), mock sprayed cluster zone with tap water, cluster zone only sprayed with kaolin (cluster), and whole canopy sprayed with kaolin (canopy). A non-sprayed control corresponded to the Schwarzmann rootstock trial. Kaolin (Surround® WP, Phoenix, Arizona, USA) [$Al_4Si_4O_{10}(OH)_8$] has been described as "a white, non-porous, non-swelling, low-abrasive, fine-grained, plate-shaped, aluminosilicate mineral" (Glenn 2005). Following the manufacturers' recommendation, approximately 0.5 L of 5% (w/v) kaolin dissolved in tap water was applied every week to each vine in the appropriate treatment class and after each rainfall event during the entire experimental period. It was applied evenly to both west and east sides of the vines using a backpack power sprayer. For cluster treatment, all clusters including those labelled for sampling were fully and evenly covered by kaolin film. For canopy treatment, kaolin was evenly applied to the whole canopy providing kaolin coverage over leaves and clusters.

Berry sampling

For the overhead shading trial, berries were taken from 5 labelled clusters (exposed exterior facing) within each replicate. Two berries were sampled from the proximal, middle and distal parts of a cluster on the exterior exposed side of the pre-labelled clusters. This was done by cutting the pedicel at the rachis junction with fine sharp scissors.

For the rootstock trial, berry samples were taken from the centre 2 vines for each replicate. Four clusters were labelled on each vine, and 3 berries were collected on each cluster (proximal, middle and distal, exposed exterior facing) for cell vitality estimation. Another 50 berries (25 from each vine) were collected randomly from each replicate for berry mass and total soluble solids estimation.

For the kaolin trial, three clusters on one vine of each replicate were labelled. Three berries were collected on each cluster (proximal, middle and distal, exposed exterior facing) for cell vitality estimation. Another 25 berries from the other vine within each replicate were collected randomly from the vines for berry mass and total soluble solids estimation.

For all trials, sampling took place between 9:00 and 11:00 am (Australian Central Daylight Time, ACDT). Berries were stored in labelled sealable plastic bags, placed in an ice-cooled container in the field and for transfer to the laboratory. Once in the laboratory, berries were stored in the dark at 4 °C until measurements were made within 24 hours of sampling.

Solar radiation

A quantum sensor (SKP 216, Skye Instruments Ltd., Wales, UK) was used to determine the photosynthetically active radiation under or outside the overhead shading.

Leaf gas exchange

For the overhead shading trial, stomatal conductance was measured using a porometer (Model AP4, DeltaT Devices, Cambridge, England). For rootstock and kaolin trials, leaf gas exchange measurements, including net CO_2 assimilation at light saturation A_{sat} (photo flux density = 919 µmol/(m^2s) and stomatal conductance g_s, were carried out using an infrared gas analyser (IRGA) (LCpro-SD Portable Photosynthesis System, ADC BioScientific, Hoddesdon, England). All measurements were made between 11:00 and 14:00 (ACDT). For each replicate, one fully exposed and expanded leaf was measured. Measurements were takin

in random order regarding replicate and treatment, IRGA readings were taken 3 mins after enclosing the leaf in the measuring chamber.

Leaf and cluster temperatures

Leaf and cluster temperatures were measured using an infrared thermometer (Fluke 568). For each replicate, three random west-facing leaves and clusters, fully exposed to sunlight, were selected for temperature measurement at around 3 pm.

Grapevine water status

For both rootstock and kaolin trials, leaf (ψ_l) and stem (ψ_s) mid-day water potential were measured using a pressure chamber (PMS Instrument Company, model 1005, Albany, OR, USA) between 11:00 and 14:00 (ACDT). For each replicate, two mid-shoot, fully exposed and expanded leaves were selected. One leaf was enclosed in a foil covered plastic bag for 1 h before measurement for ψ_s. The non-bagged leaf was used for ψ_l measurement. Leaves were placed in the chamber within 5s after excision at the stem end of the petiole, and with foil bags for ψ_s.

Berry mass and total soluble solids

Fifty berries and 25 berries sampled from each replicate for the rootstocks and kaolin trials respectively, were weighed and crushed together to obtain average berry weight and TSS.

Berry cell vitality: electrical impedance and vital staining

On each sampling day, a total of 9, 16 and 12 berries, sampled from labelled clusters in each treatment from the overhead shading, rootstock and kaolin trials respectively were used to determine cell vitality using vital staining. Additionally, impedance of berries was measured in rootstock and kaolin trials on the same batches of berries. Individual berry mass was first recorded. Impedance spectroscopy was performed on each berry as described in Caravia, et al. (2015). Briefly, a thin slice of berry skin on opposite sides of the berry equator was

removed using a fresh razor blade. Two cut surfaces of the berry were clamped between two sliver chloride coated electrodes, connecting the berry to the circuit. A 0.1 M KCl solution was used between the contacting surfaces of berry and electrodes. Thickness of the berry tissue between the electrodes was measured using a micrometre screw gauge. Impedance was measured between 1 Hz and 1 MHz using an impedance meter (Bode 100, Vector Network Analyzer, OMICRON LAB, Hong Kong). After the impedance measurement, berries were stained, using 4.8 µM fluorescein diacetate (FDA) solution with osmolality similar to the grape juice (adjusted with sucrose), on the cut medial longitudinal surface for vital staining procedures (Fuentes, et al. 2010,Tilbrook and Tyerman 2008). Berries were incubated in the dark for 15 min. The stained berries were viewed under a Nikon SMZ 800 (Nikon Co., Toyko, Japan) dissecting microscope under ultraviolet light with a green fluorescent protein filter in place. Images were taken by a Nikon DS-5Mc digital camera (Tochigi Nikon Precision Co., Ltd, Otawara, Japan) and NIS-Elements F2.30 software with the same gain and exposure settings for all images. Images were analysed with a MATLAB (Mathworks Inc., Natick, MA, USA) script for determining berry cell vitality (Fuentes, et al. 2010).

Berry internal oxygen concentration

For the overhead shading trial, a subsample of three berries of each replicate was used to determine internal berry O_2 concentrations ($[O_2]$), measured using a Clark-type oxygen microelectrode with a tip diameter of 25 µm (OX-25; Unisense A/S, Aarhus, Denmark). The microelectrodes were calibrated in a zero $[O_2]$ solution (0.1M NaOH, 0.1M $C_6H_7NaO_6$) and an aerated Milli-Q water (272 µmol/L at 22 °C), as 100% $[O_2]$ solution. Individual berries (equilibrated to room temperature, 22 ^oC) were secured on the motorized manipulator stage. To aid the penetration of the microelectrode into the berry skin, a hole was initially made through the skin at the berry equator with a stainless steel syringe needle (19G), to a depth of 200 µm. The microsensor was positioned in the berry through this hole and profiles of $[O_2]$

were taken with depth towards the centre of the berry. Previous work had established that O_2 leakage around the site of skin penetration was insignificant (Xiao, et al. 2018). Berry profiles began from 0.2 mm under the skin with 0.1 mm steps to 1.5 mm towards the centre. The electrode was not moved further to avoid damaging the tip against a seed. Each measurement lasted 10s at each position. Between each position, stable signals were recorded within 20s. Measurements were carried out and recorded using the Unisense Suite software. Means and SEM of each step (n = 3) were calculated and [O_2] profiles were compiled using GraphPad Prism 7. After the [O_2] measurements, berry temperature was measured using an IR thermometer (Fluke 568) with a type-K thermocouple bead probe (Fluke 80PK-1). Berry diameters at the equator were determined using a digital calliper.

Statistical analysis

All data are presented as mean ± SEM. For overhead shading trial, t-test was used for vine physiology measurements. One-way ANOVA was used to determine difference in pruning weight affected by rootstocks. Two-way repeated measures ANOVA and Tukey's post-test were used for assessing treatment affects over time in the three trials.

One phase associations or linear regression were fit to leaf carbon fixation at light saturation (A_{sat}) as a function of stomatal conductance (g_s). Exponential decays were fit to berry mass affected by rootstock and kaolin, and impedance affected by rootstocks. Exponential associations were fit to sugar accumulation affected by rootstock, kaolin and shading, and mass loss affected by kaolin. Linear regressions were fit to berry mass affected by shading, TSS affected in all three trials, mass loss affected by rootstock, and living tissue affected by rootstock (segmental) and kaolin. Quadratic equations were fit to mass loss as a function of living tissue affected by rootstocks. Third order polynomial functions were fit to [O_2] as a function of depth in to the berry. The Michaelis–Menten equation was fit to the relationship between percentages of berry living tissue and mean [O_2]. The Extra Sum-of-Squares F-test

was applied to test the differences of the fits between treatments. All analyses were performed in Graphpad Prism 7 (Graphpad Software, La Jolla, CA, USA). A difference was taken as being significant when $P<0.05$.

Results

Seasonal phenology and climate conditions

Full anthesis (stage EL 23) (Coombe 1995) occurred on 27 October in 2014 (shade trial) and 15 November in 2016 (rootstock/kaolin trial). Veraison occurred at around 67 DAA (shade trial) and 65 DAA (rootstock/kaolin trial). Total rainfall from flowering to 130 DAA was 68.4 (shade trial) and 178.8 mm (rootstock/kaolin trial) (Figure S1). The number of days with maximum temperature above 40 °C during the ripening period was 4 days (shade trial) and 6 days (rootstock/kaolin trial) (Figure S1).

Vine physiology

Rootstock resulted in some variations in water status and gas exchange of the Shiraz scion. Stomatal conductance (g_s) measured at 80 DAA for Schwarzmann was lower than 140 Ruggeri. 420 A showed lower ψ_s and lower A_{sat} than 140 Ruggeri at 80 DAA (Table 1). No difference was observed on other tested days (62 and 104 DAA) amongst rootstocks in midday stem and leaf water potential, g_s or A_{sat} (Table 1). For g_s ($P<0.0001$) and A_{sat} ($P<0.0001$) across rootstocks there was a significant decline during the measurement period that corresponded to a decline in ψ_s ($P<0.0001$) and ψ_l ($P<0.0001$). There were variations in scion canopy development between rootstocks as determined by pruning weights with 140 Ruggeri having higher pruning weights than the other two root stocks (Figure S2), but this was not statistically significant ($P=0.215$).

Kaolin treatment reduced A_{sat} at 80 DAA by 2-fold for canopy treated vines compared to cluster zone treated vines (P=0.012, Tukey's test), although no difference was found between the canopy treatment and the two control mock sprayed or the dry vines (Table 2). g_s of cluster zone treated vines was higher than that of the dry control vines on 80 DAA (Table 2). No difference was observed amongst kaolin treatments in ψ_s and ψ_l, g_s or A_{sat} on 62, 80 and 104 DAA except that mentioned above (Table 2). As for the rootstock results there was a general decline g_s, A_{sat}, ψ_s and ψ_l during the measurement period.

Cluster and leaf temperature measured at 86, 91 and 101 DAA did not differ amongst kaolin treatments (Table 2, Dry Control not measured)).

Light saturated photosynthesis (A_{sat}) as a function of g_s could be fit by an exponential association equation that did not differ between rootstocks (Figure 1a). Linear regressions fit best to A_{sat} versus g_s for the different kaolin treatments (except dry control, see Schwarzmann Figure 1a) and did not differ (Figure 1b).

Overhead shading treatment reduced photosynthetically active radiation by 66% from 1752.0 ± 19.7 to 587.3 ± 12.3 mmol m^{-2} s^{-1} (Table 3). This corresponded to a decrease in leaf temperature but g_s was increased by the overhead shade treatment (Table 3).

Berry ripening

The development over time of berry mass, total soluble solids (TSS), and sugar per berry are compared between treatments for the three trials in Figure 2. There was no difference in the rate of increase in berry mass amongst rootstocks and the decline in mass after the peak in mass could be fit to an exponential decay that did not differ between rootstocks (Figure 2a). A similar decline in mass was observed for the kaolin trial, where kaolin treatment compared to mock-sprayed controls showed significant difference between the fitted equations and a

smaller decline in mass (Figure 2b). The overhead shade treatment showed no significant effect on berry mass.

Berries from Schwarzmann rootstock had higher TSS over the ripening time-course compared to the other two rootstocks (2-way repeated measures ANOVA) and significant differences between the fitted linear regressions were observed (Figure 2d). No difference was found in TSS over time between kaolin or shading treatments (Figure 2e,f). The accumulation of sugar per berry was reduced in berries from 420 A compared to Scharwzmann and there was a significant difference between the fitted exponential associations (Figure 2g). No difference was found in the accumulation of sugar per berry between kaolin or shading treatments (Figure 2h, i).

Berry relative loss of mass and cell death

For the three trials, percentage loss of berry mass relative to the peak in mass, and the decline in living tissue during late ripening are compared in Figure 3. Berries from 420 A rootstock showed more percentage loss of mass compared to 140 Ruggeri (Figure 3a). Berries from kaolin sprayed vines showed less loss of mass compared to berries from control vines (Figure 3b). There was no difference between control and shaded berries in the percentage loss of mass (Figure 3c).

In the latter stages of ripening, living tissue was reduced in all three trials (Figure 3d,e,f). For the rootstock trial two clear phases of decline in living tissue could be delineated consisting of a slow and fast phase (Figure 3d). There were significant differences between the slope of the fast phase of decline in living tissue, with Scharzmann and 420 A showing a faster decline against time (DAA) compared to 140 Ruggeri. For the kaolin trial no significant difference was observed in the decline of living tissue between treatments. For the shading

trial there was a significantly smaller decline in living tissue for the shaded treatment compared to control.

Detection of living tissue using electrical impedance (Caravia *et al.* 2015) showed similar results to the vital stain technique for the rootstock trial where lower impedance was found in Scharwzmann compared to 140 Ruggeri in latter stages of ripening (Figure 4a), however no clear reduction in impedance was observed in the kaolin trial that would indicate substantial cell membrane damage and solute leakage. A reduced decline in electrical impedance was previously reported for the shade treatment in Caravia *et al* (2016).

The loss of mass relative to peak mass was correlated with berry living tissue for the rootstock trial (Figure 5). Significantly higher elevation of the fitted quadratic equations for loss of mass versus living tissue was found for 420 A compared to the other two rootstocks, indicating that for a given degree of cell death there was a greater degree of loss of mass for shiraz berries on the 420 A rootstock. Loss of berry mass was not correlated with living tissue in the kaolin trial as can be seen from inspection of Figure 3 b&e, however it is clear that for the same degree of cell death there was less loss of mass in the kaolin treatment. Insufficient data was obtained in the shading trial for this analysis.

Berry oxygen profiles for the shading trial

Oxygen concentration as a function of depth into the berry was only determined for the shading trial, and [O_2] profiles are shown for this trial at different sampling dates in Figure 6. Berries were sampled four times from after veraison (72 DAA) to pre-harvest (114 DAA). At all sample times, in both control and shaded berries, [O_2] decreased steeply with depth. On 85 and 99 DAA, third order polynomial functions were fit to the profiles and comparison of fitted curves by Extra Sum-of-Squares F-test indicated berries from shaded vines showed a different evolution of [O_2] profiles where [O_2] was on average lower in shaded berries than

control berries (Figure 6b,c). However this difference diminished when berries reached 114 DAA since one curve was found to adequately fit both [O_2] profiles of shaded and control berries (Figure 6d). The associations between berry living tissue and mean [O_2] (0.2 to 1.5 mm depth) are shown in Figure 7. Michaelis-Menten curves best fit living tissue as a function of mean [O_2] as was observed in an earlier experiment (Xiao *et al.* unpubl. data, 2018). Significantly different fits were obtained between shaded and control with shaded berries giving a low apparent K_d. This indicated that at intermediate mean [O_2] concentrations within the berry there was greater cell death in the control (unshaded treatment) than the shaded treatment.

Discussion

Here we report on preliminary trials of possible mitigation strategies that may be used to alter the evolution of cell death and berry dehydration leading to shrivel in Shiraz berries. Although it is not yet clear what causes cell death, there is good evidence that hypoxia within the berry is strongly associated with it (Xiao, et al. 2018). This hypoxia and potentially other compounding phenomena such as unregulated ROS accumulation and high ethanol concentrations may cause cell death as detected by vital stains and electrical impedance. Hypoxia within the berry mesocarp can be the result of high respiration rates at high temperature, or as a result of water stress, but anatomical changes that influence the diffusivity of O_2 within the berry are also important. In particular the lenticels on the berry pedicel were previously shown to be a major uptake pathway for O_2 into the berry (Xiao, et al. 2018). Therefore treatments, such as spray formulations, that may affect O_2 diffusion via lenticels and treatment effects on the development of internal airspaces in the berry may also impact on cell death. The link between cell death and berry dehydration is also correlative (Fuentes, et al. 2010), however, loss of membrane integrity and semi-permeability is very likely to reduce the ability of the large mesocarp cells to retain water via osmosis against the

negative tensions in the apoplast generated by the vine or berry transpiration (Scharwies and Tyerman 2017,Tilbrook and Tyerman 2008). Therefore we investigated treatments that could reduce temperature and water stress. These were: shading that reduces temperature and water stress; rootstocks that may reduce water stress or affect cluster shading, and kaolin spray formulation that may reduce leaf and cluster temperature.

Overhead shading

Overhead shading was previously reported to have the most consistent high temperature mitigation compared to other orientations of shade (Caravia, et al. 2016). In that study it was also shown that the rate of decline in berry cell vitality was reduced by overhead shade. Here we extended the Caravia, et al. (2016) study to investigate how berry [O_2] may be involved in the response. Overhead shade reduced PAR by 66% in this study and subsequently decreased leaf temperature by an average of 4 °C. This substantial reduction in temperature, particularly if there is a heatwave event, could ameliorate the potential physiological and biochemical stress on the vine. Interestingly, stomatal conductance doubled (measured on one occasion) in the shaded and cooler leaves. This is consistent with the more extensive and multiple season study of Caravia, et al. (2016). Despite the increase in g_s overall evaporative demand might be reduced by shading, which could potentially improve water status of the vines (Caravia, et al. 2016). Here we found that cell death of berries was reduced by shading consistent with Caravia, et al. (2016), but this did not translate to a significant difference in loss of berry mass in contrast to the previous study.

Contrary to expectations of the effect of reduced temperature under shade, we found that internal [O_2] for shaded berries at intermediate stages of ripening were significantly lower (more hypoxic) relative to that of the unshaded control (Figure 6). Otherwise the progression to lower and more hypoxic conditions in the pericarp as ripening progressed is consistent with previous studies (Xiao, et al. 2018) (paper 2). The difference between shaded and

unshaded berries was greatest at 99 DAA, which is normally when the rapid onset of cell death occurs (Figure 3). Respiration is highly dependent on temperature and O_2 availability. Higher temperature in the unshaded clusters should result in higher O_2 demand due to higher respiration rates, assuming O_2 diffusion and uptake were the same for control and shaded berries and that no acclimation occurred. One important pathway for berry O_2 uptake is via the lenticels on the berry pedicels. These lignified woody structures act as pores and regulate gas and vapour exchange between the atmosphere and internal tissue (Xiao, et al. 2018), and their development may be affected by the shade treatment. That some acclimation had occurred is inferred by our observation that the Michaelis-Menten fits to cell death as a function of mean [O_2] concentration within the berry were different between shaded and unshaded treatments. This indicated that shaded berries have a lower degree of cell death at the same [O_2] concentration than the unshaded berries. Unexpectedly we found that the shaded treatment was more similar to the previously determined global fit for cell death versus mean [O_2] in an unshaded experiment (Xiao *et al.*, unpubl. data, 2018). This difference may result from different Shiraz clones used between the two studies or different seasonal conditions.

Rootstocks

Some rootstocks have been consistently reported to increase drought tolerance of the scion, though the mechanisms for the effect are complex and not fully understood (Serra, et al. 2014). According to Serra, et al. (2014)the drought tolerance of Schwarzmann based on its origin as *V. riparia x V. rupestris*, would be poor-medium as is listed in online reports (e.g. UC Davis Rootstock selection: http://iv.ucdavis.edu/files/24347.pdf). 140 Ruggeri on the other hand is listed as having medium to high drought tolerance by three separate classifications (Serra et al., 2014). 420 A was classified as weak/sensitive also from three separate classifications (*ibid*). Thus the order of increasing drought tolerance of the

rootstocks used in our study is 420 A, Schwarzmann, 140 Ruggeri. Although we did not impose a drought treatment, a consistent seasonal drought effect was evident as indicated by declining g_s and stem and leaf water potentials during the season (Table 1). The relative decline in stomatal conductance was greatest for Schwarzmann (73%), intermediate for 420A (52%) and least for 140 Ruggeri (33%).

Some significant differences in vine water status and gas exchange were observed between rootstocks at 80 DAA. 420 A showed lower midday stem water potential than 140 Ruggeri indicating that the vines on 420 A might be under more stress. This is confirmed by the lower photosynthetic rate of 420 A compared to 140 Ruggeri. Despite some of these expected differences between root stock water relations, the responses of A_{sat} to g_s of the three rootstocks were similar (Figure 1a) perhaps indicating that leaf CO_2 diffusion properties and CO_2 fixation biochemistry were not greatly modified by rootstock.

Schwarzmann showed higher TSS throughout the entire period, compared to both 140 Ruggeri and 420 A, which did not differ from each other. 420 A also showed lower sugar per berry compared to Schwarzmann. Rootstock is known to affect sugar accumulation and rate of berry ripening of the same grafted variety (Corso, et al. 2016). However, the affected sugar accumulation by rootstock seemed to have limited correlation with vigour, since pruning mass did not differ amongst rootstocks (Supplementary Figure S2). Berry mass of the three rootstocks throughout the entire time was similar. However, 420 A showed an overall higher percentage of mass loss after peak mass was reached, compared to 140 Ruggeri. Although Shiraz vines on different rootstocks did not appear to have greatly different water stress towards the end of ripening, more water back-flow from 420 A berries might have occurred and 420 A showed higher mass loss compared to the other two rootstocks at similar level of living tissue (Figure 5). Rapid cell death was initiated around 94 DAA for the three rootstocks and then subsequently occurred at different rates (Figure 3d). Interestingly the rate

of decline in vitality (increase in cell death) was least in the most drought tolerant rootstock (140 Ruggeri) and this correlated with the least loss of mass. On individual sampling dates, 140 Ruggeri had more living tissue than the other rootstocks on 110 DAA and Schwarzmann on 119 DAA. This is also possibly linked to differences in water stress between the rootstocks, since the rate of cell death can be increased by water stress after cell death is initiated (Bonada, et al. 2013). We cannot exclude however, the possibility that chemical signals from the rootstocks are also involved (Serra, et al. 2014). Impedance spectroscopy measurements showed on the last sampling day that Schwarzmann berries had the lowest impedance, which indicates a higher level of membrane leakage (Caravia, et al. 2015).

Kaolin spray treatment

Kaolin particle film has been reported to reduce leaf surface temperatures on a variety of horticultural crops (Cantore, et al. 2009,Denaxa, et al. 2012,Wand, et al. 2006), Sauvignon Blanc berry temperature (Coniberti, et al. 2013) and the occurrence of temperatures over 30^{o}C in Malbec berries under reduced irrigation, but this depended on berry orientation (Shellie and King 2013). In our trial we did not find a significant decrease in leaf or berry surface temperature in response to kaolin treatment (Table 2). This is inconsistent with work on grapevine or other crops, showing kaolin application decrease the temperature of leaves and canopies (Glenn, et al. 2010,Rosati 2007). However, the effectiveness of reducing leaf and canopy temperature may also depend on other factors, such as ambient maximum temperature. For example, Tworkoski, et al. (2002) showed kaolin successfully reduced canopy temperature when ambient temperature did not exceed 30 °C. Some differences in vine water status and gas exchange were found between control and treatments. Midday leaf water potential of the full canopy treatment was lower than mock sprayed control on 104 DAA, indicating a higher stress level of canopy treated vines. There was a consistent reduction in both g_s and A_{sat} in response to kaolin treatment. Reduced assimilation has been

found previously for Malbec grapevine (Shellie and King 2013), and reduced gs has been observed in grapevine depending on cultivar (Glenn, et al. 2010). Kaolin forms a film on the grapevine leaves that increases reflection of photosynthetically active radiation (PAR) and reduces absorption of light (Rosati, et al. 2007). Kaolin film may reduce leaf photosynthesis by reflecting and blocking PAR, however if the light is already saturating photosynthesis then reduced absorption of PAR should not have a large effect depending on the degree of reduced absorption. The reflection effect of kaolin, may better distribute PAR within the canopy, which may compensate the reduced light absorption and lowered photosynthesis of the outer canopy (Rosati, et al. 2007). It is also possible that the kaolin film may physically block stomatal pores restricting CO_2 diffusion. There was no effect of kaolin on sugar accumulation in the berries indicating that if assimilation was reduced this was not sufficient to affect carbon allocation. This is consistent with a previous report on kaolin effects on Malbec (Shellie and King 2013).

Kaolin treatment had no effect on the increase in berry mass over the course of the sampling period, but there was a clear reduction in the percentage loss of mass relative to peak mass. This may be the result of reduced sunburn on the berries, which could lead to berry dehydration (Krasnow, et al. 2010). Similarly, kaolin application has been found to reduce the severity of sunburn in other fruits (Bell, et al. 2006,Cantore, et al. 2009) and grape berry dehydration (Lobos, et al. 2015). Despite reducing berry dehydration, kaolin showed no effect on the change of berry cell vitality throughout the sampling period, thereby uncoupling the normal correlation between cell death and berry dehydration (Fuentes, et al. 2010,Tilbrook and Tyerman 2008). It is possible that kaolin application reduced berry transpiration thereby slowing the dehydration that would normally occur with increasing cell death.

Conclusions

Overhead shading can reduce the rate of increase in cell death and berry dehydration in Shiraz. This treatment also affects the progression of hypoxia in the berry, but it appears to be not directly linked to temperature, rather, higher order acclimation appears to be occurring that affects the response of cell death to hypoxia in the berry. Rootstocks are a promising avenue for further research since they are becoming more common in combating abiotic stress in commercial viticulture. The more drought tolerant 140 Ruggeri has significantly less cell death and berry dehydration than the less tolerant rootstocks. Treatment with kaolin reflective film, despite the unexpected lack of effect on berry surface temperature, did reduce the loss of berry mass independently of cell death. Further research is required across multiple seasons on both rootstocks and kaolin treatments and their effects on berry oxygen concentration.

Figures

Table 1. Effect if rootstock on grapevine water potential and gas exchange properties during 2016-2017 season.

DAA	Schwarzmann	140 Ruggeri	420 A
Midday stem water potential (ψs) (MPa)			
62	-0.86 ± 0.03	-0.88 ± 0.04	-0.92 ± 0.03
80	-1.07 ± 0.06ab	-0.92 ± 0.05a	-1.15 ± 0.08b
104	-1.1 ± 0.05	-1.25 ± 0.08	-1.09 ± 0.03
Midday leaf water potential (ψl) (MPa)			
62	-1.13 ± 0.07	-1.12 ± 0.04	-1.18 ± 0.05
80	-1.31 ± 0.05	-1.26 ± 0.06	-1.44 ± 0.03
104	-1.38 ± 0.06	-1.49 ± 0.05	-1.32 ± 0.07
Stomatal conductance (g_s) (mmol m^{-2} s^{-1})			
62	188 ± 27	116 ± 38	213 ± 47
80	65 ± 19a	193 ± 30b	125 ± 47ab
104	50 ± 12	78 ± 18	103 ± 20
Photosynthetic rate (A_{sat}) (µmol m^{-2} s^{-1})			
62	10.9 ± 0.5	10 ± 1	11.5 ± 1.3
80	9.4 ± 0.9ab	13.4 ± 1a	9.2 ± 1.2b
104	3.7 ± 0.9	6.9 ± 1.6	7.5 ± 1.5

Values are (mean ± SEM) (n=4). Different letters are significantly difference between rootstocks on each sampling date (P<0.05) (Two-way repeated measures ANOVA, Tukey's test).

Table 2. Effect of kaolin spray treatment on Shiraz scion (Schwarzmann rootstock) water status, gas exchange properties, and cluster and leaf temperature.

DAA	Control* (no spray)	Control (canopy)	Control (cluster)	Cluster	Canopy
			Midday stem water potential (ψ_s) (MPa)		
62	-0.86 ± 0.03	-1.01 ± 0.03	-0.96 ± 0.05	-0.88 ± 0.04	-0.94 ± 0.03
80	-1.07 ± 0.06	-1.12 ± 0.05	-1.2 ± 0.07	-1.13 ± 0.04	-1.16 ± 0.09
104	-1.1 ± 0.05	-1.13 ± 0.03	-1.16 ± 0.04	-1.27 ± 0.05	-1.23 ± 0.07
			Midday leaf water potential (ψ_l) (MPa)		
62	-1.13 ± 0.07	-1.18 ± 0.09	-1.16 ± 0.09	-1.17 ± 0.08	-1.1 ± 0.05
80	-1.31 ± 0.05	-1.46 ± 0.04	-1.46 ± 0.07	-1.47 ± 0.04	-1.49 ± 0.05
104	-1.38 ± 0.06	-1.36 ± 0.04	-1.41 ± 0.04	-1.57 ± 0.05	-1.6 ± 0.08
			Stomatal conductance (g_s) (mmol m^{-2} s^{-1})		
62	188 ± 27	183 ± 17	178 ± 11	150 ± 18	153 ± 27
80	65 ± 19a	108 ± 31ab	103 ± 13ab	153 ± 27b	85 ± 25ab
104	50 ± 12	93 ± 17	50 ± 12	93 ± 13	77 ± 27
			Photosynthetic rate (A_{sat}) (µmol m^{-2} s^{-1})		
62	10.9 ± 0.5	11.4 ± 0.9	10.6 ± 0.4	9.9 ± 1	10.4 ± 1.4
80	9.4 ± 0.9ab	8.3 ± 1.7ab	8.8 ± 0.7ab	10.6 ± 1.4a	5.4 ± 0.3b
104	3.7 ± 0.9	6 ± 1.7	3.7 ± 0.9	4.8 ± 1.1	4.8 ± 1.1
			Cluster temperature (T_c) (°C)		
86	NM	37.8 ± 0.5	38.1 ± 0.6	37.9 ± 0.7	37.8 ± 0.4
91	NM	33.8 ± 1.8	34.3 ± 0.8	33.3 ± 1.5	32.9 ± 1.2
101	NM	28.5 ± 0.6	26.9 ± 0.8	29.1 ± 0.9	27.9 ± 0.8
			Leaf temperature (T_l) (°C)		
86	NM	35.7 ± 0.4	33.0 ± 1.2	36.4 ± 0.2	35.5 ± 1.1
91	NM	31.5 ± 1.1	31.7 ± 1.3	29.1 ± 0.6	29.6 ± 1.2
101	NM	26.2 ± 1.0	27.3 ± 0.4	26.6 ± 0.2	27.6 ± 1.0

Values (mean ± SEM) (n=4) followed by different letters are significantly different between treatments on each sampling date (P<0.05) (Two-way repeated measures ANOVA, Tukey's test)

*Same data as for Schwarzmann rootstock trial

NM = not measured

Table 3. Effect of shading treatment on Shiraz stomatal conductance, leaf temperature and photosynthetically active radiation at top of canopy on 80 DAA.

	Control	**Shaded**
g_s (mmol m^{-2} s^{-1})	537 ± 97a	1091 ± 122b
T_l (°C)	31.6 ± 0.4a	27.9 ± 0.1b
Photosynthetically active radiation (μmol m^{-2} s^{-1})	1752.0 ± 19.7a	587.3 ± 12.3b

Values (mean ± SEM) (n=3) followed by different letters are significantly different (P<0.05, t-test).

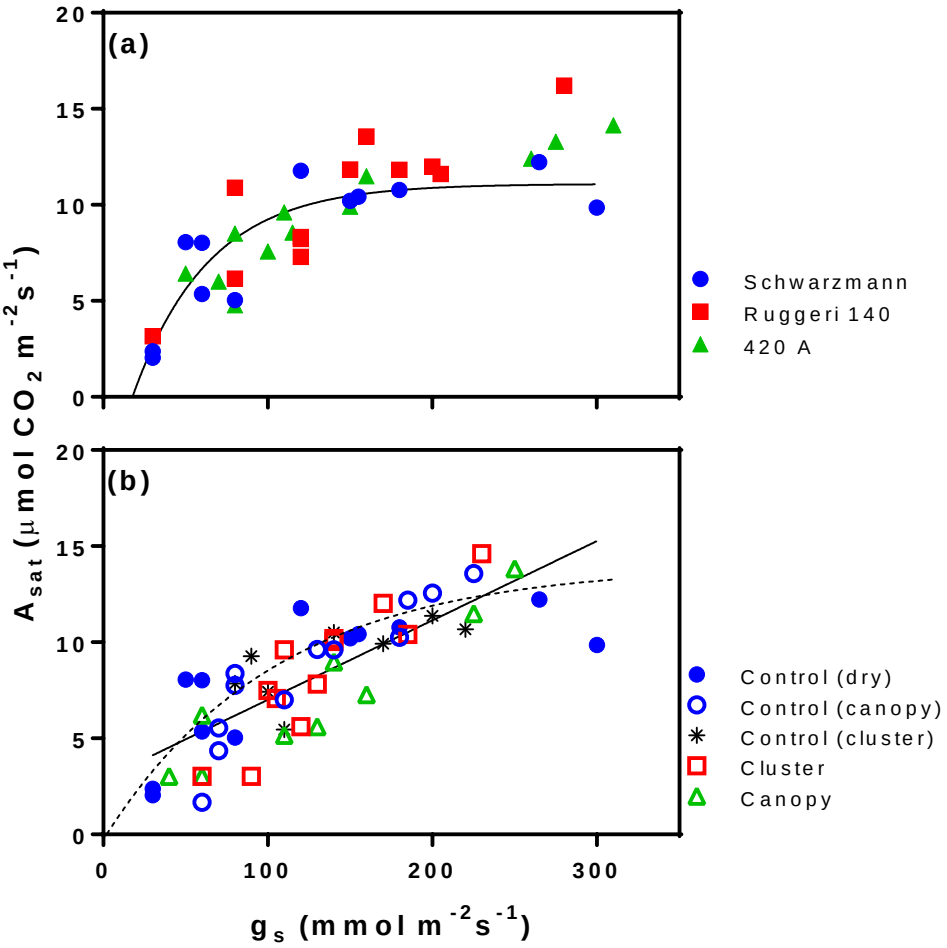

Figure 1. Shiraz leaf carbon fixation at light saturation (A_{sat}) as a function of stomatal conductance (g_s) as affected by rootstocks (a), and kaolin spray treatment (b). One regression line ($A_{sat} = 0.274 + (13.99-0.274) \times (1-\exp(-0.00961 \times g_s))$) is shown in (a), as the regressions for three rootstocks were not significantly different (Extra Sum-of-Squares F-Test, P=0.52). For the kaolin treatments linear regressions fit better to the data than exponential associations and there was no difference between the fitted equations for the kaolin spray treatments (Extra Sum-of-Squares F-Test, P=0.0507) ($A_{sat} = 2.881 + 0.0413 \times g_s$). The regression from the rootstock is reproduced in (b) (dashed line). Control (dry) in (b) and Schwarzmann (a) are the same data.

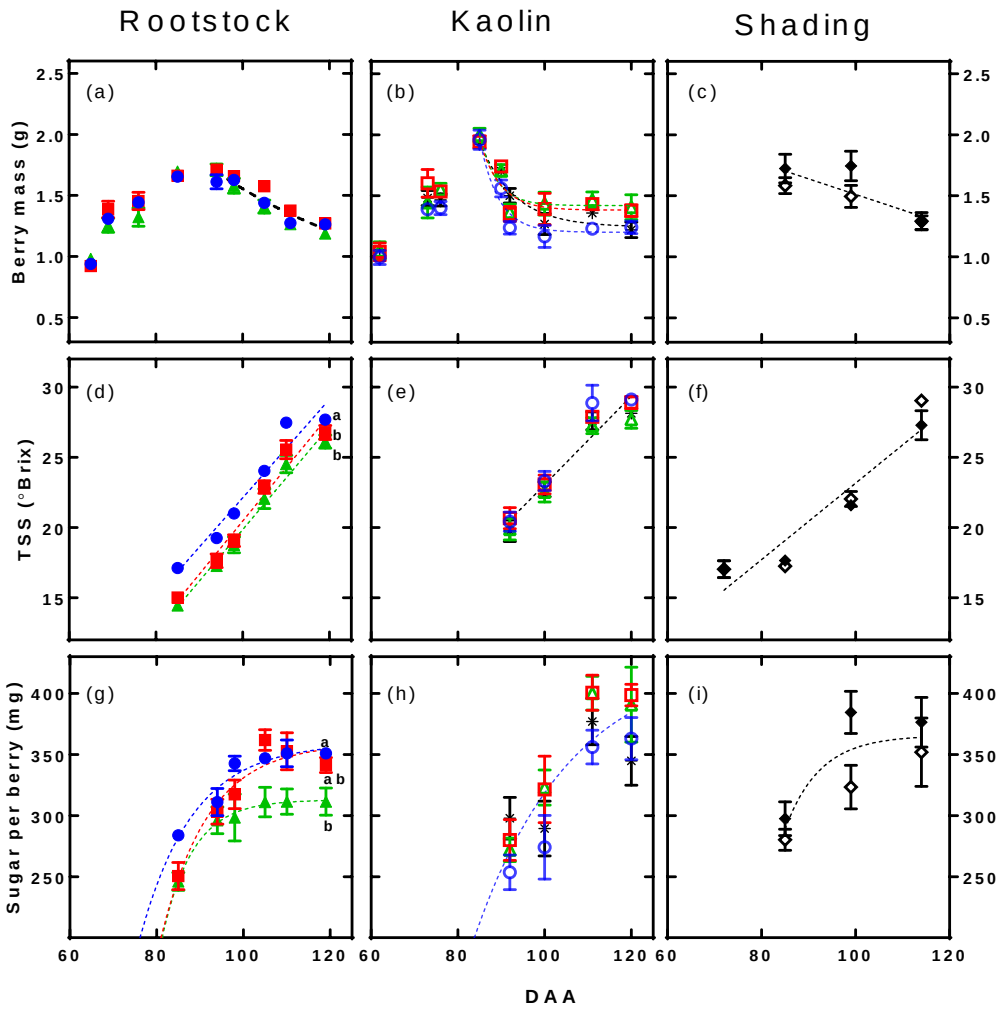

Figure 2. Shiraz berry ripening evolution showing the effect of rootstock (a,d,g), kaolin spray treatments (b,e,h), and overhead shading (c,f,i) on berry mass, TSS and sugar per berry. Rootstocks: Schwarzmann (●), 140 Ruggeri (■) and 420 A (▲). Kaolin spray: control (canopy) (○), whole canopy (△), control (cluster) (*) and cluster (□). Shading: control (◊) and overhead shading (◆). Each point is mean ± SEM (n=4 except in c,f and i n=3). Different letters indicate difference between rootstocks over the entire period (Two-way repeated measures ANOVA, $P<0.05$). Fitted lines are exponential decays in a,b; straight lines in d,e,f; exponential associations in g,h,f. Where more than one curve is shown there was a significant difference between the fits. For the loss of mass after peak mass observed for

rootstocks and kaolin treatments only kaolin treatments showed a difference (less decrease in mass) (Extra Sum-of-Squares F-test, $P = 0.009$).

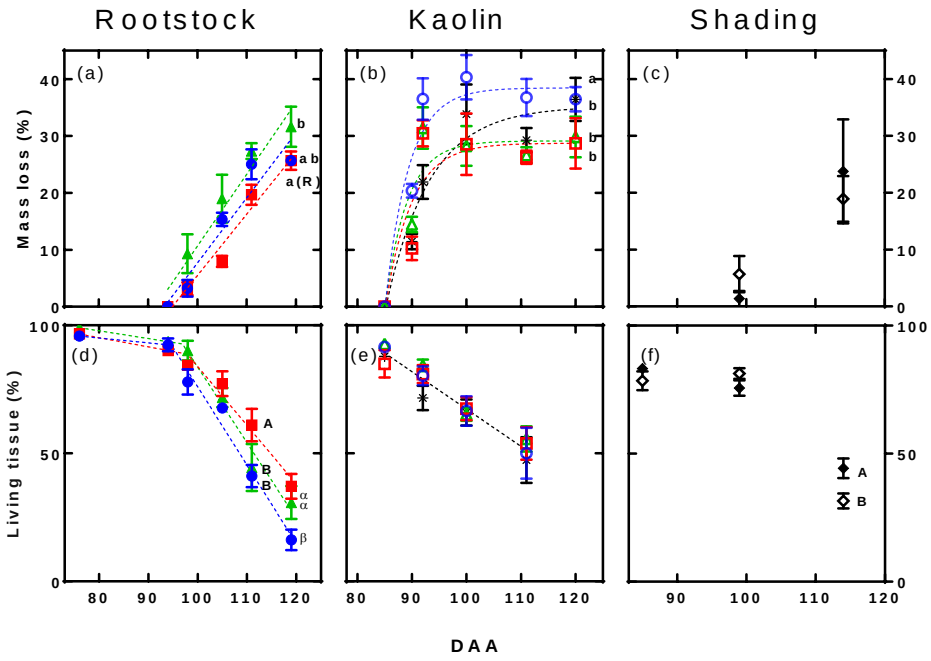

Figure 3. Evolution of Shiraz berry percentage loss of mass relative to peak in mass and living tissue showing the effect of rootstock (a,d), kaolin spray treatments (b,e), and overhead shading (c,f). Rootstock: Schwarzmann (●), 140 Ruggeri (■) and 420 A (▲). Kaolin spray: control (canopy) (○), whole canopy (△), control (cluster) (*) and cluster (□). Overhead shade: control (◊) and overhead shaded (◆).Each point is mean ± SEM (n=4 except in c and f n=3). Lower case letters indicate differences between rootstocks or kaolin treatments over the entire period (2-way repeated measures ANOVA, $P<0.05$). Upper case letters and Greek letters indicate differences within rootstocks or between shading treatments at single sampling days (2-way repeated measures ANOVA, $P<0.05$, Tukey's test). Fitted lines are linear regression (a,e), exponential associations (b) and segmental linear regression (d). Where more than one curve is shown there was a significant difference between the fits (Extra Sum-of-Squares F test, $P<0.05$).

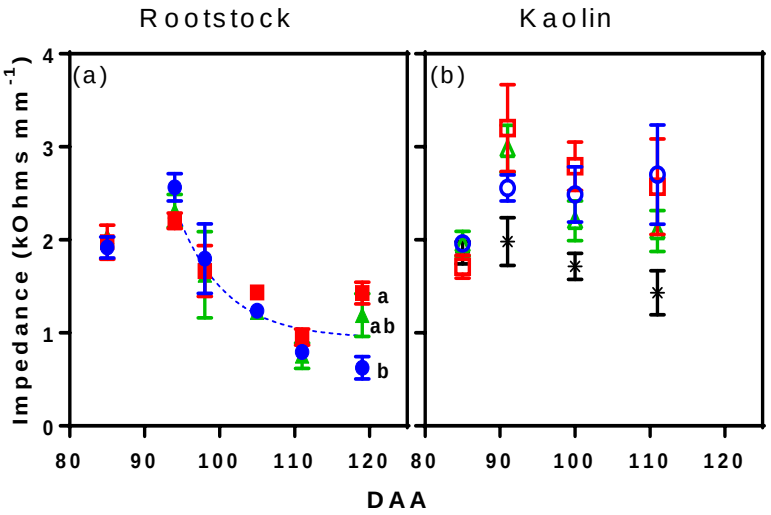

Figure 4. Evolution of Shiraz berry impedance per unit diameter showing the effect of rootstock (a), kaolin spray treatments (b). (a) Rootstocks: Schwarzmann (●), 140 Ruggeri (■) and 420 A (▲). (b) Kaolin spray treatment: control (○), bunch zone (□) and whole canopy (△). Each point is mean ± SEM (n=4). Different lower-case letters indicate difference between rootstocks at single sampling day (2-way repeated measures ANOVA, $P<0.05$). Regression in (a) is exponential decay fit to combined data.

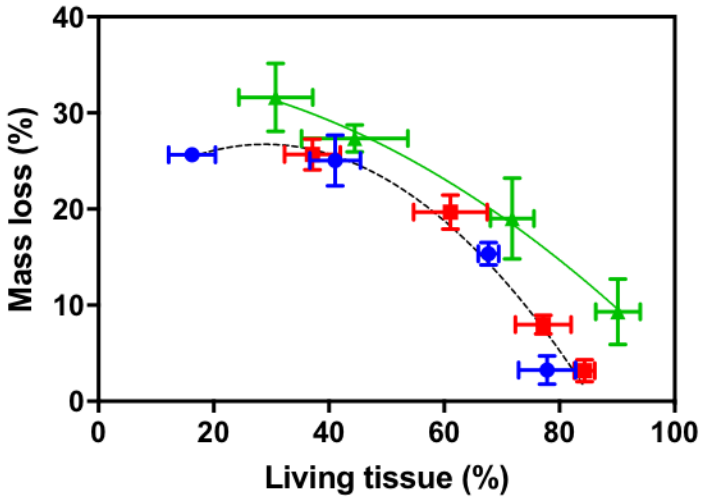

Figure 5. Loss of mass of berries as a function of living tissue of rootstocks, Schwarzmann (●), 140 Ruggeri (■) and 420 A (▲). Regressions are quadratic equations where Schwarzman and 140 Ruggeri show no significant difference (one combined curve is shown), but 420A is significantly different from the other two rootstocks (Extra Sum-of-Squares F-Test $P<0.05$). Each point is mean ± SEM (n=4).

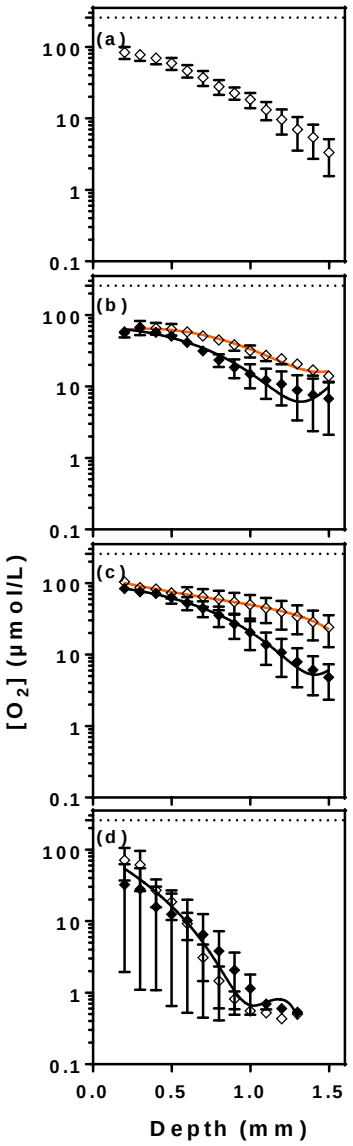

Figure 6. [O_2] profiles (log scale) from 0.2 mm beneath the skin to 1.5 mm (1.3 mm in (d)) towards the centre of the berry at different stages of development for control and overhead shaded Shiraz. Sampling times in season 2014-2015 were 72 (a), 85 (b), 99 (c), 114 (d) DAA. Dashed lines indicate the approximate O_2 saturation value for water at 25 °C. Control (◊) and overhead shaded (◆). Third order polynomial functions were fit to the data for each treatment in (b,c,d). Each point is mean ± SEM (n=3). Where separate curves are shown (b,c), the fitted lines were significantly different by F-test (P<0.05).

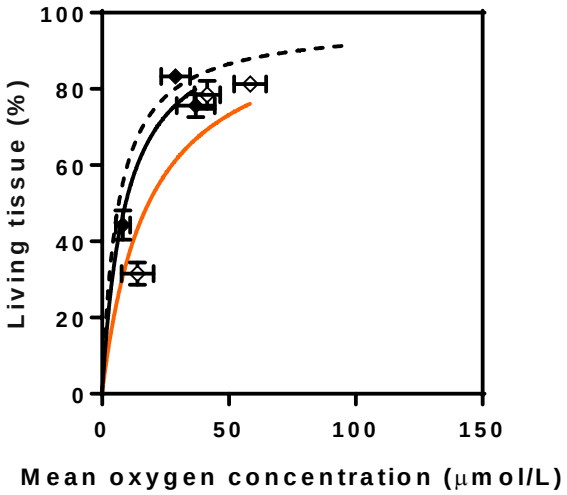

Figure 7. Dependence of berry living tissue on mean [O_2] from 0.2 mm to 1.5 mm depth from the surface of the berry. Control (◊) and overhead shaded (◆). Fitted curves are Michaelis-Menten equations: Living Tissue (LT)=LT_{max}*[O_2]/(K_d + [O_2]). Fits are different for control (unshaded, orange solid line) (R^2 =0.81) and shaded (black solid line) (R^2 =0.85) berries (P=0.02). LT_{max} = 100 for both treatments, K_d = 18.3 ± 9.7 (SE) for control and K_d = 9.3 ± 3.0 (SE) for shaded. Dashed line is Shiraz from another site (Xiao et al. unpubl. data 2018).

Supplementary materials

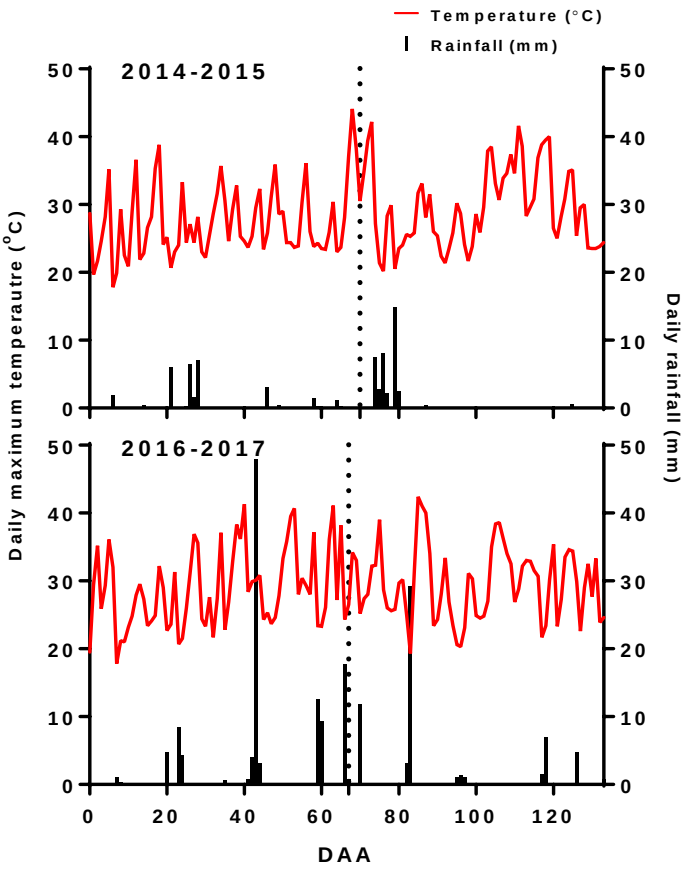

Figure S1. Maximum daily temperature and daily rainfall during season 2014-2015 and 2016-2017 in Adelaide (Kent Town weather station). Dashed black lines indicates day after anthesis (DAA) for veraison in the two seasons for Shiraz grown in the Coombe vineyard.

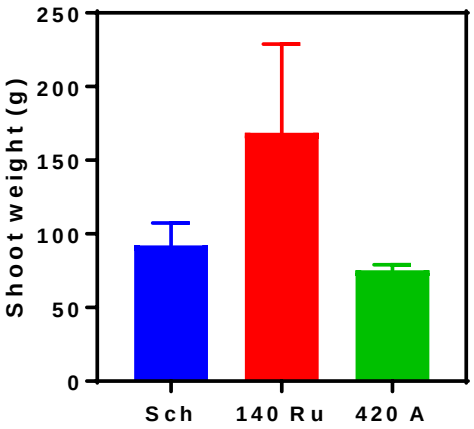

Figure S2. Effect of rootstocks, Schwarzmann (Sch), 140 Ruggeri (140 Ru), 420 A, on shoot pruning weight. Mean ± SEM (n=4). No difference found amongst rootstocks (One-way ANOVA, Tukey's test).

Literature cited

Bell, D., Ortiz V, R., Scott, C., and Phillips, N. Surround ® crop protectant for the reduction of sunburn damage and heat stress in pineapple. (International Society for Horticultural Science (ISHS), Leuven, Belgium: 179-184.

Bonada, M., Sadras, V., Moran, M., and Fuentes, S. (2013) Elevated temperature and water stress accelerate mesocarp cell death and shrivelling, and decouple sensory traits in Shiraz berries. Irrigation Science **31**, 1317-1331.

Cantore, V., Pace, B., and Albrizio, R. (2009) Kaolin-based particle film technology affects tomato physiology, yield and quality. Environmental and Experimental Botany **66**, 279-288.

Caravia, L., Collins, C., Petrie, P.R., and Tyerman, S.D. (2016) Application of shade treatments during Shiraz berry ripening to reduce the impact of high temperature. Australian Journal of Grape and Wine Research **22**, 422-437.

Caravia, L., Collins, C., and Tyerman, S. (2015) Electrical impedance of Shiraz berries correlates with decreasing cell vitality during ripening. Australian Journal of Grape and Wine Research **21**, 430-438.

Caravia, L., Collins, C., and Tyerman, S.D. (2015) Electrical impedance of Shiraz berries correlates with decreasing cell vitality during ripening. Australian Journal of Grape and Wine Research **21**, 430-438.

Coniberti, A., Ferrari, V., Dellacassa, E., Boido, E., Carrau, F., Gepp, V., and Disegna, E. (2013) Kaolin over sun-exposed fruit affects berry temperature, must composition and wine sensory attributes of Sauvignon blanc. European Journal of Agronomy **50**, 75-81.

Coombe, B.G. (1995) Growth Stages of the Grapevine: Adoption of a system for identifying grapevine growth stages. Australian Journal of Grape and Wine Research **1**, 104-110.

Corso, M., Vannozzi, A., Ziliotto, F., Zouine, M., Maza, E., Nicolato, T., Vitulo, N., Meggio, F., Valle, G., Bouzayen, M., Müller, M., Munné-Bosch, S., Lucchin, M., and Bonghi, C. (2016) Grapevine Rootstocks Differentially Affect the Rate of Ripening and Modulate Auxin-Related Genes in Cabernet Sauvignon Berries. Frontiers in Plant Science **7**, 69.

Denaxa, N.-K., Roussos, P.A., Damvakaris, T., and Stournaras, V. (2012) Comparative effects of exogenous glycine betaine, kaolin clay particles and Ambiol on photosynthesis, leaf sclerophylly indexes and heat load of olive cv. Chondrolia Chalkidikis under drought. Scientia horticulturae **137**, 87-94.

Downey, M.O., Harvey, J.S., and Robinson, S.P. (2004) The effect of bunch shading on berry development and flavonoid accumulation in Shiraz grapes. Australian Journal of Grape and Wine Research **10**, 55-73.

Ebadi, A., May, P., and Coombe, B.G. (1996) Effect of short-term temperature and shading on fruit-set, seed and berry development in model vines of V. vinifera, cvs Chardonnay and Shiraz. Australian Journal of Grape and Wine Research **2**, 1-8.

Ferris, H., Zheng, L., and Walker, M. (2012) Resistance of grape rootstocks to plant-parasitic nematodes. Journal of nematology **44**, 377.

Fuentes, S., Sullivan, W., Tilbrook, J., and Tyerman, S. (2010) A novel analysis of grapevine berry tissue demonstrates a variety-dependent correlation between tissue vitality and berry shrivel. Australian Journal of Grape and Wine Research **16**, 327-336.

Gambetta, G., Manuck, C., Drucker, S., Shaghasi, T., Fort, K., Matthews, M., Walker, M., and McElrone, A. (2012) The relationship between root hydraulics and scion vigour across Vitis rootstocks: what role do root aquaporins play? Journal of experimental botany **63**, 6445-6455.

Glenn, D. (2005) Use of Particle Film Technology,“Surround”, in Horticulture. Mew England Wegetable and Fruit Growers. Manchester **13**.
Glenn, D.M. (2012) The mechanisms of plant stress mitigation by kaolin-based particle films and applications in horticultural and agricultural crops. HortScience **47**, 710-711.
Glenn, D.M., Cooley, N., Walker, R., Clingeleffer, P., and Shellie, K. (2010) Impact of kaolin particle film and water deficit on wine grape water use efficiency and plant water relations. HortScience **45**, 1178-1187.
Glenn, D.M. and Puterka, G.J. (2005) Particle films: a new technology for agriculture. Horticultural reviews **31**, 1-44.
Greer, D.H., Weedon, M.M., and Weston, C. (2011) Reductions in biomass accumulation, photosynthesis in situ and net carbon balance are the costs of protecting Vitis vinifera 'Semillon' grapevines from heat stress with shade covering. AoB Plants **2011**, plr023.
Greer, D.H., Weston, C., and Weedon, M. (2010) Shoot architecture, growth and development dynamics of Vitis vinifera cv. Semillon vines grown in an irrigated vineyard with and without shade covering. Functional Plant Biology **37**, 1061-1070.
Jones, G.V. (2007) Climate change: observations, projections, and general implications for viticulture and wine production. Economics Department-working paper, 14.
Krasnow, M., Matthews, M., Smith, R., Benz, J., Weber, E., and Shackel, K. (2010) Distinctive symptoms differentiate four common types of berry shrivel disorder in grape. California Agriculture **64**, 155-159.
Lobos, G.A., VALDÉS-GÓMEZ, H., TAYLOR, J.A., and LAURIE, V.F. (2015) Effects of Kaolin-based particle film and fruit zone netting on Cabernet-Sauvignon grapevine physiology and fruit quality. J. Int. Sci. Vigne Vin **49**, 137-144.
McCarthy, M.G. (1999) Weight loss from ripening berries of Shiraz grapevines (Vitis vinifera L. cv. Shiraz). Australian Journal of Grape and Wine Research **5**, 10-16.
McCarthy, M.G., Cirami, R.M., and Furkaliev, D.G. (1997) Rootstock response of Shiraz (Vitis vinifera) grapevines to dry and drip-irrigated conditions. Australian Journal of Grape and Wine Research **3**, 95-98.
Oliveira, M., Teles, J., Barbosa, P., Olazabal, F., and Queiroz, J. (2014) Shading of the fruit zone to reduce grape yield and quality losses caused by sunburn. Journal International des Sciences de la Vigne et du Vins **48**, 179-187.
Petrie, P.R. and Sadras, V.O. (2008) Advancement of grapevine maturity in Australia between 1993 and 2006: putative causes, magnitude of trends and viticultural consequences. Australian Journal of Grape and Wine Research **14**, 33-45.
Rahmstorf, S. and Coumou, D. (2011) Increase of extreme events in a warming world. Proceedings of the National Academy of Sciences **108**, 17905-17909.
Ristic, R., Downey, M.O., Iland, P.G., Bindon, K., Francis, I.L., Herderich, M., and Robinson, S.P. (2007) Exclusion of sunlight from Shiraz grapes alters wine colour, tannin and sensory properties. Australian Journal of Grape and Wine Research **13**, 53-65.
Rogiers, S., Hatfield, J., and Keller, M. (2004) Irrigation, nitrogen, and rootstock effects on volume loss of berries from potted Shiraz vines. VITIS-GEILWEILERHOF- **43**, 1-6.
Rojas-Lara, B. and Morrison, J.C. (1989) Differential effects of shading fruit or foliage on the development and composition of grape berries. Vitis **28**, 27-63.
Rosa, C., Jimenez, J.F., Margaria, P., and Rowhani, A. (2011) Symptomatology and effects of viruses associated with Rugose Wood complex on growth of four different rootstocks. American Journal of Enology and Viticulture, ajev. 2011.10104.
Rosati, A. (2007) Physiological effects of kaolin particle film technology: A review. Funct. Plant Sci. Biotech. **1**, 100-105.

Rosati, A., Metcalf, S.G., Buchner, R.P., Fulton, A.E., and Lampinen, B.D. (2007) Effects of kaolin application on light absorption and distribution, radiation use efficiency and photosynthesis of almond and walnut canopies. Annals of Botany **99**, 255-263.
Sadras, V. and Petrie, P. (2012) Predicting the time course of grape ripening. Australian Journal of Grape and Wine Research **18**, 48-56.
Scharwies, J.D. and Tyerman, S.D. (2017) Comparison of isohydric and anisohydric Vitis vinifera L. cultivars reveals a fine balance between hydraulic resistances, driving forces and transpiration in ripening berries. Functional Plant Biology **44**, 324-338.
Serra, I., Strever, A., Myburgh, P., and Deloire, A. (2014) the interaction between rootstocks and cultivars (Vitis vinifera L.) to enhance drought tolerance in grapevine. Australian Journal of Grape and Wine Research **20**, 1-14.
Shellie, K.C. and King, B.A. (2013) Kaolin particle film and water deficit influence malbec leaf and berry temperature, pigments, and photosynthesis. American Journal of Enology and Viticulture **64**, 223-230.
Soar, C.J., Dry, P.R., and Loveys, B.R. (2006) Scion photosynthesis and leaf gas exchange in Vitis vinifera L. cv. Shiraz: Mediation of rootstock effects via xylem sap ABA. Australian Journal of Grape and Wine Research **12**, 82-96.
Song, J., Shellie, K.C., Wang, H., and Qian, M.C. (2012) Influence of deficit irrigation and kaolin particle film on grape composition and volatile compounds in Merlot grape (Vitis vinifera L.). Food Chemistry **134**, 841-850.
Steiman, S.R., Bittenbender, H.C., and Idol, T.W. (2007) Analysis of kaolin particle film use and its application on coffee. HortScience **42**, 1605-1608.
Šuklje, K., Zhang, X., Antalick, G., Clark, A.C., Deloire, A., and Schmidtke, L.M. (2016) Berry Shriveling Significantly Alters Shiraz (Vitis vinifera L.) Grape and Wine Chemical Composition. Journal of agricultural and food chemistry **64**, 870-880.
Tilbrook, J. and Tyerman, S.D. (2008) Cell death in grape berries: varietal differences linked to xylem pressure and berry weight loss. Functional Plant Biology **35**, 173-184.
Tworkoski, T.J., Michael Glenn, D., and Puterka, G.J. (2002) Response of bean to applications of hydrophobic mineral particles. Canadian journal of plant science **82**, 217-219.
Walker, R.R., Blackmore, D.H., Clingeleffer, P.R., and Correll, R.L. (2004) Rootstock effects on salt tolerance of irrigated field-grown grapevines (Vitis vinifera L. cv. Sultana) 2. Ion concentrations in leaves and juice. Australian Journal of Grape and Wine Research **10**, 90-99.
Wallis, C.M., Wallingford, A.K., and Chen, J. (2013) Grapevine rootstock effects on scion sap phenolic levels, resistance to Xylella fastidiosa infection, and progression of Pierce's disease. Frontiers in Plant Science **4**, 502.
Wand, S.J., Theron, K.I., Ackerman, J., and Marais, S.J. (2006) Harvest and post-harvest apple fruit quality following applications of kaolin particle film in South African orchards. Scientia horticulturae **107**, 271-276.
Webb, L., Whetton, P., and Barlow, E. (2011) Observed trends in winegrape maturity in Australia. Global Change Biology **17**, 2707-2719.
Xiao, Z., Rogiers, S., Sadras, V., and Tyerman, S.D. (2018) Hypoxia in grape berries: the role of seed respiration and lenticels on the berry pedicel and the possible link to cell death. Journal of experimental botany.

Chapter 5 General discussion

The growth and development of grape (*Vitis vinifera* L.) berries follows a double sigmoid pattern that can be delineated into three main phases as outlined previously; the last phase, that of berry shrinkage, is marked by loss of water and concentration of sugars and is, depending on cultivar, correlated with loss of cell vitality within the pericarp (Coombe and McCarthy, 2000; Fuentes *et al.*, 2010; McCarthy and Coombe, 1999; Sadras and McCarthy, 2007; Tilbrook and Tyerman, 2008). This shrinkage (dehydration or shrivel), is particularly common in Shiraz growing in warm wine regions and is usually accompanied by cell death (Bonada *et al.*, 2013b). Cell death is characterized by a breakdown in cell membrane integrity that has been hypothesised as a phenological stage during berry ripening aiding seed dispersal in some cultivars (Caravia *et al.*, 2015; Clarke *et al.*, 2010; Fuentes *et al.*, 2010; Tilbrook and Tyerman, 2009). Cell death and late ripening berry shrivel can be modulated by temperature and drought (Bonada *et al.*, 2013a; Bonada *et al.*, 2013b). They are associated with altered chemical composition and sensory characteristics of the berries (Bonada *et al.*, 2013a; Suklje *et al.*, 2016). This thesis has provided new knowledge and understanding of the phenomenon of berry cell death during late ripening. Firstly, Chapter 2 described the possible physiological cause of cell death, the occurrence of hypoxia within the berries, during berry ripening of Chardonnay and Shiraz. Second, Chapter 3 showed how water stress and elevated temperature affect Shiraz berry cell death and internal oxygen status. Lastly, Chapter 4 reported on some preliminary trials for the mitigation of cell death and berry shrivel in Shiraz by examination of the effect of overhead shading, rootstocks and kaolin application.

Cell death during late ripening in berry mesocarp of *Vitis vinifera* L. is cultivar dependent and correlates with berry dehydration in some cultivars (Fuentes *et al.*, 2010). Late ripening dehydration and cell death are also modulated by temperature and drought. This is a concern for viticulture practice in warm regions. Because of global warming, the changing climate

might result in berries ripening under warmer months with more frequent stressful events such as heatwaves (Jones, 2007; Petrie and Sadras, 2008; Webb *et al.*, 2011). Cultivars such as Shiraz, that commonly show berry cell death can have up to 30% yield loss due to berry shrivel (McCarthy and Coombe, 1999). Oxygen is essential to normal cell function. However, oxygen availability in the parenchyma of the grape berry mesocarp might be limited by high internal respiration demand and low gas intake. In Chapter 2, berry internal [O_2] of Chardonnay, Shiraz and Ruby Seedless during berry ripening, was correlated with changes in berry cell vitality during ripening. There was a close similarity between the pattern of cell death across the berry mesocarp and [O_2] profiles where the central regions of the mesocarp had both the highest cell death and the lowest [O_2] in both Shiraz and Chardonnay berries. The roles of seed respiration and O_2 permeation through pedicel lenticels were examined. First, seeds contributed to berry respiration substantially around veraison but decreased to a negligible demand late in ripening. Both seeded cultivars showed substantial amounts of cell death during ripening, while Ruby Seedless grapes maintained higher levels of cell vitality as well as higher internal [O_2]. Second, lower lenticel surface area in Shiraz could be indicative of a greater restriction on O_2 uptake compared to Chardonnay. The increased ethanol concentration within Chardonnay berries after blocking pedicel lenticels confirmed that lenticels are indeed an important pathway for oxygen uptake, and that blocking these gas permeable structures can lead to increased hypoxia in the berry mesocarp. O_2 concentration increased towards the central axis corresponding to the presence of central air spaces visualised using x-ray micro-CT. These air spaces connect to the pedicel where lenticels are located, further confirming the critical function of lenticels for berry O_2 uptake especially at high temperatures when respiratory demand is high. The results provide a basis for explaining the cultivar differences in cell death due to the presence of seeds and differences in lenticel morphology and surface area.

Because cell death and berry shrivel are modulated by ambient temperature and water stress, as an extension of the findings in Chapter 2, the connection was explored between cell death and berry internal [O_2] in Shiraz berries grown under water and heat stress conditions in the field. Using micro-oxygen electrodes and micro X-ray CT analysis, Shiraz berry cell death was shown to be correlated with hypoxia in the mesocarp and decreased berry porosity (air spaces within the berry pericarp), perhaps induced by stress, that could potentially restrict the diffusion of O_2 and lead to hypoxia and cell death. Berry internal [O_2] decreased with both depth in Shiraz berry tissues and berry ripeness irrespective of growing conditions. The progression of cell death during berry ripening correlated with mean berry internal [O_2] across all growing conditions. Water stress decreased Shiraz berry internal [O_2] and increased ethanol accumulation and cell death. Total berry porosity decreased across the ripening period independent of treatment while locule cavity space increased. This suggested that earlier in ripening, Shiraz berry internal air spaces occur as fine pores and that later in ripening, locule air space becomes larger relative to the total berry volume. Air channels connected the internal air space to the pedicels, where lenticels occur at high density, similar to that which was observed Chardonnay berries using micro-CT in Chapter 2. This further confirmed the physiological importance of pedicel lenticels in gas exchange and oxygen uptake. Overall, the reduced berry internal [O_2] is related to the reduction in porosity and percentage of living tissue. Cell death, and by implication berry shrivel, are strongly linked to oxygen supply and demand. Potentially any biotic or abiotic stress that may influence oxidative processes, berry respiration or berry anatomy will likely impact on cell death, with implications for oenologically relevant berry traits.

Increased temperature advances the onset and increases the rate of CD in Chardonnay and Shiraz berries (Bonada *et al.*, 2013b). This could relate to the temperature dependence of respiration. In pear fruit it was shown that increasing temperature should strongly increase

respiration rate but not to affect the gas diffusion properties resulting in predicted very low core [O_2] (Ho *et al.*, 2009). In Chapter 2 the direct measures of berry mesocarp [O_2] profiles concur with this prediction. We also observed typical Q_{10} and activation energy for respiration of 2.47 and 2.27 for whole berry respiration rates between 10 and 40 ^oC for Chardonnay and Shiraz berries respectively, and blocking the pedicel lenticels at 40 ^oC that reduced respiration. Wine-grape berries ripen on the plant and can become considerably hotter than the surrounding air (Caravia *et al.*, 2016; Smart and Sinclair, 1976; Tarara *et al.*, 2008). Transient high temperatures would create a large respiratory demand and low [O_2] in the centre of the mesocarp as we observed. However, subsequent cooling during the night or during milder weather will reduce the respiratory demand and increase internal [O_2] if the diffusivity for O_2 remained the same. Water deficit can also modulate mesocarp CD and berry shrivel in Shiraz (Bonada *et al.*, 2013a). Under field conditions (Chapter 3), the effect of water stress was dominant in comparison to elevated canopy ambient temperature, causing the onset of cell death to be advanced. In contrast to Bonada *et al.* (2013a), elevated temperature did not affect berry cell death under the experimental conditions imposed. Notwithstanding differences in seasonal base temperatures and possible acclimation caused by long term heating, it is interesting to note the very large difference in the onset of cell death in thermal time between the Bonada *et al.* (2013a) and my study. In contrast, the onset of cell death in time after anthesis was the same for the two studies and consistent across many previous studies on Shiraz berry cell death (Tilbrook and Tyerman, 2008). This may suggest that cell death, and probably the development of hypoxia in the berry, although modulated by temperature and water stress, are strongly dependent on phenological timing relative to anthesis. How this timing could be "measured" by the berry/vine is not clear, but candidates could be day length or sugar accumulation in the berry.

Further research

Oxygen concentration increased towards the central axis in both Chardonnay and Ruby Seedless grapes. As ripening progressed, there was a reduction of [O_2] in the central axis in Chardonnay, however, this was not evident in Ruby Seedless. Differences in lenticel morphology could account for this difference in O_2 availability in the central axis region. Therefore, classification of cluster morphology (pedicel length and cluster compactness) could be integrated in to [O_2] monitoring during berry ripening across cultivars. Berry transpiration contributes to late ripening dehydration and might associate with the change of berry internal oxygen concentration. Oxygen status monitoring on berries attached to the vines in field conditions warrants further investigation. Furthermore, the resistance to hypoxia in table grape cultivars could result from genetic differences in metabolic regulation under hypoxia. The expression patterns and function of an important programmed cell death inhibitor gene *VvBAP1* during berry development under water stress have been reported by Cao *et al.* (unpublished 2018). *VvBAP1* inhibits cell death induced by ROS and is found to over expression in water stress berries (Cao *et al.* unpublished 2018). Further research could address the signal transduction mechanism of the upregulation of the gene and whether the expression of the gene and/or the triggering mechanism could be phenotypically different. The regulation of hypoxia-responsive genes was found to contribute to bud burst in grapevines, a highly oxygen-dependent development process (Meitha *et al.*, 2018). N-end rule of protein degradation is important in regulating expression of hypoxia related genes in plants, including grapevine (Gibbs *et al.*, 2011; Meitha *et al.*, 2018). Enhanced hypoxia-responsive ethylene responsive factor (HRE2) stability improves survival under hypoxia of *Arabidopsis* (Gibbs *et al.*, 2011). Haemoglobin is an important O_2 binding protein. Under hypoxia, maize root haemoglobin may contribute to maintaining ATP supply and to delay the onset of cell death (Sowa *et al.*, 1998). The increased level of haemoglobin enhances survival

under hypoxic stress in *Arabidopsis* (Hunt *et al.*, 2002). Hypoxia responsive protein levels and gene expressions in grape berries across cultivars during berry development warrant further investigation.

The function of key signalling molecules such as reactive oxygen species (ROS) and the role of potassium relating to grape berry cell death are yet to be defined. Plant tissue oxygen status plays important signalling roles in developmental regulation (Considine *et al.*, 2017; Gibbs *et al.*, 2011). Hydrogen peroxide accumulation and the modulation of reactive oxygen species (ROS) scavenging enzymes potentially play an important role in controlling grapevine development, notably during events such as budburst and berry veraison (Considine *et al.*, 2017; Pilati *et al.*, 2007; Sudawan *et al.*, 2016). ROS generation can be a signal in biotic and abiotic stress responses but can also be harmful causing oxidative stress (Noctor and Foyer, 1998). ROS generation is also linked with hypoxia in cells (Blokhina *et al.*, 2001). The oxidative burst during berry ripening has been associated with altered lipid metabolism (Pilati *et al.*, 2007) and large increases in expression of lipoxygenase genes occurs during ripening that may be important for flavour development (Podolyan *et al.*, 2010). Hypoxia-induced oxidative stress decreases lipid and membrane integrity (Blokhina *et al.*, 2001), the latter being clearly evident in most wine grape berries by vitality stains (Tilbrook and Tyerman, 2008). In the meantime, increased CD in Shiraz grapes can be reflected by decreased extracellular electrical resistance indicating electrolyte leakage (Caravia *et al.*, 2015). This leakage corresponds to the accumulation of potassium in the extracellular space of Merlot berries (Keller and Shrestha, 2014), a cultivar that also displayed cell death (Fuentes *et al.*, 2010). It has been speculated that potassium and ROS regulation might be strongly connected during berry development involving oxidative processes. Research in this direction will add to the understanding of berry ripening and senescence (Rogiers *et al.*, 2017).

Further field studies on the effect of application of kaolin and the use of rootstocks on cell death and berry shrivel are warranted. These would allow a more thorough examination of effectiveness of the kaolin and the performance of rootstocks in relation to berry water retention under drought and heat stress.

Chapter 6 Literature cited (literature review and general discussion)

Alexander LV, Arblaster JM. 2009. Assessing trends in observed and modelled climate extremes over Australia in relation to future projections. *International Journal of Climatology* **29**, 417-435.
Anwar SA, McKenry M, Ramming D. 2002. A search for more durable grape rootstock resistance to root-knot nematode. *American Journal of Enology and Viticulture* **53**, 19-23.
Bailey-Serres J, Voesenek L. 2008. Flooding stress: acclimations and genetic diversity. *Annual Review of Plant Biology* **59**, 313-339.
Becker T, Grimm E, Knoche M. 2012. Substantial water uptake into detached grape berries occurs through the stem surface. *Australian Journal of Grape and Wine Research* **18**, 109-114.
Beikircher B, Mayr S. 2013. Winter peridermal conductance of apple trees: lammas shoots and spring shoots compared. *Trees (Berlin, Germany : West)* **27**, 707-715.
Blokhina O, Virolainen E, Fagerstedt KV. 2003. Antioxidants, oxidative damage and oxygen deprivation stress: a review. *Annals of Botany* **91** 179-194.
Blokhina OB, Chirkova TV, Fagerstedt KV. 2001. Anoxic stress leads to hydrogen peroxide formation in plant cells. *Journal of Experimental Botany* **52**, 1179-1190.
Bonada M, Sadras V, Moran M, Fuentes S. 2013a. Elevated temperature and water stress accelerate mesocarp cell death and shrivelling, and decouple sensory traits in Shiraz berries. *Irrigation science* **31**, 1317-1331.
Bonada M, Sadras VO. 2015. Review: critical appraisal of methods to investigate the effect of temperature on grapevine berry composition. *Australian Journal of Grape and Wine Research* **21**, 1-17.
Bonada M, Sadras VO, Fuentes S. 2013b. Effect of elevated temperature on the onset and rate of mesocarp cell death in berries of Shiraz and Chardonnay and its relationship with berry shrivel. *Australian Journal of Grape and Wine Research* **19**, 87-94.
Bottcher C, Harvey KE, Boss PK, Davies C. 2013. Ripening of grape berries can be advanced or delayed by reagents that either reduce or increase ethylene levels. *Functional Plant Biology* **40**, 566-581.
Cadot Y, Minana-Castello MT, Chevalier M. 2006. Anatomical, histological, and histochemical changes in grape seeds from Vitis vinifera L. cv Cabernet franc during fruit development. *Journal of Agricultural and Food Chemistry* **54**, 9206-9215.
Caravia L, Collins C, Petrie PR, Tyerman SD. 2016. Application of shade treatments during Shiraz berry ripening to reduce the impact of high temperature. *Australian Journal of Grape and Wine Research* **22**, 422-437.
Caravia L, Collins C, Tyerman SD. 2015. Electrical impedance of Shiraz berries correlates with decreasing cell vitality during ripening. *Australian Journal of Grape and Wine Research* **21**, 430-438.
Carbonneau A. 1985. The early selection of grapevine rootstocks for resistance to drought conditions. *American Journal of Enology and Viticulture* **36**, 195-198.
Castellarin SD, Gambetta GA, Wada H, Krasnow MN, Cramer GR, Peterlunger E, Shackel KA, Matthews MA. 2016. Characterization of major ripening events during softening in grape: turgor, sugar accumulation, abscisic acid metabolism, colour development, and their relationship with growth. *Journal of Experimental Botany* **67**, 709-722.

Castellarin SD, Gambetta GA, Wada H, Shackel KA, Matthews MA. 2011. Fruit ripening in Vitis vinifera: spatiotemporal relationships among turgor, sugar accumulation, and anthocyanin biosynthesis. *Journal of experimental botany* **62**, 4345-4354.
Choat B, Gambetta GA, Shackel KA, Matthews MA. 2009. Vascular function in grape berries across development and its relevance to apparent hydraulic isolation. *Plant Physiology* **151**, 1677-1687.
Clarke SJ, Hardie WJ, Rogiers SY. 2010. Changes in susceptibility of grape berries to splitting are related to impaired osmotic water uptake associated with losses in cell vitality. *Australian Journal of Grape and Wine Research* **16**, 469-476.
Considine JA, Knox RB. 1979. Development and histochemistry of the cells, cell walls, and cuticle of the dermal system of fruit of the grape,Vitis vinifera L. *Protoplasma* **99**, 347-365.
Considine MJ, Diaz-Vivancos P, Kerchev P, Signorelli S, Agudelo-Romero P, Gibbs DJ, Foyer CH. 2017. Learning to breathe: developmental phase transitions in oxygen status. *Trends in plant science* **22**, 140-153.
Coombe BG. 1960. Relationship of growth and development to changes in sugars, auxins, and gibberellins in fruit of seeded and seedless varieties of Vitis Vinifera. *Plant Physiology* **35**, 241-250.
Coombe BG. 1973. The regulation of set and development of the grape berry. International Society for Horticultural Science (ISHS), Leuven, Belgium, 261-274.
Coombe BG. 1976. The Development of Fleshy Fruits. *Annual Review of Plant Physiology* **27**, 207-228.
Coombe BG. 1987. Distribution of solutes within the developing grape berry in relation to its morphology. *American Journal of Enology and Viticulture* **38**, 120-127.
Coombe BG. 1992. Research on development and ripening of the grape berry. *American Journal of Enology and Viticulture* **43**, 101-110.
Coombe BG, McCarthy MG. 2000. Dynamics of grape berry growth and physiology of ripening. *Australian Journal of Grape and Wine Research* **6**, 131-135.
Cramer GR, Ergül A, Grimplet J, Tillett RL, Tattersall EA, Bohlman MC, Vincent D, Sonderegger J, Evans J, Osborne C. 2007. Water and salinity stress in grapevines: early and late changes in transcript and metabolite profiles. *Functional & integrative genomics* **7**, 111-134.
Dai ZW, Vivin P, Barrieu F, Ollat N, Delrot S. 2010. Physiological and modelling approaches to understand water and carbon fluxes during grape berry growth and quality development: a review. *Australian Journal of Grape and Wine Research* **16**, 70-85.
Davies C, Robinson SP. 1996. Sugar accumulation in grape berries (cloning of two putative vacuolar invertase cDNAs and their expression in grapevine tissues). *Plant Physiology* **111**, 275-283.
Davis DD. 1980. Anaerobic metabolism and the production of organic acids. *Metabolism and Respiration*: Elsevier, 581-611.
De Freitas V, Glories Y, Monique A. 2000. Developmental changes of procyanidins in grapes of red Vitis vinifera varieties and their composition in respective wines. *American Journal of Enology and Viticulture* **51**, 397-403.
DellaPenna D, Pogson BJ. 2006. Vitamin synthesis in plants: tocopherols and carotenoids. *Annual Review of Plant Biology* **57**, 711-738.
Famiani F, Farinelli D, Palliotti A, Moscatello S, Battistelli A, Walker RP. 2014. Is stored malate the quantitatively most important substrate utilised by respiration and ethanolic fermentation in grape berry pericarp during ripening? *Plant Physiology and Biochemistry* **76**, 52-57.

Fuentes S, Sullivan W, Tilbrook J, Tyerman S. 2010. A novel analysis of grapevine berry tissue demonstrates a variety-dependent correlation between tissue vitality and berry shrivel. *Australian Journal of Grape and Wine Research* **16**, 327-336.
Fukao T, Bailey-Serres J. 2004. Plant responses to hypoxia - is survival a balancing act? *Trends in Plant Science* **9**, 449-456.
Gadjev I, Stone JM, Gechev TS. 2008. Chapter 3: Programmed Cell Death in Plants: New Insights into Redox Regulation and the Role of Hydrogen Peroxide. *International Review of Cell and Molecular Biology*, Vol. 270: Academic Press, 87-144.
Gambetta GA, Manuck CM, Drucker ST, Shaghasi T, Fort K, Matthews MA, Walker MA, McElrone AJ. 2012. The relationship between root hydraulics and scion vigour across Vitis rootstocks: what role do root aquaporins play? *Journal of experimental botany* **63**, 6445-6455.
Gibbs DJ, Lee SC, Isa NM, Gramuglia S, Fukao T, Bassel GW, Correia CS, Corbineau F, Theodoulou FL, Bailey-Serres J, Holdsworth MJ. 2011. Homeostatic response to hypoxia is regulated by the N-end rule pathway in plants. *Nature* **479**, 415-418.
Good AG, Crosby WL. 1989. Anaerobic induction of alanine aminotransferase in barley root tissue. *Plant Physiology* **90**, 1305-1309.
Good AG, Muench DG. 1992. Purification and characterization of an anaerobically induced alanine aminotransferase from barley roots. *Plant Physiology* **99**, 1520-1525.
Gout E, Boisson A-M, Aubert S, Douce R, Bligny R. 2001. Origin of the Cytoplasmic pH Changes during Anaerobic Stress in Higher Plant Cells. Carbon-13 and Phosphorous-31 Nuclear Magnetic Resonance Studies. *Plant Physiology* **125**, 912-925.
Granett J, Walker MA, Kocsis L, Omer AD. 2001. Biology and management of grape phylloxera. *Annual review of entomology* **46**, 387-412.
Gray JD, Kolesik P, Hoj PB, Coombe BG. 1999. Confocal measurement of the three-dimensional size and shape of plant parenchyma cells in a developing fruit tissue. *Plant Journal* **19**, 229-236.
Groh B, Hübner C, Lendzian KJ. 2002. Water and oxygen permeance of phellems isolated from trees: the role of waxes and lenticels. *Planta* **215**, 794-801.
Hardie WJ, O'Brien TP, Jaudzems VG. 1996. Morphology, anatomy and development of the pericarp after anthesis in grape, Vitis vinifera L. *Australian Journal of Grape and Wine Research* **2**, 97-142.
Harris J, Kriedemann P, Possingham J. 1968. Anatomical aspects of grape berry development. *Vitis* **7**, 106-119.
Harris J, Kriedemann P, Possingham J. 1971. Grape berry respiration: effects of metabolic inhibitors. *Vitis* **9**, 291-298.
Herremans E, Verboven P, Verlinden BE, Cantre D, Abera M, Wevers M, Nicolaï BM. 2015. Automatic analysis of the 3-D microstructure of fruit parenchyma tissue using X-ray micro-CT explains differences in aeration. *BMC Plant Biology* **15**, 264.
Hertog MLATM, Peppelenbos HW, Evelo RG, Tijskens LMM. 1998. A dynamic and generic model of gas exchange of respiring produce: the effects of oxygen, carbon dioxide and temperature. *Postharvest Biology and Technology* **14**, 335-349.
Ho QT, Verboven P, Ambaw A, Verlinden BE, Nicolaï BM. 2016. Transport properties of fermentation metabolites inside 'Conference' pear fruit. *Postharvest Biology and Technology* **117**, 38-48.
Ho QT, Verboven P, Mebatsion HK, Verlinden BE, Vandewalle S, Nicolai BM. 2009. Microscale mechanisms of gas exchange in fruit tissue. *New Phytologist* **182**, 163-174.
Ho QT, Verboven P, Verlinden BE, Schenk A, Delele MA, Rolletschek H, Vercammen J, Nicolai BM. 2010. Genotype effects on internal gas gradients in apple fruit. *Journal of Experimental Botany* **61**, 2745-2755.

Hunt PW, Klok EJ, Trevaskis B, Watts RA, Ellis MH, Peacock WJ, Dennis ES. 2002. Increased level of hemoglobin 1 enhances survival of hypoxic stress and promotes early growth in Arabidopsis thaliana. *Proceedings of the National Academy of Sciences of the United States of America* **99**, 17197-17202.
Ikbal FE, Hernández JA, Barba-Espín G, Koussa T, Aziz A, Faize M, Diaz-Vivancos P. 2014. Enhanced salt-induced antioxidative responses involve a contribution of polyamine biosynthesis in grapevine plants. *Journal of plant physiology* **171**, 779-788.
Iland P, Dry P, Proffitt T, Tyerman S. 2011. The grapevine: from the science to the practice of growing vines for wine: Patrick Iland Wine Promotions.
Jones GV. 2007. Climate change: observations, projections, and general implications for viticulture and wine production. *Economics Department-working paper*, 14.
Jones KH, Senft JA. 1985. An improved method to determine cell viability by simultaneous staining with fluorescein diacetate-propidium iodide. *Journal of Histochemistry & Cytochemistry* **33**, 77-79.
Keller M, Mills LJ, Wample RL, Spayd SE. 2005. Cluster thinning effects on three deficit-irrigated vitis vinifera cultivars. *American Journal of Enology and Viticulture* **56**, 91-103.
Keller M, Shrestha PM. 2014. Solute accumulation differs in the vacuoles and apoplast of ripening grape berries. *Planta* **239**, 633-642.
Keller M, Smith JP, Bondada BR. 2006. Ripening grape berries remain hydraulically connected to the shoot. *Journal of Experimental Botany* **57**, 2577-2587.
Keller M, Zhang Y, Shrestha PM, Biondi M, Bondada BR. 2015. Sugar demand of ripening grape berries leads to recycling of surplus phloem water via the xylem. *Plant Cell and Environment* **38**, 1048-1059.
Kennedy JA, Matthews MA, Waterhouse AL. 2000. Changes in grape seed polyphenols during fruit ripening. *Phytochemistry* **55**, 77-85.
Kennedy JA, Matthews MA, Waterhouse AL. 2002. Effect of maturity and vine water status on grape skin and wine flavonoids. *American Journal of Enology and Viticulture* **53**, 268-274.
Kidman CM, Olarte Mantilla S, Dry PR, McCarthy MG, Collins C. 2014. Effect of water stress on the reproductive performance of Shiraz (Vitis vinifera L.) grafted to rotstocks. *American Journal of Enology and Viticulture* **65**, 96-108.
Knipfer T, Fei J, Gambetta GA, McElrone AJ, Shackel KA, Matthews MA. 2015. Water transport properties of the grape pedicel during fruit development: insights into xylem anatomy and function using microtomography. *Plant Physiology* **168**, 1590-1602.
Krasnow M, Matthews M, Shackel K. 2008. Evidence for substantial maintenance of membrane integrity and cell viability in normally developing grape (Vitis vinifera L.) berries throughout development. *Journal of Experimental Botany* **59**, 849-859.
Lee Y, Rubio MC, Alassimone J, Geldner N. 2013. A Mechanism for Localized Lignin Deposition in the Endodermis. *Cell* **153**, 402-412.
Lendzian KJ. 2006. Survival strategies of plants during secondary growth: barrier properties of phellems and lenticels towards water, oxygen, and carbon dioxide. *Journal of Experimental Botany* **57**, 2535-2546.
Longhurst T, Tung H, Brady C. 1990. Developmental regulation of the expression of alcohol dehydrogenase in ripening tomato fruits. *Journal of Food Biochemistry* **14**, 421-433.
Mayor L, Moreira R, Sereno A. 2011. Shrinkage, density, porosity and shape changes during dehydration of pumpkin (Cucurbita pepo L.) fruits. *Journal of Food Engineering* **103**, 29-37.
Meitha K, Agudelo-Romero P, Signorelli S, Gibbs DJ, Considine JA, Foyer CH, Considine MJ. 2018. Developmental control of hypoxia during bud burst in grapevine. Plant, cell & environment.

McCarthy M, Cirami R, Furkaliev D. 1997. Rootstock response of Shiraz (Vitis vinifera) grapevines to dry and drip-irrigated conditions. *Australian Journal of Grape and Wine Research* **3**, 95-98.
McCarthy MG. 1997. The effect of transient water deficit on berry development of cv. Shiraz (Vitis vinifera L.). *Australian Journal of Grape and Wine Research* **3**, 102-108.
McCarthy MG, Coombe BG. 1999. Is weight loss in ripening grape berries cv. Shiraz caused by impeded phloem transport? *Australian Journal of Grape and Wine Research* **5**, 17-21.
McMinn WAM, Magee TRA. 1997. Physical characteristics of dehydrated potatoes — Part II. *Journal of Food Engineering* **33**, 49-55.
Mebatsion H, Verboven P, Ho Q, Verlinden B, Mendoza F, Nguyen T, Nicolaï B. 2006. Modeling fruit microstructure using an ellipse tessellation algorithm. *13th World Congress of Food Science & Technology 2006*, 246-246.
Mendoza F, Verboven P, Mebatsion HK, Kerckhofs G, Wevers M, Nicolai B. 2007. Three-dimensional pore space quantification of apple tissue using X-ray computed microtomography. *Planta* **226**, 559-570.
Mullins MG, Bouquet A, Williams LE. 1992. *Biology of the grapevine*: Cambridge University Press.
Nelson K. 1979. *Harvesting and handling California table grapes for market*. Division of Agricultural Sciences, University of California: Agricultural Sciences Publications, University of California, Berkeley.
Nelson KE, Ahmedullah M. 1973. Effect of temperature change on the release rate of sulfur dioxide from two-stage sodium bisulfite generators. *American Journal of Enology and Viticulture* **24**, 75-80.
Nicholas P. 1997. Rootstock characteristics. *The Australian Grapegrower and Winemaker* **400**, 30.
Noctor G, Foyer CH. 1998. Ascorbate and glutathione: keeping active oxygen under control. *Annual Review of Plant Biology* **49**, 249-279.
Nunan KJ, Sims IM, Bacic A, Robinson SP, Fincher GB. 1998. Changes in cell wall composition during ripening of grape berries. *Plant Physiology* **118**, 783-792.
Ojeda H, Deloire A, Carbonneau A, Ageorges A, Romieu C. 1999. Berry development of grapevines: relations between the growth of berries and their DNA content indicate cell multiplication and enlargement. *Vitis* **38**, 145-150.
Olarte Mantilla SM, Collins C, Iland PG, Kidman CM, Ristic R, Boss PK, Jordans C, Bastian SEP. 2017. Shiraz (Vitis vinifera L.) berry and wine sensory profiles and composition are modulated by rootstocks. *American Journal of Enology and Viticulture*.
Palliotti A, Cartechini A. 2001. Developmental changes in gas exchange activity in flowers, berries, and tendrils of field-grown Cabernet Sauvignon. *American Journal of Enology and Viticulture* **52**, 317-323.
Patrick JW. 1997. Phloem unloading: sieve element unloading and post-sieve element transport. *Annual Review of Plant Physiology and Plant Molecular Biology* **48**, 191-222.
Paul V, Srivastava G. 2006. Role of surface morphology in determining the ripening behaviour of tomato (Lycopersicon esculentum Mill.) fruits. *Scientia Horticulturae* **110**, 84-92.
Perkins S, Alexander L, Nairn J. 2012. Increasing frequency, intensity and duration of observed global heatwaves and warm spells. *Geophysical Research Letters* **39**.
Petrie PR, Sadras VO. 2008. Advancement of grapevine maturity in Australia between 1993 and 2006: putative causes, magnitude of trends and viticultural consequences. *Australian Journal of Grape and Wine Research* **14**, 33-45.

Pilati S, Brazzale D, Guella G, Milli A, Ruberti C, Biasioli F, Zottini M, Moser C. 2014. The onset of grapevine berry ripening is characterized by ROS accumulation and lipoxygenase-mediated membrane peroxidation in the skin. *BMC Plant Biology* **14**, 87.
Pilati S, Perazzolli M, Malossini A, Cestaro A, Dematte L, Fontana P, Dal Ri A, Viola R, Velasco R, Moser C. 2007. Genome-wide transcriptional analysis of grapevine berry ripening reveals a set of genes similarly modulated during three seasons and the occurrence of an oxidative burst at veraison. *BMC Genomics* **8**, 428.
Pitzschke A, Forzani C, Hirt H. 2006. Reactive oxygen species signaling in plants. *Antioxidants & redox signaling* **8**, 1757-1764.
Podolyan A, White J, Jordan B, Winefield C. 2010. Identification of the lipoxygenase gene family from Vitis vinifera and biochemical characterisation of two 13-lipoxygenases expressed in grape berries of Sauvignon Blanc. *Functional Plant Biology* **37**, 767-784.
Possner D, Kliewer WM. 1985. The localization of acids, sugars, potassium and calcium in developing grape berries. *Vitis* **24**, 229-240.
Reape TJ, McCabe PF. 2008. Apoptotic-like programmed cell death in plants. *New Phytol* **180**, 13-26.
Reynolds AG, Naylor AP. 1994. 'Pinot noir' and 'Riesling' grapevines respond to water stress duration and soil water-holding capacity. *HortScience* **29**, 1505-1510.
Ristic R, Iland PG. 2005. Relationships between seed and berry development of Vitis Vinifera L. cv Shiraz: Developmental changes in seed morphology and phenolic composition. *Australian Journal of Grape and Wine Research* **11**, 43-58.
Roberts J, Callis J, Jardetzky O, Walbot V, Freeling M. 1984. Cytoplasmic acidosis as a determinant of flooding intolerance in plants. *Proceedings of the National Academy of Sciences* **81**, 6029-6033.
Rogiers S, Hatfield J, Keller M. 2004a. Irrigation, nitrogen, and rootstock effects on volume loss of berries from potted Shiraz vines. *Vitis* **43**, 1-6.
Rogiers S, Holzapfel B. 2015. *The plasticity of berry shrivelling in 'Shiraz': A vineyard survey*.
Rogiers SY, Coetzee ZA, Walker RR, Deloire A, Tyerman SD. 2017. Potassium in the grape (Vitis vinifera L.) berry: transport and function. *Frontiers in Plant Science* **8**, 1629.
Rogiers SY, Hatfield JM, Jaudzems VG, White RG, Keller M. 2004b. Grape Berry cv. Shiraz Epicuticular Wax and Transpiration during Ripening and Preharvest Weight Loss. *American Journal of Enology and Viticulture* **55**, 121-127.
Sadras VO, Collins M, Soar CJ. 2008. Modelling variety-dependent dynamics of soluble solids and water in berries of Vitis vinifera. *Australian Journal of Grape and Wine Research* **14**, 250-259.
Sadras VO, McCarthy MG. 2007. Quantifying the dynamics of sugar concentration in berries of Vitis vinifera cv. Shiraz: a novel approach based on allometric analysis. *Australian Journal of Grape and Wine Research* **13**, 66-71.
Saglio PH. 1985. Effect of path or sink anoxia on sugar translocation in roots of maize seedlings. *Plant Physiology* **77**, 285-290.
Santesteban LG, Royo JB. 2006. Water status, leaf area and fruit load influence on berry weight and sugar accumulation of cv. 'Tempranillo' under semiarid conditions. *Scientia Horticulturae* **109**, 60-65.
Scharwies JD, Tyerman SD. 2017. Comparison of isohydric and anisohydric Vitis vinifera L. cultivars reveals a fine balance between hydraulic resistances, driving forces and transpiration in ripening berries. *Functional Plant Biology* **44**, 324-338.
Serra I, Strever A, Myburgh P, Deloire A. 2014. the interaction between rootstocks and cultivars (Vitis vinifera L.) to enhance drought tolerance in grapevine. *Australian Journal of Grape and Wine Research* **20**, 1-14.

Shabala S. 2017. Signalling by potassium: another second messenger to add to the list? *Journal of Experimental Botany* **68**, 4003-4007.
Shi JX, Goldschmidt EE, Goren R, Porat R. 2007. Molecular, biochemical and anatomical factors governing ethanol fermentation metabolism and accumulation of off-flavors in mandarins and grapefruit. *Postharvest Biology and Technology* **46**, 242-251.
Shimada Y, Roos Y, Karel M. 1991. Oxidation of methyl linoleate encapsulated in amorphous lactose-based food model. *Journal of Agricultural and Food Chemistry* **39**, 637-641.
Smart RE, Sinclair TR. 1976. Solar heating of grape berries and other spherical fruits. *Agricultural Meteorology* **17**, 241-259.
Sowa AW, Duff SM, Guy PA, Hill RD. 1998. Altering hemoglobin levels changes energy status in maize cells under hypoxia. *Proceedings of the National Academy of Sciences* **95**, 10317-10321.
Spayd SE, Tarara JM, Mee DL, Ferguson JC. 2002. Separation of sunlight and temperature effects on the composition of Vitis vinifera cv. Merlot berries. *American Journal of Enology and Viticulture* **53**, 171-182.
Streeter JG, Thompson JF. 1972. Anaerobic accumulation of γ-aminobutyric acid and alanine in radish leaves (Raphanus sativus, L.). *Plant Physiology* **49**, 572-578.
Sudawan B, Chang C-S, Chao H-f, Ku MSB, Yen Y-f. 2016. Hydrogen cyanamide breaks grapevine bud dormancy in the summer through transient activation of gene expression and accumulation of reactive oxygen and nitrogen species. *BMC Plant Biology* **16**, 202.
Suklje K, Zhang X, Antalick G, Clark AC, Deloire A, Schmidtke LM. 2016. Berry shriveling significantly alters Shiraz (Vitis vinifera L.) grape and wine chemical composition. *Journal of Agricultural and Food Chemistry* **64**, 870-880.
Sweetman C, Deluc LG, Cramer GR, Ford CM, Soole KL. 2009. Regulation of malate metabolism in grape berry and other developing fruits. *Phytochemistry* **70**, 1329-1344.
Swift J, Buttrose M, Possingham J. 1973. Stomata and starch in grape berries. *Vitis* **12**, 38-45.
Taiz L, Zeiger E. 2010. *Plant Physiology*. Sunderland, Massachusetts U.S.A.: Sinauer Associates Inc.
Terrier N, Romieu C. 2001. Grape berry acidity. In: Roubelakis-Angelakis KA, ed. *Molecular Biology & Biotechnology of the Grapevine*: Springer Netherlands, 35-57.
Thomas TR, Shackel KA, Matthews MA. 2008. Mesocarp cell turgor in Vitis vinifera L. berries throughout development and its relation to firmness, growth, and the onset of ripening. *Planta* **228**, 1067-1076.
Tilbrook J, Tyerman SD. 2008. Cell death in grape berries: varietal differences linked to xylem pressure and berry weight loss. *Functional Plant Biology* **35**, 173-184.
Tilbrook J, Tyerman SD. 2009. Hydraulic connection of grape berries to the vine: varietal differences in water conductance into and out of berries, and potential for backflow. *Functional Plant Biology* **36**, 541-550.
Tournaire-Roux C, Sutka M, Javot H, Gout E, Gerbeau P, Luu D-T, Bligny R, Maurel C. 2003. Cytosolic pH regulates root water transport during anoxic stress through gating of aquaporins. *Nature* **425**, 393.
Tyerman SD, Tilbrook J, Pardo C, Kotula L, Sullivan W, Steudle E. 2004. Direct measurement of hydraulic properties in developing berries of Vitis vinifera L. cv Shiraz and Chardonnay. *Australian Journal of Grape and Wine Research* **10**, 170-181.
Van Doorn WG, Woltering EJ. 2005. Many ways to exit? Cell death categories in plants. *Trends in plant science* **10**, 117-122.

Vergara R, Parada F, Rubio S, Pérez FJ. 2012. Hypoxia induces H2O2 production and activates antioxidant defence system in grapevine buds through mediation of H2O2 and ethylene. *Journal of Experimental Botany* **63**, 4123-4131.
Wada H, Matthews MA, Shackel KA. 2009. Seasonal pattern of apoplastic solute accumulation and loss of cell turgor during ripening of Vitis vinifera fruit under field conditions. *Journal of Experimental Botany* **60**, 1773-1781.
Walker RR, Blackmore DH, Clingeleffer PR, Correll RL. 2002. Rootstock effects on salt tolerance of irrigated field-grown grapevines (Vitis vinifera L. cv. Sultana).: 1. Yield and vigour inter-relationships. *Australian Journal of Grape and Wine Research* **8**, 3-14.
Wallis CM, Wallingford AK, Chen J. 2013. Grapevine rootstock effects on scion sap phenolic levels, resistance to Xylella fastidiosa infection, and progression of Pierce's disease. *Frontiers in Plant Science* **4**, 502.
Webb LB, Whetton PH, Barlow EWR. 2007a. Modelled impact of future climate change on the phenology of winegrapes in Australia. *Australian Journal of Grape and Wine Research* **13**, 165-175.
Webb LB, Whetton PH, Barlow EWR. 2011. Observed trends in winegrape maturity in Australia. *Global Change Biology* **17**, 2707-2719.
Webb LB, Whetton PH, Barlow EWR. 2007b. Modelled impact of future climate change on the phenology of winegrapes in Australia. *Australian Journal of Grape and Wine Research* **13**, 165-175.
White KL, Bell L. 1999. Glucose loss and Maillard browning in solids as affected by porosity and collapse. *Journal of Food Science* **64**, 1010-1014.
Wigginton MJ. 1973. Diffusion of oxygen through lenticels in potato tuber. *Potato Research* **16**, 85-87.
Williams LE. 2010. Interaction of rootstock and applied water amounts at various fractions of estimated evapotranspiration (ETc) on productivity of Cabernet Sauvignon. *Australian Journal of Grape and Wine Research* **16**, 434-444.
Zhang W-H, Tyerman SD. 1999. Inhibition of water channels by HgCl2 in intact wheat root cells. *Plant Physiology* **120**, 849-858.
Zhang X-Y, Wang X-L, Wang X-F, Xia G-H, Pan Q-H, Fan R-C, Wu F-Q, Yu X-C, Zhang D-P. 2006. A shift of phloem unloading from symplasmic to apoplasmic pathway is involved in developmental onset of ripening in grape berry. *Plant physiology* **142**, 220-232.
Zhang Y, Keller M. 2015. Grape berry transpiration is determined by vapor pressure deficit, cuticular conductance, and berry size. *American Journal of Enology and Viticulture* **66**, 454-462.
Zhang Y, Keller M. 2017. Discharge of surplus phloem water may be required for normal grape ripening. *Journal of Experimental Botany* **68**, 585-595.